Three Paradigms of Emotional Learning Differentially Affect Brainstem, Hypothalamic, and Limbic Circuits in the Rat

by

Elizabeth Anne Myers

Bachelor of Science, University of Pittsburgh, 2002

Submitted to the Graduate Faculty of

Faculty of Arts and Sciences in partial fulfillment

of the requirements for the degree of

Master of Science

University of Pittsburgh

2004

UNIVERSITY OF PITTSBURGH

FACULTY OF ARTS AND SCIENCES

This dissertation was presented

by

Elizabeth Anne Myers

It was defended on

June 29, 2004

and approved by

Anthony Grace, Ph.D.

John P. Card, Ph.D.

Linda Rinaman, Ph.D.
Thesis Director

Three Paradigms of Emotional Learning Differentially Affect Brainstem, Hypothalamic, and Limbic Circuits in the Rat

Elizabeth A. Myers, M.S.

University of Pittsburgh, 2004

Noradrenergic (NA) signaling in limbic forebrain regions, such as the central nucleus of the amygdala (CeA), shapes the encoding and expression of emotional learning, and modulates responses to stress and anxiety. The present study examined whether categorically different emotional stress models, [cholecystokinin (CCK), trimethylthiazoline (TMT), and yohimbine (YO)] support behaviorally aversive conditioning and differentially activate CRH-positive neurons in the hypothalamus, medullary and pontine NA neurons, and ascending inputs to the CeA. A conditioned flavor avoidance (CFA) paradigm using a flavor preference test was implemented as a measure of aversive conditioning for each stressor. In a terminal experiment, rats received either an injection of CCK (10 μg/kg, i.p.), YO (5 mg/kg. i.p.), or 15 min exposure to an aversive odor, TMT, and were perfused 60-120 min later. In a subset of rats, retrograde neural tracer was microinjected into the CeA prior to stressor treatment and perfusion. Brainstem and forebrain sections were processed for immunocytochemical localization of cFos and either dopamine beta hydroxylase (DβH) to identify NA neurons, corticotropin-releasing hormone (CRH), or neural tracer to identify hindbrain CeA-projecting neurons. All stressors activated hypothalamic CRH neurons, produced a relatively strong CFA in a 2-bottle choice test, and recruited similar proportions of CeA-projecting neurons arising from the parabrachial nucleus, a projection path critical for this behavioral paradigm. All stressors recruited NA

neurons within the medullary A2 cell group to a similar extent, whereas those in the medullary A1 cell group and pontine A6 cell group were recruited more selectively by TMT and YO compared to CCK. Afferent inputs to the CeA arising in these hindbrain cell groups were activated in a parallel manner, with TMT and YO recruiting a much greater proportion of CeA-projecting neurons in the A1 and A6 cell groups. These findings lend support to the working hypothesis that different emotional stimuli may potentially influence emotional learning via stressor-specific ascending NA projection pathways to the CeA. In general, elucidating stressor-specific neural circuitry may provide new insight into how to design effective therapeutic measures for a wide range of human disorders and conditions involving the NA system.

TABLE OF CONTENTS

LIST OF TABLES

LIST OF FIGURES

PREFACE

I would like to whole heartily thank my mentor, Dr. Linda Rinaman, for her dedication, commitment, and support of my goals as both a scientist and a person. Linda's unconditional encouragement and constant willingness to present me with every opportunity to shape my learning experience during my time in her lab has fostered tremendous growth in me as both a scientist and person. I thank her for allowing me to think independently, to pursue projects of personal interest, and for valuing my intellectual contributions to both experimental projects and manuscripts. Her passion for science is contagious and has left an indelible imprint on the fond memories I have of working in her lab and of my time in Pittsburgh.

I would like to thank the additional members of my master's committee, Dr. Pat Card and Dr. Anthony Grace, who have provided me with guidance and support throughout the process of completing this thesis. I want to further thank Pat Card for being an excellent advisor. I want to extend a special thanks to Dr. Susan Sesack, who has been a listening ear throughout both my undergraduate and graduate education. I thank her for offering me unlimited advice and for always being an advocate for me as both a student and person. I also recognize and thank my fellow graduate students in the program and other faculty members of the neuroscience department that have been integral to my success as a student, including Drs. Alan and Judy Sved, Dr. David Wood, and Dr. Edward Stricker.

I would like to kindly thank the Rinaman lab technicians Victoria Maldovan, Judith Joyce Balcita-Pedicino, and Jen-Shew Yen for both their technical assistance and their friendship. These three remarkable individuals often put a smile on my face and never ceased to amaze me with their endless array of talents both inside and outside of the lab. Their continuous intellectual efforts and support of my goals, both academically and personally, made it possible

for me to complete this body of scientific work- they will be greatly missed. I would like to thank Tom Koehnle for his assistance with the statistical analysis for this manuscript. I would also like to thank Shnehal Patel and Layla Banihashemi for allowing me to share my knowledge and experience with them and for greatly enriching me as a person by sharing their scholarship and culture.

I would like to extend a thank you to the ladies in the fiscal office for always having patience with my questions, to Marlene and Joan for always guaranteeing me a few laughs in my day, and to my undergraduate advisor, Andrea Abt, for always providing a listening ear.

I would like to especially thank both Ingrid Kuo, a friend and mentor who has always inspired me to pursue my dreams, and Dr. John Rosenberg for providing me with my first opportunity to engage in scientific research through my own project as an undergraduate. This project became the catalyst for my interest in laboratory research.

Most of all, I would like to thank my parents and my brother, who have provided me with unconditional support for every life endeavor I have pursued. Their continuous love, encouragement, and listening ears have provided me with a foundation for life happiness and success. They are incredible parents, mentors, and friends. Lastly, but certainly not least, I would like to thank my most devoted and cherished companions, Fonzi and Petie.

1. Chapter 1: General Introduction

Stress: A Brief Historical Perspective

In 1936, endocrinologist, Hans Selye marked his pivotal role in the development of the stress concept when he coined and defined the term *stress* as "the body's nonspecific response to a demand placed on it," and named its causal agents, *stressors* (Selye 1936, 1946). Prior to Selye's hypothesis, physiologist Walter Cannon had put forth the widely accepted notion that a primal sympathoadrenal system was activated in response to external challenges placed on the body (Cannon 1929). Cannon noted that both physical and emotional disturbances alike elicited this response from an organism. Selye's concept of stress greatly extended upon Cannon's theory and shifted attention to the additional important role of the hypophysis in generating responses to stress. Notably, today this is the hallmark biological system most often associated with the body's response to stress and elevated activity of this neuroendocrine axis is now generally accepted as a valid "operational" definition of *stress*. However, the validity of Selye's ideas and the use of this definition of stress have since been questioned as significant advances have been made in stress research.

Despite significant development in this field and subsequent attempts by other researchers to adequately define the abstract concept of *stress*, there still abounds considerable ambiguity in the meaning of the word. Nevertheless, stress is something that is experienced by all living organisms. In humans, stress is linked to the underlying pathophysiology of a wide array of psychiatric disorders and medical problems prevalent among the general population, including hypertension, irritable bowel syndrome, depression, and numerous anxiety-related disorders. Consequently, gaining a solid understanding of the neural correlates of stress and

anxiety through elucidation of the underlying brain circuits involved in mediating emotional responses will provide important insight into the brain mechanisms by which stress and anxiety can influence physiology and behavior. Moreover, expounding the specific neural systems involved may suggest better treatments strategies and offer more effective therapeutic outcomes for these relatively prevalent disorders.

The Stress Response

Stress responses involve specific somatic (behavioral), autonomic, and neuroendocrine adjustments that may be interpreted as adaptive mechanisms to improve an organism's ability to maintain homeostasis and increase its chances of survival. In animals, behavioral responses often include the promotion of adaptive mechanisms such as fighting, fleeing, freezing, increased alertness, nausea, as well as the inhibition of nonadaptive mechanisms including feeding and reproduction. In humans, behavioral responses to stress frequently consist of health-related behaviors such as substance abuse, eating problems, alcohol consumption, smoking, and generalized feelings of anxiety. These behavioral responses are intricately tied with physiological responses to stress; thus, each has the potential to influence the other, which is often detrimental to an organism's well being.

The autonomic component of the stress response includes the immediate release of catecholamines (epinephrine/norepinephrine) from the sympathetic nervous system and the associated adrenal medulla. This sympathetic arousal provides an organism with a rapidly responding global alarm mechanism that initiates a fight or flight response, which serves as an adaptive strategy for an organism to deal with an imposing threat. A longer sustaining and delayed-onset physiological response to stress is generated by the neuroendocrine hypothalamo-

pituitary adrenal (HPA) axis. HPA activation is regulated primarily by a discreet population of neurons in the hypothalamic medial parvocellular parventricular nucleus (mpPVN). Upon stimulation from a converging set of neural inputs, this population of neurons releases corticotropin-releasing hormone (CRH) and arginine vasopressin (AVP) directly into a specialized pituitary portal circulation. This specialized blood supply allows CRH to target endocrine cells of the anterior pituitary and promotes the release of adrenocorticotropin (ACTH) which, in turn, potentiates both the synthesis and secretion of glucocorticoids [mainly corticosterone (CORT) in rats and cortisol in humans] from the adrenal cortex. Glucocorticoids are released into the general circulation and act on receptors distributed throughout the brain to help maintain the fight or flight response and to limit the magnitude of the HPA stress response. Together, the autonomic and neuroendocrine components of the stress response act in a coordinated fashion to provide the necessary neurohumoral adaptations for an organism to maintain homeostasis in the face of threatening stimuli.

Stressor Categorization

A wide range of experimental stimuli (i.e., stressors) induce stereotypical behavioral and physiological responses in both animals and humans, yet an enigma surrounds the question of whether the brain deals with such stimuli in a categorical fashion. Consistent with this view is the notion that if the brain discriminates between different types of stressors, these stimuli should elicit category-specific patterns of neural activity in the central nervous system (Dayas et al., 2001). This hypothesis was first proposed by Fortier in 1951 to explain why stimuli such as epinephrine, cold, and histamine could elicit corticosteroid release when the pituitary was removed while stimuli such as immobilization and sounds required an intact pituitary to generate

such responses (reviewed in Herman et al., 2003; Fortier 1951). In more recent years, Herman's group suggests that there are two general categories of stressors the brain may recognize that are, in part, defined by a general underlying neural circuitry: *limbic-insensitive* and *limbic-sensitive stress pathways*. However, Herman's group is careful to point out that it is important to understand that the distinction made between these general classifications does not assume that all stressors within each category use identical circuitry. Limbic-insensitive stress pathways are most responsive to stressors that pose an immediate threat to homeostasis, involve direct inputs to the PVN via visceral efferent pathways, and do not require higher order cognitive processing or limbic appraisal. Stimuli that fall into this general category are often termed *systemic, physical or interoceptive stressors*, and include models such as hemorrhage, immune challenge (IL-1β), hypoxia, and supraphysiological doses of cholecystokinin (CCK). In contrast, limbic-sensitive stress pathways are most responsive to stressors that do not pose an immediate threat to physiological homeostasis, induce anticipation of suffering, require limbic appraisal, and necessitate assembly and processing from multiple sensory modalities prior to the initiation of a stress response. Stimuli that are placed in this category are widely termed *processive, neurogenic, psychogenic, or exteroceptive stressors*, and often include models such as predator-related stimuli (i.e., live exposure or odor cues), novelty, and restraint stress (Herman and Cullinan 1997).

In view of this, HPA responses to restraint, fear conditioning, or exposure to a novel environment are affected by lesions of the prefrontal cortex and amygdala, whereas HPA responses to physiologic threats such as ether or hypoxia are unaffected by lesions of the limbic system (Herman and Cullinan 1997). These findings suggest that although the physiological responses (i.e., autonomic and neuroendocrine adjustments) are a common feature observed

among different stressors, the underlying neural circuitry that governs such responses may vary depending on the nature of the stimulus involved. Whereas such classifications make discussing general differences among stressor paradigms an easier task for researchers, it is important to point out that numerous stressors are not easily placed into either of these general categories, and consequently, may recruit overlapping neural circuitry.

The Amygdala, Emotional Learning, and Stress

Stressors are often discussed as being "emotionally arousing stimuli" that impose a challenge on an organism and generate an emotional response that emerges as a wide array of behavioral output. According to LeDoux, emotions can be operationally defined as "unconscious biological functions of the brain that are essential for the survival of all living organisms." For example, the emotion of fear and the associated fight or flight response is essential to an animal avoiding a predator in the wild (LeDoux 1996).

The hypothalamus was once implicated as a key subcortical region in emotional processing; however, this notion was challenged when Weiskrantz published a seminal paper that first proposed the amygdala to be the centerpiece of the neural networks implicated in recognizing and responding to threats (Weiskrantz 1956). The amygdala appears to play an essential role in detecting emotionally arousing stimuli, generating subsequent emotional responses, and mediating emotional learning and the formation of emotional memories concerning such stimuli. In particular, the amygdala is implicated to play a role in a form of Pavlovian conditioning: *fear conditioning*. In Pavlovian fear conditioning, an emotionally neutral conditioned stimulus (CS), usually a tone or flavor in the case of flavor avoidance learning, is presented in conjunction with an aversive unconditioned stimulus (US), such as

footshock or exposure to an aversive odor. After single or multiple pairings, the CS comes to elicit responses that typically are observed with the US, such as defensive behavior (i.e., freezing or avoidance responses), changes in physiological parameters such as heart rate and blood pressure, and neuroendocrine responses (LeDoux 2003). Various studies report that lesions of the amygdala in various species suppress fear-related behaviors and disrupt fear conditioning (reviewed in Davis 1992a,b). Specifically, the central nucleus of the amygdala (CeA) appears to be necessary for the acquisition and expression of fear and anxiety responses to conditioned and short duration unconditioned stimuli. Evidence in support of this comes from lesion studies which demonstrate that lesions of the CeA disrupt behavioral, autonomic, and neuroendocrine responses to conditioned fear (LeDoux et al., 1984, 1986, 1995). Furthermore, the CeA is implicated as an essential brain region for condition taste aversion learning (Lasiter and Glanzman 1985; Lamprecht and Dudai 1996; Yamamoto et al., 1997).

Although a large body of literature focuses on the role of the amygdala in producing conditioned fear responses, a few studies suggest that this structure is additionally important for generating unconditioned fear responses. The role of specific amygdaloid nuclei in unconditioned fear responses is less understood, as experiments addressing this question have produced mixed results. For example, in one study large amygdala lesions or those that damaged the cortical medial, and in some cases the CeA, blocked a reliable measure of innate fear in that these lesions dramatically increased the number of contacts rats made with a sedated cat (reviewed in Davis 2001; Blanchard and Blanchard 1972). In another study, electrolytic or chemical lesions of the CeA attenuated increases in plasma CORT produced by restraint stress (Beaulieu et al., 1987; Van de Kar et al., 1991) and blocked unconditioned analgesia to cat exposure or footshock (Fox and Sorenson 1994; Werka 1997). In contrast, a recent study

examined the effects of lesions to the CeA and medial amygdala (MeA) on cat odor-induced unconditioned fear. The findings of the study revealed that fiber-sparing lesions of the MeA, but not the CeA, disrupted unconditioned fear behavior (i.e., freezing) in response to predator odor (Chun-I et al., 2004). This finding is not surprising given the known direct chemosensory information pathway directly from the accessory and main olfactory bulbs to the MeA (Scalia and Winans 1975). Given these mixed results, one view of the role of the amygdala in fear conditioning suggests that the amygdala is selectively involved in the mediation of unconditioned fear responses.

Information from external stimuli can trigger emotional responses without conscious awareness via direct pathways to the amygdala through the gateway for sensory information, the thalamus. The lateral nucleus of the amygdala receives critical information about conditioned and aversive unconditioned stimuli from converging neural inputs, and then relays this information to the CeA, where a learned association is formed between the two stimuli. Subsequent neural transmission from the CeA to hypothalamic and brainstem areas involved in stress and anxiety coordinates the behavioral, neuroendocrine, and autonomic responses that form an integrated emotional response (Gallagher and Chiba 1996). Selective damage to these CeA output areas can interrupt the expression of individual responses. For example, damage to the periaqueductal gray interferes with freezing behavioral responses but not blood pressure responses whereas damage to the lateral hypothalamus disrupts autonomic, but not behavioral responses (LeDoux et al., 1988). Selective lesions of the CeA also decrease ACTH and CORT responses to immobilization and fear conditioning (Beaulieu et al., 1987; Van der Kar et al., 1991), and reduce the number of CRH neurons expressing cFos (a marker of neuronal activation) in the PVN following immune challenge (Xu et al., 1999). Interestingly, other reports suggest

that CeA lesions do not have an effect on HPA axis regulation. For example, in one study ACTH release and PVN cFos expression appear to be unaltered by CeA lesions in restrained animals (Dayas et al., 1999). Perhaps, variations in the experimental design used across different studies may contribute to the inconsistent results observed with different stress stimuli. Furthermore, stress responses to certain stimuli are differentially affected by lesions of different divisions of the CeA (Marchilhac and Siaud 1996). A more probable and widely debated notion is that the CeA is involved in generating stress responses to selective stimuli as selective induction of cFos is observed in the CeA following hemorrhage and infusion of cytokines (Sawchenko et al., 1996; Thrivikraman et al., 1997), whereas little cFos expression is seen following foot shock or restraint stress (Cullinan et al., 1995; Sawchenko et al., 1996).

Role of Viscerosensory Feedback

Emotional and cognitive functions of the brain are intimately tied with the autonomic nervous system (ANS). For example, we often use expressions such as there are "butterflies in my stomach" or my "stomach is tied in knots" when we experience a stressful situation (Mayer et al., 2000). Exteroceptive stimuli (i.e., external to the body) have the ability to generate interoceptive stress-related signals within the body that provide important feedback on autonomic, neuroendocrine, and behavioral outputs of brain regions involved in emotional processing. In contrast to signals processed by our special senses (i.e., olfaction, audition, vision), the majority of interoceptive feedback signals do not reach conscious awareness.

States of peripheral autonomic arousal are represented within several key brain regions that are also implicated in emotional processing (Critchley et al., 2000, 2001), including brainstem viscerosensory nuclei, the hypothalamus, BNST, and CeA, which is implicated in the

generation of autonomic arousal in response to conditioned fear stimuli (LeDoux 1992). The positioning of these select brain regions throughout the neuroaxis, and their reciprocal interconnections, forms a *central autonomic network* (Benarroch 1993), which plays a pivotal role in mediating changes in bodily states that influence ongoing emotional experience. A recent clinical report provides compelling evidence that the ANS greatly influences our emotions by showing that the absence of peripheral autonomic arousal, in patients with pure autonomic failure (PAF), leads to decreased fear conditioning-related anxiety in the amygdala (Critchley et al., 2001, 2002). Importantly, the amygdala receives direct neural input from brainstem viscerosensory nuclei including the hindbrain nucleus of the solitary tract (NST; the sensory nucleus of the dorsal vagal complex, ventrolateral medulla (VLM), and pontine parabrachial nucleus (PBN). Specifically, primary sensory afferents from peripheral visceroreceptors course through the vagus nerve and terminate in the NST, the first brainstem synaptic relay by which subsequent transmission of interoceptive feedback to forebrain limbic brain regions occurs (Spyer 1982; Ciriello and Calaresu 1980; Kannan and Yamashita 1985). This notion suggests that all categories of stress likely induce both neuroendocrine and autonomic alterations that generate subsequent interoceptive feedback which can influence emotional processing in the brain.

Ascending neural inputs to the CeA

There is growing evidence to suggest that noradrenergic (NA) transmission in the CeA plays a central role in integrating somatic and interoceptive (neuroendocrine and autonomic) responses during adaptive responses to stress and anxiety, and is important for conditioned learning and the encoding of memories for emotionally provoking experiences (Williams et al.,

2000; Zardetto-Smith and Gray 1990). The majority of catecholaminergic (i.e., noradrenergic or adrenergic) inputs to the CeA arise from the aforementioned dorsomedial and ventromedial medullary regions including the NST (A2/C2 NA cell group), and VLM (A1/C1 NA cell group). The CeA, in addition to other limbic forebrain regions, contains a high density of adrenergic receptors in divisions that receive input from the NST and VLM (Sawchenko and Swanson 1982; ETC Jr. et al., 1990). Other catecholaminergic inputs to the CeA arise from the locus coeruleus (LC; A6 cell group), although to a lesser extent than those arising in the caudal medulla (Zardetto-Smith and Gray 1990, 1995). The LC projects directly to the CeA as well as several other subnuclei of the amygdala (Nitecka et al., 1980) whereas inputs from the NST and VLM appear to be more selective for the CeA. Specifically, catecholaminergic CeA-projecting neurons of the NST are primarily noradrenergic (A2 neurons) whereas a substantial proportion of the VLM catecholaminergic projections to the CeA arise from adrenergic cells of the C1 group (Zardetto-Smith and Gray 1990, 1995). Importantly, these hindbrain inputs to the CeA are largely reciprocal and highly interconnected.

The parabrachial nucleus (PBN) of the pons also provides a massive non-catecholaminergic reciprocal innervation of the CeA, PVN, and bed nucleus of the stria terminalis (BNST) that potentially shapes stress and anxiety-related responses. Similar to the amygdala, the PBN is clearly necessary for the acquisition of conditioned taste/flavor aversion/avoidance learning as evidenced through various lesion studies (Sakai and Yamamoto 1998; Grigson et al., 1998; Reilly 1999; Wang and Chambers 2002). Furthermore, bidirectional projections between the PBN and CeA form a well-defined classical viscerosensory neural circuit (Fulwiler and Saper 1984; Van der Kooy et al., 1984; Veening et al., 1984; Jhamandas et al., 1996). The PBN contains neurons immunoreactive for a wide array of stress-related

neuropeptides, that are implicated as key components in relaying visceral information to the PVN and CeA from the periphery (Saper and Loewy, 1980; Herbert and Saper 1990; Jia et al., 1994; Norgren 1995). Afferent inputs to the CeA arising from the PBN are primarily calcitonin gene related peptide-positive neurons (Schwaber et al., 1988). The lateral viscerosensory PBN, including the external lateral division, receives dense inputs from both NA and non-NA neuronal populations (i.e., peptidergic cell populations) located within the NST (Shapiro and Miselis, 1985; Herbert and Saper 1990; Jia et al., 1994).

The NST serves as the first brainstem synaptic relay for a large number of viscerosensory and gustatory afferents coming from the periphery (via the vagus nerve); thus, it is adequately positioned to signal feedback relating to peripheral physiological changes following an emotionally arousing event through direct NA input to forebrain regions, including the limbic forebrain, and through indirect input to these forebrain areas via non-catecholaminergic projections routed through the PBN.

Mechanisms of CeA influence on the hypothalamus

Interestingly, though the CeA appears to have pronounced influences on HPA function, it has sparse direct neural projections to the PVN (Gray et al., 1989). Therefore, the neural mechanisms by which the CeA governs HPA function are currently unclear. One view is that the CeA has the potential to contribute to HPA function via indirect neuronal pathways that do provide direct projections to the mpPVN.

For example, the CeA provides direct neural input, via the stria terminalis, to the BNST (Sun et al., 1991; Petrovich and Swanson 1997), a subcortical limbic region that densely innervates the parvocellular portion of the PVN (Sawchenko and Swanson 1983; Magnuson and

Gray 1989) and has strong connections with brainstem viscerosenosry nuclei, including the NST and PBN (Dong et al., 2001). Furthermore, many studies implicate a role for the BNST in anxiety responses to unconditioned anxiety (reviewed in Walker et al., 2003) and suggest that it contributes to the shaping of HPA responses (Dunn 1987). The oval and fusiform subnuclei of the lateral BNST, in particular, have been implicated in behavioral and endocrine responses to both exterocpetive and interoceptive stress (Casada and Dafny 1991; Pacak et al., 1995; Crane et al., 2003). Interestingly, the BNST is often thought of as a continuum of the CeA as they are anatomically, neurochemically, cytoarchitectonically, and embryologically related, and project to a common set of target areas (Alheid et al., 1995). However, the BNST is more generally implicated in stress-induced anxiety as opposed to fear, insofar as fear is triggered by an immediate threat whereas anxiety is often a prolonged state of apprehension and increased vigilance unrelated to immediate environmental threats (Walker et al., 2003).

As previously described, the CeA is also reciprocally interconnected with dorsomedial and ventromedial hindbrain catecholaminergic cell groups. These select hindbrain catecholamine-producing pathways not only provide important afferent drive to the CeA, but also supply direct input to CRH-containing neurons of the mpPVN. Consonant with this view, it has been reported that many different types of stress stimuli recruit these medullary noradrenergic cell groups (Ceccatelli et al., 1989; Sawchenko et al., 2000) and that these stimuli orchestrate HPA function. An excitatory role for these ascending catecholaminergic inputs on the PVN is supported by studies that show stimulation of the central noradrenergic bundle, which includes ascending axons from the A1/A2 medullary cell groups, initiates CRH release into portal blood (Plotsky 1987), and deafferentation of these inputs to the PVN inhibits cFos protein in CRH neurons following immune challenge (Li et al., 1996). Together, this afferent drive to

the CeA and PVN is presumed to play an important role in shaping emotional learning and modulating behavioral and neuroendocrine responses to stress and anxiety.

Aims of Study

While it is clear that afferent inputs from the NST, VLM, LC, and PBN to the limbic forebrain play an important role in mediating stress and anxiety, it is currently unclear whether CeA-projecting inputs from these cell groups are differentially activated by categorically different paradigms of emotional learning (i.e., interoceptive vs exteroceptive stimuli). The present study investigated behavioral responses related to stress and anxiety, and possible correlating central patterns of neural activation in adult rats following presentation of three different stressors: administration of an aversive visceral stimulus [(cholecystokinin (CCK)], exposure to an aversive odor stimulus [trimethylthiazoline (TMT)], and systemic treatment with an anxiogenic pharmacological agent [yohimbine (YO)].

To achieve these objectives, a comparative analysis on the effects of each stressor was carried out by implementing a behavioral conditioning paradigm and by using immunocytochemical detection methods in order to label dual cFos and neuronal phenotypic markers. The cFos protein product of the c-fos immediate early gene is used in this study as a marker of stimulus-induced neuronal activity, as this gene accumulates in nuclei of stimulated neurons (Sagar et al., 1988) and is now well established as a relatively reliable marker of neuronal activity (Kovacs 1998). Neuronal phenotypical analysis centered on stressor-induced activation of CRH-positive neurons in the hypothalamus, activation of medullary and pontine NA neurons, and activation of ascending neural inputs to the CeA. The rationale for undertaking this investigation was that our experimental findings might identify the potential overlapping vs.

differential central neural mechanisms which underlie the observed behavioral responses associated with these three categorically different stressor paradigms. Elucidating stressor-specific neural circuitry may provide us with new insights into how to design effective treatments for a wide range of human disorders.

2. Chapter 2: Viscerosensory Activation of Noradrenergic Inputs to the Amygdala in Rats

Norepinephrine (NE) acts in the amygdala to regulate processes underlying acquisition and expression of emotional learning. The present study investigated whether stimulation of gastric vagal sensory afferents activates neurons immunoreactive for the NE synthetic enzyme, dopamine beta hydroxylase (DßH), in medullary and pontine cell groups that innervate the central nucleus of the amygdala (CeA) in rats. To identify such neurons, retrograde neural tracers were microinjected bilaterally into the CeA. Seven to ten days later, rats were injected i.p. with saline vehicle (controls) or cholecystokinin octapeptide (CCK; 10 μg/kg) to stimulate gastric vagal afferents, then perfused with fixative 60-90 min later. Brain sections were processed for localization of neural tracer and cFos protein (to identify activated cells). Approximately 30% of retrogradely-labeled neurons in the nucleus of the solitary tract (NST; A2/C2 region) and 19% of retrogradely-labeled neurons in the ventrolateral medulla (A1/C1 region) were activated in rats after CCK treatment. Triple immunolabeling of cFos, neural tracer, and DβH confirmed that the large majority of activated, CeA-projecting neurons were noradrenergic (or adrenergic). Conversely, CCK activated less than 4% of CeA-projecting neurons in the locus coeruleus (A6 cell group), similar to control cases. These findings suggest that vagal afferent stimulation may modify amygdalar processes of emotional learning via direct noradrenergic/adrenergic projections from the caudal medulla to the CeA.

2.1. Introduction

Norepinephrine (NE) modulates amygdala activity during the encoding and expression of emotional memories (Ferry et al., 1999). Activation of NE inputs to the amygdala may occur as a consequence of viscerosensory feedback associated with emotional arousal (e.g., adrenal epinephrine release, altered cardiac and gastrointestinal functions). Adrenergic and noradrenergic inputs to the amygdala include neurons in the locus coeruleus (LC; A6 cell group), NST (A2/C2 cell group), and ventrolateral medulla (VLM; A1/C1 cell group). LC projections to the amygdala are distributed to several subnuclei (Nitecka et al., 1980), whereas amygdala-projecting NST and VLM neurons preferentially target the CeA (Zardetto-Smith and Gray, 1990; Zardetto-Smith and Gray 1995; Ricardo and Koh 1978). Whether amygdalar-projecting neurons in the LC, NST, or VLM are actually activated by viscerosensory stimuli that affect emotional learning remains an important question.

Systemic administration of CCK has memory-enhancing effects in rats and mice (Voits et al., 2001; Lemaire et al., 1994; Gerhardt et al., 1994), consistent with evidence that vagal afferent activity affects learning and memory in rodents and in humans (Slaughter and Hahn 1974; Clark et al., 1999; Clark et al., 1998). Synthetic CCK binds to CCK-A receptors on gastric vagal afferents, thereby pharmacologically activating inputs to the NST (Schwartz and Moran 1998; Day et al., 1994) and inducing robust cFos expression in the NST, VLM, and other central regions (including the CeA) that receive viscerosensory signals (Day et al., 1994; Rinaman et al., 1993). Thus, CCK is a useful pharmacological tool to identify brain neurons activated by vagal sensory stimulation. The present study determined whether CCK activates neurons in the A1/C1, A2/C2, and/or A6 cell groups that project to the CeA.

2.2. Materials and Methods

Animals

Fourteen male Sprague-Dawley rats (Harlan Laboratories; 240-310 g body weight) were used in this investigation. Rats were housed separately in stainless steel cages in a controlled environment (20-22°C, 12:12 hr photoperiod) with free access to water and pelleted chow (Purina 5001).

Tracer injections

Rats were anesthetized with halothane (Halocarbon Laboratories; 1.5-3% in oxygen) and mounted into a stereotaxic frame. Two retrograde tracers were used: Fluorogold (FG; Fluorochrome, Inc.; 2% in 150mM NaCl) and cholera toxin (CTb; List Biological Laboratories, Inc.; 0.25% in 150mM NaCl). Rats received a FG injection targeted to the left CeA, and a CTb injection targeted to the right CeA. This increased the chance of obtaining at least one accurate injection site in each rat, thereby reducing the number of rats needed. A 1.0-µl Hamilton syringe filled with FG or CTb was attached to the stereotaxic injector guide. CeA coordinates were based on the Paxinos and Watson rat brain atlas (Paxinos and Watson 1997). Tracer (50 nl) was delivered by pressure injection over a period of 1-2 min. A different 1-µl Hamilton syringe was used to repeat the procedure using the second tracer on the opposite side of the brain. Afterwards, the skin was closed with stainless steel clips, and rats were returned to their home cages.

CCK administration and animal perfusion

Seven to ten days after tracer injections, rats were injected i.p. with sulfated CCK (Bachem) dissolved in 2.0 ml vehicle (150 mM NaCl) to yield a dose of 10 μg/kg body weight. Controls were injected with vehicle. Rats were returned to their home cages and left undisturbed for 60-90 min, then were anesthetized by i.p. injection of sodium pentobarbital (50 mg/kg). Rats were perfused transcardially with 150 mM NaCl followed by fixative (4% paraformaldehyde with lysine and sodium metaperiodate). Brains were post-fixed overnight at 4°C, then blocked and cryoprotected in 20% sucrose.

Histology and immunocytochemistry

Using a freezing microtome, coronal 35-μm sections were cut from the caudal extent of the NST through the rostral extent of the corpus callosum. Sections were collected serially in six sets and stored at –20°C in cryopreservant (Watson et al., 1986). Sections were removed from storage and rinsed for 1 hr in buffer (0.1 M sodium phosphate, pH 7.4) prior to immunocytochemical procedures. Antisera were diluted in buffer containing 0.3% Triton-X and 1% normal donkey serum. Biotinylated secondary antisera (Jackson Immunochemicals) were used at a dilution of 1:500.

Two sets of tissue sections from each rat were processed for localization of cFos protein using a rabbit antiserum provided by P. Larsen (1:50,000) and ABC immunoperoxidase procedures, as described previously (Rinaman et al., 1995). Sections were processed using a nickel sulfate-intensified DAB reaction to generate a blue-black cFos nuclear reaction product. One set of cFos-labeled tissue sections was subsequently processed for immunoperoxidase localization of FG (rabbit anti-FG; Chemicon; 1:30,000), while the second set was processed for localization of CTb (goat anti-CTb; List Biological Laboratories, Inc.; 1:50,000). Plain DAB

was used to generate a brown reaction product at the amygdalar FG and CTb injection sites, and in the cytoplasm of retrogradely labeled brainstem neurons.

For triple immunolabeling of retrograde tracer, cFos, and DβH, a third set of cFos-reacted tissue sections was incubated for 48 hrs in a cocktail of mouse anti-DβH (Chemicon; 1:3,000) and either rabbit anti-FG (1:3,000) or goat anti-CT (1:5,000). After buffer rinsing, sections were incubated for 2 hr in a cocktail of fluorescent-tagged secondary antisera (Cy^2–conjugated donkey anti-mouse IgG and either Cy^3–conjugated donkey anti-rabbit IgG or Cy^3–conjugated donkey anti-goat IgG), then rinsed in buffer.

After immunocytochemical staining, tissue sections were mounted onto Superfrost Plus microscope slides (Fisher Scientific), air dried, dehydrated and defatted in graded ethanols and xylene, and coverslipped using Cytoseal 60 (VWR).

Quantitative Analysis

Double immunoperoxidase-reacted sections were used for quantification of retrogradely labeled (CeA-projecting) neurons. Analysis was limited to three regions that provide adrenergic/noradrenergic inputs to the amygdala: the LC (pontine A6 cell group), the NST (medullary A2/C2 cell groups), and the caudal VLM (medullary A1/C1 cell groups). Counts of retrogradely labeled LC neurons were summed across rostrocaudal levels in each experimental case. Counts of retrogradely labeled NST and VLM neurons were grouped by rostrocaudal level: 1) caudal to the AP (caudal NST and VLM); 2) at the AP level (mid NST and VLM); and 3) rostral to the AP (rostral NST and VLM). A minimum of 4 coronal sections (spaced by 210 μm) through the LC and 10 coronal sections through the NST and VLM were analyzed in each rat that received at least one tracer injection accurately centered in the CeA (n = 9 rats; see

Results). FG- or CTb-positive neurons were counted bilaterally at 40x magnification. Criteria for counting a neuron as retrogradely labeled included the presence of brown cytoplasmic immunoreactivity, and a visible nucleus. Neurons were considered cFos-positive if their nucleus displayed any visible blue-black immunoreactivity, and cFos-negative if their nucleus was devoid of blue-black immunolabel. Cell counts thus obtained were used to determine the percentage of retrogradely labeled LC, NST, and VLM neurons that were activated after i.p. injection of vehicle or CCK. Regional differences in the proportion of CeA-projecting neurons activated after CCK were tested for statistical significance by using two-way ANOVA, with treatment group (control or CCK) and brain region (NST, VLM, or LC) as independent variables. When f values indicated a significant overall main effect of treatment group and brain region on cFos activation values, the ANOVA was followed up with planned t comparisons between treatment groups and brain regions. Differences were considered statistically significant when $P < 0.05$.

2.3. Results

Tracer injection sites and distribution of retrogradely labeled neurons

Nine rats had at least one tracer injection accurately centered in the CeA (Fig. 1). Of these, five were CCK-treated and four were vehicle controls (Table 1). So that each rat contributed only one set of data to the experimental analysis, we quantified labeling produced only by the most accurate tracer injection site in each case (results described below). In seven rats, FG produced the most accurate tracer injection, whereas CTb produced the most accurate injection in two rats. To varying degrees, amygdalar regions adjacent to the CeA (i.e.,

basolateral and medial subnuclei) were included within the outer boundaries of CeA-centered injection sites (see Fig. 1).

Retrogradely labeled neurons were present in the LC, NST, and VLM in all nine cases (Table 1, Figs. 2 and 3), although the absolute number of labeled neurons in each region varied among cases (Table 1). Counts of retrogradely labeled NST and VLM neurons in sections rostral to the AP were discontinued at the level at which the NST moves laterally away from the floor of the fourth ventricle, because labeled NST or VLM neurons were rarely observed at more rostral levels. Labeled neurons were present bilaterally in each brainstem region, with an ipsilateral predominance relative to the injection site. The largest number of retrogradely labeled NST and VLM neurons were found at rostrocaudal levels through the AP and just rostral to it (Fig. 3), consistent with previous reports (Zardetto-Smith and Gray 1990; Zardetto-Smith and Gray 1995; Roder and Ciriello 1993).

Five rats had tracer injection sites that were centered dorsal, ventral, medial, or lateral to the CeA. The outer boundaries of such injection sites extended into the CeA, but produced few or no retrogradely labeled neurons in the NST or VLM (i.e., 0-2 neurons per section). Conversely, the LC consistently contained retrogradely labeled neurons in all five cases. These observations are consistent with previous reports that retrograde tracer transport occurs primarily from the center of the tracer injection site, and that the NST and VLM selectively target the CeA (Zardetto-Smith and Gray 1990; Zardetto-Smith and Gray 1995; Roder and Ciriello 1993) whereas the LC innervates additional amygdala subnuclei (Nitecka et al., 1980).

Distribution of activated neurons after vehicle or CCK treatment

In agreement with our previous studies (Rinaman et al., 1993,1995), relatively few cFos-positive neurons were observed in the brainstems of vehicle-injected control rats. Quantitative analysis indicated that relatively low percentages of retrogradely-labeled NST, VLM, and LC neurons were activated in control rats (Table 1). One control case (#02-91) displayed an unusually high activation of CeA-projecting VLM neurons (14.8%) that was not duplicated in the other three control cases.

Robust cFos expression was observed within the NST, VLM, and several other brainstem and forebrain regions in CCK-treated rats, as previously reported (Day et al., 1994; Rinaman et al., 1993, 1995). Activation of retrogradely labeled NST and VLM neurons averaged 30.3% and 18.6%, respectively (Table 1). Conversely, activation of retrogradely labeled LC neurons averaged just 3.8% (Table 1).

Two-way ANOVA revealed a significant interaction between treatment group (vehicle vs. CCK) and brainstem region (NST, VLM, LC) in the proportion of activated, retrogradely-labeled neurons [$F(1, 2) = 14.8$, $P < 0.01$)]. Post-hoc t comparisons between treatment groups revealed that significantly larger proportions of retrogradely-labeled NST neurons were activated in CCK-treated rats compared to controls ($P< 0.001$). Treatment group differences in activation of retrogradely-labeled VLM neurons approached (but did not reach) statistical significance ($P = 0.056$). Activation of retrogradely-labeled LC neurons did not differ significantly between groups ($P = 0.31$).

Among the five CCK-treated rats, larger proportions of retrogradely labeled neurons were activated in the NST compared to the VLM or LC, and larger proportions of neurons in the VLM were activated compared to the LC ($P < 0.05$ for each comparison). When retrogradely labeled

NST and VLM neurons were grouped according to rostrocaudal level, and then summed across the five CCK-treated cases (Fig. 3), the proportion of activated neurons was found to be most prominent at "mid" and "rostral" levels of the NST (36% and 38%, respectively), and at "mid" and "caudal" levels of the VLM (24% and 26%, respectively).

Chemical phenotype of activated, retrogradely labeled NST and VLM neurons

Triple labeled tissue sections processed for localization of cFos, retrograde tracer, and DβH were examined qualitatively to determine the chemical phenotype of activated, CeA-projecting neurons. The apparent majority of retrogradely labeled NST and VLM neurons were DβH-positive, including those expressing cFos in CCK-treated rats (see Fig. 2).

2.4. Discussion

The CeA is implicated in the acquisition and expression of both autonomic (visceral) and somatic (behavioral) learned emotional responses. For example, the CeA contributes to the acquisition and expression of conditioned heart rate and behavioral "freezing" responses to threatening stimuli (LeDoux et al., 1988). It has been suggested that the most critical step of integration before the amygdala generates a behavioral response takes place within local CeA circuits (Pitkanen et al., 1997).

Emerging evidence indicates that enhancement or blockade of NE signaling processes in the amygdala can modulate the efficacy of conditioned learning and memory about emotionally arousing events (reviewed in Ferry et al., 1999). However, it has been unclear whether amygdala-projecting NE neurons are actually activated in natural or experimental conditions of emotional learning, and the extent to which different populations of NE neurons may be

involved. The present results indicate that a significant proportion of NST neurons and, to a lesser extent, VLM neurons innervating the amygdala are activated after CCK-induced stimulation of gastric vagal afferents. The apparent majority of these neurons are DßH immunopositive, identifying them as NE (or adrenergic) neurons. Although not quantified, the overall extent of cFos activation in DβH-positive neurons was similar to our previous studies in which systemic CCK activated approximately 50% of catecholaminergic neurons in the NST and 25% of those in the VLM, but few or none in the LC (Rinaman et al., 1993).

The NST receives and processes interoceptive information carried by vagal (and other) sensory afferents, and conveys this information to the amygdala and other forebrain regions via direct and indirect neural pathways (Ricardo and Koh 1978); the latter includes projections relayed through the VLM (Sawchenko and Swanson 1981). NST and VLM projection neurons are primarily catecholaminergic (Zardetto-Smith and Gray 1990, 1995; Rinaman et al., 1995; Roder and Ciriello 1993; Sawchenko and Swanson 1981), and stimulation of NST neurons leads to increased extracellular levels of NE in the amygdala (Clayton and Williams 2000; Williams et al., 2000). Extracellular NE levels in the amygdala also are elevated after vagal afferent stimulation with CCK (Kaneyuki et al., 1989). Thus, our results indicate that DβH-positive projection neurons in the NST (and perhaps the VLM) may be responsible for increased NE release in the amygdala after stimulation of viscerosensory pathways. Such pathways evidently include those that convey gastrointestinal signals, and also may include those that convey cardiovascular or other types of viscerosensory feedback.

We did not determine what subset of DβH-positive, CeA-projecting neurons in the NST and VLM were NE neurons, as opposed to adrenergic neurons; DβH immunolabeling identifies both populations. Previous studies addressed this issue by using tyrosine hydroxylase (TH) and

phenylethanolamine-*N*-methyltransferase (PNMT) immunolabeling combined with retrograde tracing from the CeA (Zardetto-Smith and Gray 1990, 1995; Roder and Ciriello 1993). The results indicated that the large majority of CeA-projecting neurons in the NST and VLM are catecholaminergic (TH-positive). Less than 10% of the NST projection neurons were identified as being adrenergic (PNMT-positive; Zardetto-Smith and Gray 1990), whereas larger proportions of VLM neurons projecting to the CeA are PNMT-positive (Zardetto-Smith and Gray 1995; Roder and Ciriello 1993). It is possible that NE and epinephrine exert different effects at adrenergic receptors in the CeA, but evidence for this is lacking. Thus, it currently is unclear whether parcellation of medullary NE and adrenergic projections to the CeA is functionally meaningful.

Results from several studies suggest that vagal afferents play a critical role in mediating the effects of interoceptive feedback signals on amygdalar mechanisms of emotional learning (Slaughter and Hahn 1974; Clark et al., 1998, 1999), and CCK appears to be a useful experimental tool with which to test this idea. CCK improves retention of inhibitory avoidance training in intact mice, but not in vagotomized mice (Flood et al., 1987), evidence that the memory-enhancing effect is mediated through vagal afferents. The effect also depends on intact afferent inputs to the amygdala (Flood et al., 1995). Other studies in rats indicate that systemic CCK improves performance in a variety of learning and memory tasks (Voits et al., 2001; Lemaire et al., 1994; Gerhardt et al., 1994). Although CCK injection is a pharmacological treatment that is unlikely to reproduce any normal physiological state, improved memory retention also has been reported after "natural" vagal stimulation, such as occurs when food-deprived mice receive a meal as a posttraining reinforcer (Flood et al., 1987). We previously reported that voluntary ingestion of a large, satiating meal in rats activates approximately the

same proportion of catecholaminergic NST neurons as are activated after systemic administration of CCK at the dose used in the present study (10 μg/kg), suggesting that this dose may stimulate gastric vagal afferents in a manner that is roughly equivalent to the stimulation produced by consumption of a large meal (Rinaman et al., 1998).

In summary, we have provided evidence that CeA-projecting, DβH-positive neurons in the caudal medulla are activated in rats after CCK-induced stimulation of vagal sensory afferents, whereas few or no CeA-projecting neurons in the pontine LC are activated. These results suggest that NE projection pathways arising from neurons in the NST (and perhaps the VLM) may play a key role in the modulatory effects of viscerosensory stimuli on emotional learning.

APPENDIX A: Chapter 2 Figures

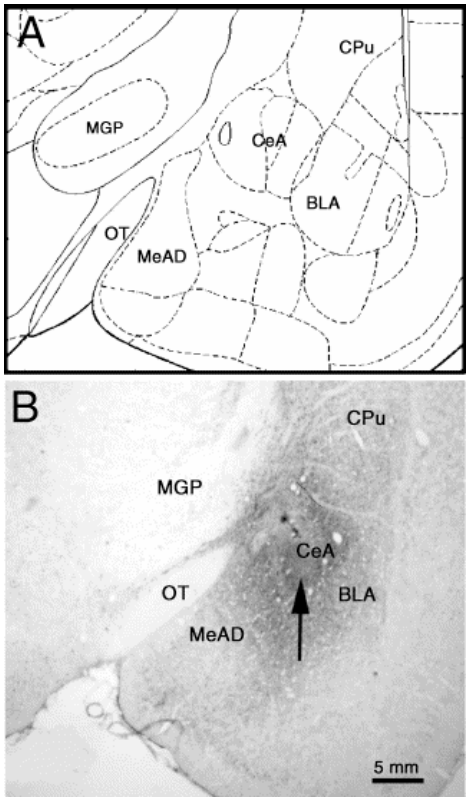

Figure 1. Illustration of an "accurate" tracer injection site into the central nucleus of the amygdala (CeA). (A) schematic of the CeA and surrounding regions (adapted from Paxinos and Watson 1997, corresponding to their level 28, 2.56 mm caudal to Bregma). (B) immunoperoxidase localization of FG in rat # 02-66 (see Table 1) in a tissue section closely matched to the schematic in panel A. The center of the injection site is indicated by an arrow. Retrograde labeling in this animal is illustrated in Figure 2A,B. MGP = medial globus pallidus; OT = optic tract; CPu = caudate putamen; BLA = basolateral nucleus of the amygdala; MeAD = anterodorsal medial nucleus of the amygdala.

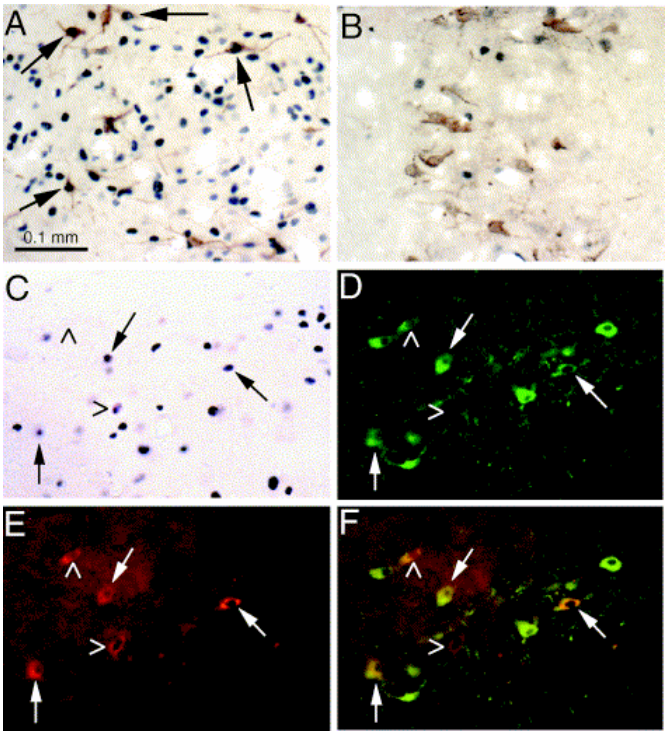

Figure 2. Retrograde labeling, cFos expression, and dopamine beta hydroxylase (DβH) immunolabeling of CeA-projecting neurons. Panels A and B depict labeling in rat # 02-66; see Figure 1 for the tracer injection site. Panels C-F are photomicrographs of a single tissue section through the NST (mid-AP level) from rat # 02-52, processed for triple immunocytochemical detection of cFos, CTb, and DβH. (A) retrograde labeling (brown cytoplasmic label) and cFos expression (blue-black nuclear label) in the NST at a level just rostral to the area postrema (AP). Arrows point out NST neurons that are retrogradely labeled with FG and activated to express cFos. The tracer injection site for this animal is shown in Figure 1. (B) Retrograde neuronal labeling of LC neurons, none of which are cFos-positive. In panels (C-F), arrows indicate triple-labeled neurons (i.e., retrogradely labeled with CTb, activated to express cFos, and DβH immunoreactive). ^ points out a retrogradely labeled, DβH-positive neuron that is not cFos immunoreactive. > points out a retrogradely labeled, cFos-positive neuron that is not DβH immunoreactive. (C) CCK-induced cFos expression. (D) DβH (green fluorescent) immunolabeling. (E) Retrogradely labeled (CTb-positive; red fluorescent) neurons. (F) Double exposure photomicrograph of DβH and CTb immunolabeling. Scale bar in A applies to all panels.

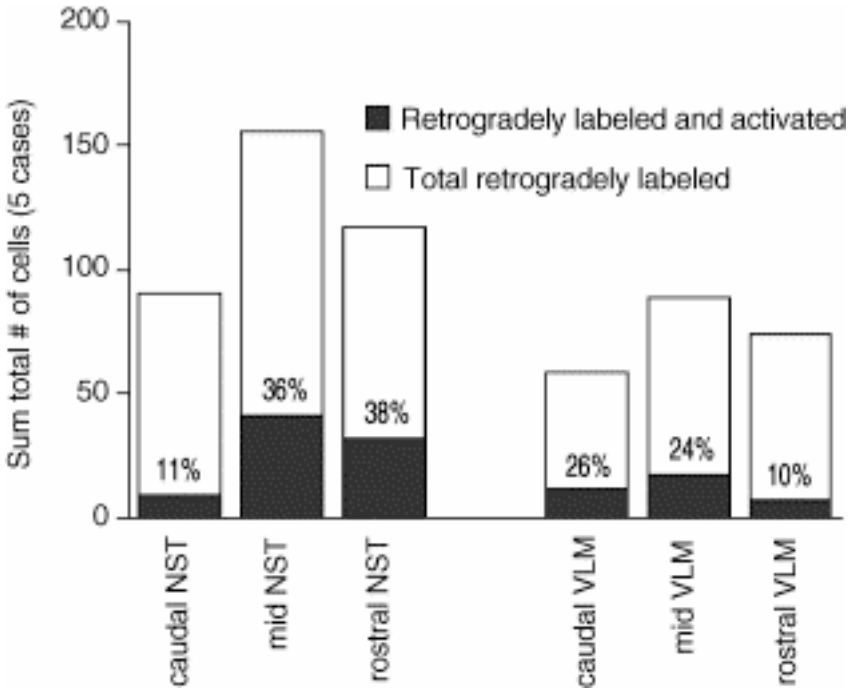

Figure 3. Summary of quantitative data for NST (A2/C2 region) and VLM (A1/C1 region) labeling at three rostrocaudal levels in CCK-treated rats. Each set of bars represents the total number of labeled neurons summed across all five experimental cases. Caudal NST and VLM counts were made in tissue sections caudal to the area postrema (AP). Mid NST and VLM counts were made in sections through the level of the AP. Rostral NST and VLM counts were made in sections rostral to the AP (see text). The % values indicate the proportion of all retrogradely neurons counted in each region that were cFos-positive.

Table 1. Treatment-induced activation of retrogradely-labeled brainstem neurons projecting to the CeA.

Rat	Activated neurons (% activated/total retrogradely labeled)		
	NST	VLM	LC
Vehicle treatment			
#02-91	5.9/68	14.8/27	8.6/35
#02-92	0/23	0/6	6.3/16
#02-104	6.7/15	0/24	4/99
#02-105	1.1/88	3.6/83	7.4/68
Mean±S.E.	3.4±1.7% (out of 194)	4.6±3.5% (out of 140)	6.6±1.0% (out of 218)
CCK treatment			
#02-52	28.6/42	17.9/39	10/10
#02-54	29.2/48	7.1/42	0/42
#02-64	30.3/33	22.2/9	9/55
#02-65	26.7/116	31.7/60	0/4
#02-66	36.6/41	13.9/36	0/24
Mean±S.E.	30.3±1.7% (out of 280)	18.6±4.1% (out of 186)	3.8±2.3% (out of 135)

3. Chapter 3: The Predator Odor Trimethylthiazoline Supports Conditioned Flavor Avoidance and Activates Brainstem Noradrenergic Neurons, Hypothalamic CRH Neurons, and Ascending Inputs to the Central Nucleus of the Amygdala in Rats

The ability of interoceptive stimuli to activate the HPA axis and modulate emotional state is mediated, in part, by recruitment of noradrenergic (NA) inputs to the hypothalamus and limbic forebrain. It is unclear whether similar pathways are recruited during responses to emotionally significant exteroceptive stimuli, such as predator odors. The present study investigated behavioral conditioned avoidance responses and central activation of neural cFos expression in rats after exposure to trimethylthiazoline (TMT; isolated from fox feces) or a novel control odor (banana extract, BE). Experiment 1 demonstrated that rats avoid consuming novel flavors that previously were paired with TMT exposure, but do not avoid consuming flavors previously paired with BE. Experiment 2 investigated potential neural correlates for the unique ability of TMT to support conditioned flavor avoidance. Naïve rats were exposed to low or high levels of either TMT or BE, then were perfused with fixative 60-90 minutes later. In a subset of rats, retrograde neural tracers were microinjected into the central nucleus of the amygdala (CeA) 7-10 days before acute odor exposure and perfusion. Brainstem and forebrain sections were processed for immunocytochemical localization of cFos and either dopamine beta hydroxylase to identify NA neurons, corticotropin-releasing hormone (CRH), or retrograde neural tracer. Exposure to high levels of TMT or BE activated significantly greater cFos expression by NA neurons in the nucleus of the solitary tract (NST), ventrolateral medulla (VLM), and locus coeruleus (LC) compared to activation in rats after exposure to low levels of each odorant. Compared to activation after the high BE exposure condition, high TMT activated significantly greater proportions of discretely localized NA neurons within the NST and VLM, LC NA neurons, hypothalamic CRH neurons, and CeA neural inputs arising from the NST and lateral

parabrachial nucleus. We propose that the unique ability of TMT to support conditioned avoidance responses in rats is related to its ability to recruit neural activation in viscerosensory regions of the caudal medulla and pons, including neurons that project directly to the CeA.

3.1. Introduction

Stress and anxiety responses in humans and animals include somatic, autonomic, and neuroendocrine components, and can be induced by a wide variety of interoceptive and exteroceptive stimuli under natural and experimental conditions. There has been a recent shift to implement more ethologically relevant stress and anxiety paradigms in animal studies designed to probe the central neural mediation of relevant behavioral and physiological responses (discussed in Dielenberg et al., 2001). Olfactory cues, for example, exert a powerful influence on behavior in rodents; thus, odors such as trimethylthiazoline (TMT) may provide an appropriate experimental model with which to examine stress and anxiety responses in rats. TMT is a volatile sulfur-containing compound isolated from the feces of the fox, a natural predator of rats. A growing number of behavioral studies suggest that in addition to being repugnant, TMT may serve as a partial predator stimulus to rats. Acute or repeated exposure of laboratory rats to TMT elicits unconditioned freezing responses indicative of fear (Wallace and Rosen 2000; Fendt et al. 2003), reduces food intake (Burwash et al., 1998), and elevates plasma corticosterone levels (Perrot-Sinal et al., 1999; Morrow et al., 2000). TMT also elicits strong avoidance responses in wild rats that are naïve to foxes (Vernet-Maury et al., 1984). It is unclear, however, whether olfactory stimuli such as TMT can serve as unconditioned stimuli (US) for conditioned avoidance responses, as has been demonstrated for other types of stressful, aversive, and/or anxiogenic treatments in rats (i.e., lithium chloride, electric shock, etc.).

The present study demonstrates that TMT can serve as an olfactory US to support the formation of conditioned flavor avoidance (CFA) in rats, whereas CFA is not observed after similar exposure of rats to a novel but presumably non-aversive control odor, banana extract (BE). We then compare central patterns of neural cFos protein expression in rats after acute exposure to TMT or BE, with a specific focus on odor-induced recruitment of brainstem NA

neurons, hypothalamic CRH neurons, and brainstem inputs to the central nucleus of the amygdala (CeA).

3.2. Materials and Methods

Animals

Adult male Sprague-Dawley rats (Harlan Laboratories; 250-320 g BW) were used. Rats were housed singly in stainless steel cages in a controlled environment (20-22°C, 12:12 h light:dark cycle; lights on at 0700 hr) with ad libitum access to water and pelleted chow (Purina 5001).

Experiment 1: Conditioned Flavor Avoidance (CFA)

A sensitive two-bottle choice procedure (Deutsch and Hardy, 1977) was used to determine whether acute exposure to TMT (Experiment 1A) or a novel control odor (BE; Experiment 1B) supports the formation of CFA. CFA training and testing was conducted during the light cycle of the photoperiod, between 1500 and 1700 hr.

Experiment 1A: TMT exposure. A group of 6 naïve adult male rats (~300 g BW) underwent 22 hr water deprivation, then were transported to a quiet training/testing room and acclimated to novel plastic test chambers (46 x 25 x 20 cm) with a wire cage top and white Sani-Chip bedding material. Half of the rats were presented with almond flavored tap water to drink from a graduated tube, and the others with vanilla flavored water (both 0.5% McCormick flavor extract). The left-right position of the bottle on each training/testing cage was switched after 15 min, with cumulative fluid intakes recorded at 15 and 30 min. Rats remained in the training/testing room for 45 min after the end of fluid access; this training day provided the "non odor-paired flavor" condition. Rats then were returned to their home cages and 24 hr of water ad

libitum. Rats were then water deprived again for 22 hr, transported to the training/testing room, and placed into test chambers containing milled corn-cob bedding material, where they were allowed to drink the alternate flavor (i.e., vanilla or almond) for 30 min with bottle position on the cage switched after 15 min. Thirty minutes after the end of fluid access, rats were exposed to TMT (PheroTech Inc.; 40 µl neat pipetted onto filter paper on top of the wire cage top) for 15 min. This provided the "TMT-paired flavor" condition. Rats were then returned to their home cages and 24 hr of water ad libitum. Rats were then water deprived again for 22 hr, transported to the training/testing room and given 30-min simultaneous access to two bottles containing almond and vanilla flavored water. A 50-50 mixture of Sani-Chips and corn-cob bedding material was present during this two-bottle choice test. The volume of each flavor consumed was recorded at 15 min, bottle positions switched, and cumulative intake recorded at 30 min. Rats then were returned to their home cages with ad libitum water access for four days.

Experiment 1B: BE exposure. Four days after completing the TMT exposure experiment described above, the CFA training and testing procedure was repeated using the same group of rats (n=6), but using different novel flavors (i.e., 0.5 % McCormick coconut or brandy extract) in the "no-odor paired flavor" and "BE-paired flavor" conditions.

CFA data analysis: Within each CFA experiment, flavor preference ratios displayed by each rat were determined by dividing the volume consumed from each bottle during the 30-min choice test by the total volume consumed from both bottles. Outcomes indicating flavor preference ratios that do not differ significantly (i.e., close to 50%:50%) are interpreted as an absence of CFA, whereas outcomes indicating significantly shifted preference ratios (i.e., 30%:70%) are interpreted as evidence for conditioned avoidance of the flavor pairing condition represented by the lower value in the ratio. Individual rat preference ratio data were averaged to

obtain group preference ratios (mean ± SE) for no-odor paired flavors relative to odor-paired flavors within each experiment. Student's t-test was used to determine whether group preference ratios for odor-paired and non-odor paired flavors were statistically different, with significance set at $P < 0.05$.

Experiment 2: Odor-Induced cFos Expression

New groups of rats naïve to TMT or BE were acclimated to daily handling for approximately one week. On the day of odor exposure and sacrifice, rats were placed individually in novel 19 x 29 x 13 cm plastic cages with a wire top, transported to a new location within the building, and then exposed for 15 min to either TMT or BE. Distinct odor conditions were used on different days to avoid odor contamination across treatment groups. In each case, 40 µl of TMT (PheroTech Inc.) or BE (McCormick brand; local supermarket) was pipetted onto a small piece of filter paper placed onto the wire top of each cage. To determine whether odorant concentration (i.e., exposure level) affected observed patterns of neural activation, odor exposure was carried out under two conditions: 1) cages were placed in a quiet area located immediately adjacent to an operating fume hood (low odor exposure condition) or 2) cages were placed in a quiet area without a fume hood (high odor exposure condition). After 15 min of odor exposure, filter papers were removed from the cage tops and rats were returned to their home cages in the animal facility. Rats were left undisturbed in their home cages for 90 min, then were anesthetized and perfused transcardially with fixative (described below). After each odor exposure session, cages and wire tops were cleaned thoroughly with a germicidal detergent and deodorant (Quatricide PV; Pharmacal Research Laboratories, Inc) and allowed to air dry for at least 24 hr before re-use in order to reduce residual odor traces.

Perfusion and tissue preparation

Rats were anesthetized with sodium pentobarbital (Nembutal; 50 mg i.p.) and perfused transcardially with 50-100 ml of 150 mM NaCl followed by 500 ml of fixative solution (4% paraformaldehyde in 0.1 M phosphate buffer with lysine and sodium metaperiodate;(McLean and Nakane 1974). Brains were post-fixed overnight at 4˚C, then blocked and cryoprotected in aqueous 20% sucrose prior to sectioning.

Neural tracer injections

A subset of rats received bilateral, stereotaxically guided microinjections of retrograde neural tracer into the CeA 7-10 days prior to odor exposure and perfusion. For tracer injections, rats were anesthetized with halothane (Halocarbon Laboratories; 1-3% in oxygen) and mounted into a stereotaxic frame. Two retrograde tracers were used: FluoroGold (FG, Fluorochrome, Inc; 2% in 150 mM NaCl) and cholera toxin, beta subunit (CTb, List Biological Laboratories; 0.25% in 150 mM NaCl). Rats received FG injections targeted to the left CeA and CTb injections targeted to the right CeA. The dual tracer injection procedure increased the chance of obtaining at least one accurate tracer injection site in each rat. A 1.0-µl Hamilton syringe filled with either FG or CTb was attached to the stereotaxic arm. CeA coordinates (2.2 mm posterior, 4.0 mm lateral, and 8.2 mm ventral to bregma) were selected based on a standard rat brain atlas (Paxinos and Watson 1997). The syringe was lowered into the brain and was left in place for 5 min prior to injection. FG (50 nl) or CTb (100-150 nl) was delivered by manual pressure over a 1-2 minute period. The syringe was left in place for an additional 7 min after each injection to reduce tracer diffusion up the needle tract. The skin was closed with stainless steel clips, 2% lidocaine was applied to the incision site, and rats were returned to their home cages after

recovery from anesthesia. Rats were given 7-10 days to recover from surgery prior to acute odor exposure, described above.

Histology and immunocytochemistry

Coronal 35-μm tissue sections were cut from the caudal extent of the NST through the rostral extent of the corpus callosum using a freezing microtome. Sections were collected serially in six adjacent sets and stored at –20°C in cryopreservent (Watson et al., 1986). Sections were removed from storage and rinsed for 1 h in buffer (0.1 M sodium phosphate, pH 7.4) prior to immunocytochemical procedures. Antisera were diluted in buffer containing 0.3% Triton-X and 1% normal donkey serum. Biotinylated secondary antisera (Jackson Immunochemicals) were used at a dilution of 1:500.

Tissue sections were processed for localization of cFos protein using a rabbit polyclonal antiserum (1:50,000; provided by Dr. Philip Larsen, Denmark) and Vectastain Elite ABC immunoperoxidase reagents (Vector Laboratories). The specificity of this antibody for cFos protein has been reported (Rinaman et al., 1997). Sections were processed using a nickel sulfate-intensified DAB reaction to generate a blue-black cFos reaction product in the nuclei of activated cells. In tracer-injected rats, two sets of cFos-labeled tissue sections were subsequently processed for immunoperoxidase localization of FG (rabbit anti-FG: Chemicon; 1:30,000) or CTb (goat anti-CTb; List Biological Laboratories; 1:50,000). DAB was used to generate a brown reaction product at the amygdalar FG and CTb injection sites, and in the cytoplasm of retrogradely labeled neurons. Other sets of cFos-labeled tissue sections were processed for immunoperoxidase localization of CRH (rabbit anti-CRH, 1:15,000; Penninsula) in the forebrain and the NA synthetic enzyme, DβH (mouse anti-DβH, 1:30,000; Chemicon), in the brainstem.

After immunocytochemical processing, tissue sections were mounted onto Superfrost Plus microscope slides (Fisher Scientific), allowed to air dry overnight, dehydrated and defatted in graded ethanols and xylene, and coverslipped using Cytoseal 60 (VWR).

Quantitative analysis

Dual immunoperoxidase-labeled tissue sections were analyzed with a light microscope to determine the number and proportions of phenotypically identified neurons activated to express cFos. Criteria for counting a neuron as retrogradely labeled (i.e., CTb- or FG-positive), DβH-positive, or CRH-positive included the presence of brown cytoplasmic immunoreactivity and a visible nucleus. Neurons were considered cFos-positive if their nucleus contained visible blue-black immunoreactivity, regardless of intensity, and cFos-negative if their nucleus was unlabeled. Cell counts thus obtained were used to determine the percentage of phenotypically identified neurons that were activated in each experimental case.

The distribution of CRH-positive PVN neurons and the proportion activated to express cFos in each rat was documented at 100x magnification using oil immersion with the assistance of Stereo Investigator X-Y plotting software (MicroBrightField, Inc). CRH-positive neurons in the PVN were summed bilaterally and averaged in each rat across two sections spaced 210 □m apart that contained the highest density of CRH neural labeling. Activated CRH neurons (i.e., those with nuclear cFos labeling) were expressed as a percentage of the total number of CRH-positive neurons counted within the PVN.

Quantitative analysis of cFos expression by retrogradely labeled neurons and DβH-positive NA neurons was limited to brainstem regions that provide direct input to the CeA, including the pontine LC (location of the A6 NA cell group), the lateral parabrachial nucleus, the

nucleus of the solitary tract (location of the A2/C2 cell groups), and the caudal ventrolateral medulla (location of the A1/C1 cell groups). Retrogradely labeled or DβH-positive neurons were counted bilaterally in each region at 40x magnification. In each rat, counts of activated DβH-positive neurons in the LC were summed bilaterally within each region across 6-11 tissue sections spaced 210 μm apart. Retrogradely labeled neurons within the external portion of the lateral parabrachial nucleus (PBN) were summed unilaterally and averaged over two sections spaced 210 μm apart that contained the highest density of retrograde labeling ipsilateral to the CeA tracer injection site in each rat. Counts of retrogradely labeled and DβH-positive NST and VLM neurons were grouped according to 3 rostrocaudal levels of the visceral NST defined with respect to the area postrema (AP): (1) sections caudal to the AP (caudal NST and VLM); (2) sections at the level of the AP (mid NST and VLM); and (3) sections rostral to the AP (rostral NST and VLM). Retrogradely labeled NST and VLM neurons were counted at the same rostrocaudal levels at which activation of NA neurons was assessed. Counts in rostral sections were discontinued at the level at which the NST moves laterally away from the floor of the fourth ventricle. Statistical comparisons were examined by either 2- or 3-WAY ANOVA. When f values indicated significant overall main effects of treatment group and/or brain region, the ANOVA was followed up with selected comparisons of interest using planned t-tests. Differences were considered statistically significant when $P < 0.05$.

3.3. Results

Behavioral observations during odor exposure

We qualitatively observed behavioral responses by rats to TMT and BE in both the CFA paradigm and terminal cFos studies. These behavioral observations were not monitored

throughout the course of the 15 min odor exposure session in an effort to prevent placing further stress on the animals, but were assessed at the onset and conclusion of each experiment. In all odor exposure sessions, rats reliably approached the odor source (filter paper) at the onset of the exposure session; however, at the conclusion of the experiment rats exposed to TMT showed pronounced freezing and avoidance behavior that was not observed with BE exposure. Furthermore, freezing and avoidance responses were observed during both the "low" and "high" TMT exposure paradigms.

Experiment 1: Conditioned Flavor Avoidance (CFA)

CFA data from Experiments 1A and 1B were analyzed separately by Student's t test to determine whether there were significant differences between group mean preference ratios for non odor-paired flavors vs. TMT-paired flavors (Experiment 1A), and for non odor-paired flavors vs. BE-paired flavors (Experiment 1B). Results from Experiment 1A revealed a significant preference of rats for non odor-paired flavors compared to TMT-paired flavors (Fig. 4A). Fluid intake in the 30 min two bottle choice test consisted of 12.0 ± 1.3 ml of the non odor-paired flavor and 6.7 ± 1.9 ml of the TMT-paired flavor ($P < 0.05$), evidence for a relatively strong CFA response to TMT. Conversely, results from Experiment 1B revealed no evidence for conditioned avoidance of BE-paired flavors (Fig. 4B). Fluid intake in the 30 min two bottle choice test consisted of 9.7 ± 1.6 ml of the non odor-paired flavor and 10.5 ± 1.7 ml of the BE-paired flavor (difference not significant).

Experiment 2: Odor-induced activation of phenotypically identified neurons

DβH-positive NA neurons

Medulla

NST (A2/C2 cell groups): Three-way repeated measures ANOVA revealed significant main effects (between subjects) of odor intensity (low vs. high) [$F(1,30) = 154$, $P < 0.05$] and odor type (BE vs. TMT) [$F(1,30) = 5.4$, $P < 0.05$] on activation of NA neurons in the NST, with high exposure levels of TMT and BE activating significantly more NA neurons per tissue section than low exposure levels of the corresponding odorants (Fig. 5A). There was no significant interaction between odor intensity and odor type. Within subjects, there was a significant effect of rostrocaudal level (cNST, mNST, rNST) [$F(2,60) = 43.5$, $P < 0.05$] and a significant interaction between odor intensity and NST rostrocaudal level on NA neuron activation [$F(2,60) = 30.6$, $P < 0.05$]. There was no significant interaction between odor type and rostrocaudal level. At all 3 rostrocaudal levels of the NST, activation of NA cells was significantly greater in rats after low TMT exposure compared activation after low BE exposure (Fig. 5A). Interestingly, however, activation of NA cells within the NST was similar in rats after high BE and high TMT exposure, with the exception of significantly greater activation of NA neurons in the rNST after high TMT compared to high BE (Fig. 5A). Figure 7 shows representative photomicrographs of cFos activation within the mNST in rats after exposure to TMT at low levels (Fig. 7A) or high levels (Fig. 7D).

VLM (A1/C1 cell groups): Similar to the NST results described above, three-way repeated measures ANOVA revealed significant main effects (between subjects) of odor intensity (low vs. high) [$F(1,31) = 358.87$, $P < 0.05$] and odor type (BE vs. TMT) [$F(1,31) = 19.16$, $P < 0.05$] on NA neuron activation in the VLM, with high exposure levels of TMT and

BE activating significantly more NA neurons per tissue section than low exposure levels of the same odorants (Fig. 5B). No significant interactions were observed between odor intensity level and odor type. Within subjects, there was a significant effect of rostrocaudal level (cVLM, mVLM, rVLM) [$F(2,62) = 11.68$, $P < 0.05$] and a significant interaction between odor intensity and VLM rostrocaudal level on NA neuron activation [$F(2,62) = 3.58$. $P < 0.05$]. There was no significant interaction between odor type and rostrocaudal level. High BE exposure increased NA cell activity within the VLM to a degree similar to high TMT exposure, with the exception of significantly greater activation in the mVLM after high TMT (Fig. 5B). Activation of NA cells within the cVLM was significantly greater in rats after exposure to low TMT compared to activation after low BE, whereas activation in the mVLM and rVLM was similar in these two treatment groups (Fig. 5B). Figure 7 shows representative photomicrographs of cFos activation within the mVLM in rats after exposure to TMT at low levels (Fig. 7B) or high levels (Fig. 7E).

Pons

LC (A6 cell group): Two-way ANOVA revealed significant main effects of odor intensity (low vs. high) [$F(1,30) = 60.1$, $P < 0.05$] and odor type (BE vs. TMT) [$F(1,30) = 6.68$, $P < 0.05$] on cFos expression by NA neurons within the LC. A possible interaction between odor intensity and odor type approached but did not reach statistical significance [$F(1,30) = 3.6$, $P = 0.067$]. Post hoc *t* comparisons revealed that significantly more NA cells were activated in rats after high BE and high TMT exposure compared to activation after low exposure levels of the same odorants (Fig. 6; $P < 0.05$ for each comparison). Figure 7 shows representative photomicrographs of cFos activation within the LC in rats after exposure to TMT at low levels (Fig. 7C) or high levels (Fig. 7F).

Activation of CRH-positive PVN neurons

Two-way ANOVA revealed significant main effects of odor intensity (low vs. high) [$F(1,23)=57.38$, $P < 0.05$] and odor type (BE vs. TMT) [$F(1,23)=14.27$, $P < 0.05$], and a significant interaction between odor intensity and type in the proportion of CRH neurons in the mpPVN activated to express cFos [$F(1,23)= 9.52$, $P < 0.05$]. Post hoc *t* comparisons revealed that high BE and high TMT exposure activated significantly greater proportions of CRH neurons compared to activation after low levels of the same odorants ($P < 0.05$ for each comparison; Fig. 8). Relatively few cFos-positive neurons were observed within the medial parvocellular PVN in rats after exposure to low levels of BE or TMT, and there was no significant difference between these groups in the proportion of CRH neurons expressing cFos (Fig. 8). Exposure to high levels of TMT produced robust cFos expression within CRH-positive PVN neurons that was significantly greater than all other treatment groups, including activation after high BE (Fig. 8). Figure 9 shows representative photomicrographs of cFos expression by CRH-positive PVN neurons in rats after exposure to low or high levels of BE or TMT.

cFos expression in additional brain regions

As previously reported in other studies using predator-related stimuli (reviewed in Blanchard 2003; Dielenberg 2001), the following brain regions showed a relative increase in cFos expression after high TMT exposure: piriform and dorsal endopiriform cortices, interpeduncular nucleus, dorsal and ventral premammillary nuclei of the hypothalamus, paraventricular thalamus, lateral septum, median preoptic area, medial amygdala, central nucleus of the amygdala (Fig. 10), and the fusiform nucleus, and to a lesser extent, the oval nucleus of the BNST (Fig. 11). Though these data were only qualitative observations, it was apparent that

high TMT exposure activated many more neurons compared to all other odors in this study. More moderate cFos expression was observed after high BE compared to low BE in these same regions, but not to the extent seen with high TMT.

Tracer injection sites and distribution of retrograde labeling

Analysis of tracer injection sites revealed that 23 rats had at least one injection accurately targeted to the center of the CeA (high TMT, n = 5; high BE, n = 8; low TMT, n = 7; low BE, n=3). FG produced the most effective retrograde labeling in the majority of rats. To varying degrees, amygdalar regions adjacent to the CeA (i.e., the basolateral and medial nuclei) generally were included within the outer boundaries of CeA-centered tracer injection sites. A typical tracer injection site is illustrated in Chapter 2 (see Fig. 1). Although these extra-CeA regions do not receive direct neural input from the NST or VLM (Myers and Rinaman 2002), neural tracer diffusing to these sites could contribute to some degree of retrograde labeling observed within the LC.

Retrogradely labeled neurons were present within the NST, VLM, and LC in all 23 cases, although the absolute number of labeled neurons in each region varied among cases. Robust retrograde labeling also was observed in lateral and medial subdivisions of the pontine PBN, although double-labeled (i.e., cFos-positive) neurons were present only within the lateral PBN (see below). Retrogradely labeled neurons were present bilaterally in all 4 brainstem regions, with an ipsilateral predominance relative to the side of tracer injection. No clear trends in the number of retrogradely-labeled NST or VLM neurons or in the proportion activated to express cFos were observed at different rostro-caudal levels of the NST or VLM, and so NST and VLM cell counts were collapsed within each experimental case.

Quantitative analysis of activated brainstem inputs to the CeA

Three-way repeated measures ANOVA revealed significant main effects (between subjects) of odor intensity (low vs. high) [$F(1,19) = 130.74$, $P < 0.05$] and odor type (BE vs. TMT) [$F(1,19) = 50.5$, $P < 0.05$] on odor-induced activation of retrogradely labeled brainstem neurons, but no significant interaction between odor intensity and type. Within subjects, there was a significant main effect of brain region (NST, VLM, LC, or PBN) [$F(3,57)=56.32$, $P < 0.05$] and significant interactions between odor intensity and region [$F(3,57)=14.67$, $P < 0.05$] and between odor type and region [$F(3,57)=6.74$, $P < 0.05$] on the proportion of retrogradely labeled brainstem neurons activated to express cFos. There also was a significant three-way interaction between odor intensity, odor type, and brain region [$F(3,57)=5.0$, $P < 0.05$]. Post hoc *t* comparisons revealed that significantly larger proportions of retrogradely labeled NST, VLM, and LC neurons were activated in rats exposed to high BE or high TMT compared to activation in rats exposed to low levels of the same odors ($P < 0.05$ for each comparison; Fig. 12). Low TMT exposure activated a significantly larger proportion of retrogradely labeled neurons compared to low BE in all brainstem regions except the lateral PBN, where the difference approached but did not achieve statistical significance. High TMT exposure activated a significantly larger proportion of NST and PBN neurons compared to high BE exposure (Fig. 12), whereas activation of retrogradely labeled neurons within the VLM and LC was not significantly different between rats exposed to high levels of TMT or high levels of BE. Figure 13 shows representative photomicrographs of activated CeA inputs within the NST and LC in rats after exposure to TMT at low levels (Fig. 13A, B) or high levels (Fig. 13C, D).

3.4. Discussion

Several research groups have reported that exposure to TMT, a volatile chemical component of fox feces, elicits innate behavioral responses in rats that are indicative of fear and anxiety. These include increased freezing and avoidance behaviors, and reduced nondefensive behaviors such as grooming and exploration (Morrow et al., 2002; Wallace and Rosen 2000; Wallace and Rosen 2001; Fendt et al. 2003). Furthermore, TMT exposure activates the HPA axis in rats, as evidenced by increased serum levels of adrenocorticotropic hormone (ACTH) and corticosterone (CORT) that parallel increases observed in other well-established models of stress and anxiety (Morrow et al, 2000; Vernet-Maury et al., 1999; 1984). The present study is the first to demonstrate that TMT can serve as an unconditioned stimulus to support conditioned flavor avoidance, and the first to report neuroanatomical data regarding central neural circuits activated by this odorant. We demonstrate that TMT exposure activates CRH neurons at the apex of the HPA axis in a concentration-dependent manner, and elicits a unique activation profile of brainstem NA cell populations, including those that provide direct afferent input to the CeA.

Odor Exposure Paradigm. The experimental testing environment may play a significant role in shaping the behavioral and neural responses to various predator-related cues. Consequently, rats in our study were not acclimated to the odor exposure environment as one previous study reported that rats were less responsive to TMT when it was presented in a familiar environmental context (Morrow et al., 2002). Furthermore, behavioral responses to predator odors, such as TMT, appear to depend on the size of the testing chamber. Accordingly, several studies report robust freezing responses when rats are exposed to TMT in a small-enclosed environment (Hotsenpillar and Williams 1997; Wallace and Rosen 2000, 2001; Fendt et al. 2003) whereas other studies have failed to note observable freezing responses in rats confronted

with TMT (Perrot-Sinal et al., 1999; Morrow et al., 2000; McGregor et al., 2002). Importantly, the studies which did not observe freezing responses implement a much larger testing chamber in which the rats can easily move to the opposite side of the chamber and create sufficient distance from the odor source to reduce its intensity. For example, several studies using cat odor exposure (McGregor et al., 2002; Dielenberg and McGregor 2001) give odor-exposed rats the opportunity to retreat to a "hide box" at the opposite side of the experimental chamber. Therefore, escape responses (i.e., retreating to a hide box) may serve as an appropriate behavioral response to a predator cue when the environment is conducive to it, whereas freezing responses may become more advantageous to rats when the predator cue is inescapable (i.e., in small-enclosed environments).

Aversive Nature of TMT. Conflicting reports have described TMT as a predator odor that evokes unconditioned fear and/or anxiety responses in rats, or as a repugnant odor that is aversive to rats without necessarily producing fear responses. The fact that TMT exposure supported the formation of a relatively strong CFA response, and exposure to a novel control odor (BE) clearly did not, suggests that this odor compound is highly aversive to rats, although the specific properties which make it aversive cannot be identified based on our experimental findings. Moreover, while TMT and BE exposure evoked similar initial exploratory behavior and approach to the odor source, we qualitatively observed profound freezing and avoidance behavior by TMT-exposed rats at the conclusion of the experiment that was not seen with the BE exposure. This observation is consonant with other reports and is indicative of fear (Morrow et al., 2002; Wallace and Rosen 2000; Wallace and Rosen 2001; Fendt et al. 2003).

Comparison of TMT and BE. The control odor used in this study (BE) was selected based on its qualitatively similar potency (to human observers) and on our unpublished observations that rats do not avoid close contact with BE or avoid drinking water that has been flavored with BE. Nevertheless, exposure of odor-naiive rats to high levels of BE produced a statistically significant increase in the proportion of CRH neurons activated to express cFos compared to activation in rats after exposure to low levels of BE. These findings highlight that the novelty of the odor likely contributed to the behavioral and neural responses observed in this study. It is important to note, however, that CRH activation in rats after high BE reached only half the magnitude of CRH activation in rats after high TMT exposure; therefore, TMT elicited a significantly greater response of neurons at the apex of the HPA axis, an index of the stressful nature of TMT exposure.

Similarly, although NA neurons within most regions of the NST and VLM were activated to a similar extent after exposure of rats to high BE or high TMT, TMT recruited a significantly larger number of NA cells within the LC (A6 cell group). The LC is known to provide widespread input to many subcortical and cortical brain regions, several of which showed increased cFos expression following TMT exposure in the present study. Interestingly, these brain regions included areas that are implicated in defensive and/or aggressive behavior. Therefore, the apparently selective response of the LC to TMT may reflect heightened arousal associated with this aversive predator cue whereas other similarities in NA cell activation observed in the NST and VLM may reflect odor novelty and/or intensity level regardless of the odor's potential behavioral significance.

TMT-Induced Activation of Inputs to the CeA. There is growing evidence to suggest that NA transmission in the amygdala plays a central role in integrating somatic and visceral responses during adaptive responses to stress, and is important for conditioned learning and the encoding of memories for emotionally provoking experiences (Clayton and Williams 2000; Williams et al., 2000; Zardetto-Smith and Gray 1990). However, it is currently unclear whether amygdalar-projecting NA projections are actually activated by an unconditioned aversive odor stimulus. Interestingly, in the low exposure paradigm, TMT recruited a greater proportion of afferent inputs to the CeA arising in the NST, VLM, and LC compared to the control banana odor. However, in the high exposure paradigm, the differential effect of TMT was observed only within the NST and the PBN. Thus, TMT may recruit a specific CeA-projecting pathway arising in the NST or PBN. The observed TMT-induced increases in cFos expression in both the CeA and external lateral PBN, as well as the activation of CeA inputs arising from this region, correspond with the observed CFA response to TMT, as CFA responses are dependent on involvement of both of these structures and the connections between them (Lasiter and Glanzman 1985; Lamprecht and Dudai 1996; Yamamoto et al., 1997; Sakai and Yamamoto 1998; Grigson et al., 1998; Reilly 1999; Wang and Chambers 2002).

We did not determine the neurochemical phenotypes of CeA-projecting neurons in this study, but previous reports indicate that CeA-projecting neurons within the NST are primarily noradrenergic (A2 cell group) and located within cNST and mNST levels described in the present study. Conversely, VLM projections to the CeA arise primarily from adrenergic cells of the C1 group (Zardetto-Smith and Gray 1990, 1995), corresponding in the present study to the rostrocaudal level described as rVLM. CeA-projecting neurons arising from the PBN are

primarily calcitonin-gene related peptide (CGRP)-positive (Schwaber et al., 1988). Accordingly, TMT exposure activated CGRP-positive neurons in PBN in the present study (data not shown). Interestingly, we qualitatively observed increased cFos expression in both the CeA and the medial amygdala (MeA). While increased cFos expression in the MeA has been reported in other studies using the cat odor paradigm, the CeA is not reported to show increased cFos expression in these studies (Dielenberg et al., 2001; Dielenberg and McGregor 2001). As previously discussed, in several studies where rats were given the option to retreat to a "hide box," the rats showed negligible freezing response (Dielenberg and McGregor 2001; McGregor et al., 2001; McGregor et al., 2002). In our study we qualitatively observed robust freezing responses and the odor exposure sessions were carried out in a small enclosed environment which did not allow for the rats to escape the odor. These findings, taken together with other reports, suggest that the CeA may play a central role in mediating unconditioned, fear-related freezing to TMT (Blanchard and Blanchard 1973; Fox and Sorenson 1994). Thus, increased cFos expression in the CeA may not be expected in experimental paradigms where rats do not display freezing responses to predator odors, but instead show retreat/escape behavior.

Conclusion. In summary, we report that TMT is a highly aversive stimulus in rats, as it supports conditioned flavor avoidance learning. Furthermore, acute TMT exposure results in a distinct pattern of activation of hypothalamic neurons and hindbrain NA neurons that provide afferent input to the amygdala. These results suggest that TMT may exert its effects on emotional learning via NA projection pathways arising from the hindbrain, especially the pontine LC. The behavioral responses and corresponding fingerprint of odor-induced neural activity

reported in this study provide a general framework for the development of future experiments, which can probe the specific neural substrates necessary for the observed responses to TMT.

APPENDIX B: Chapter 3 Figures

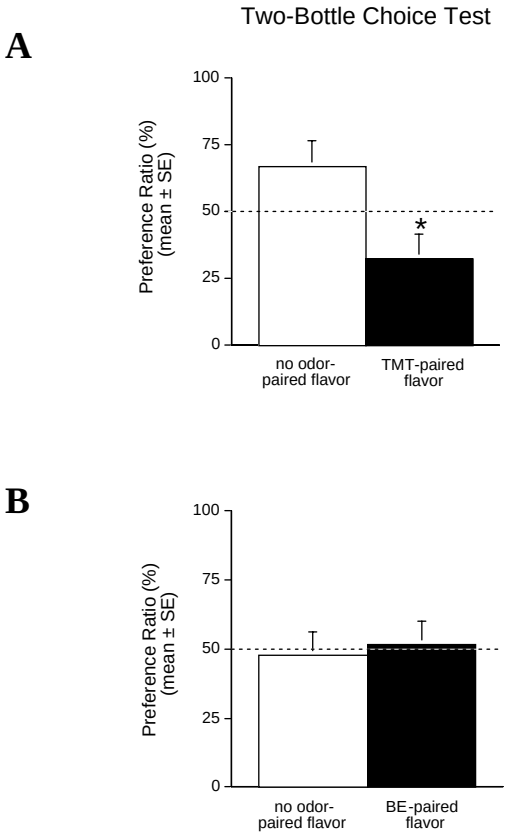

Figure 4. Average group preference ratios (n = 6) for novel flavors after pairing with no odor (non odor-paired flavor) or TMT (panel A), or after pairing with no odor (non odor-paired flavor) or BE (panel B). Dashed lines indicate expected preference ratio with no effect of treatment (50%). * $P < 0.05$, significantly less than intake of non odor-paired flavor, indicating conditioned avoidance of the TMT-paired flavor.

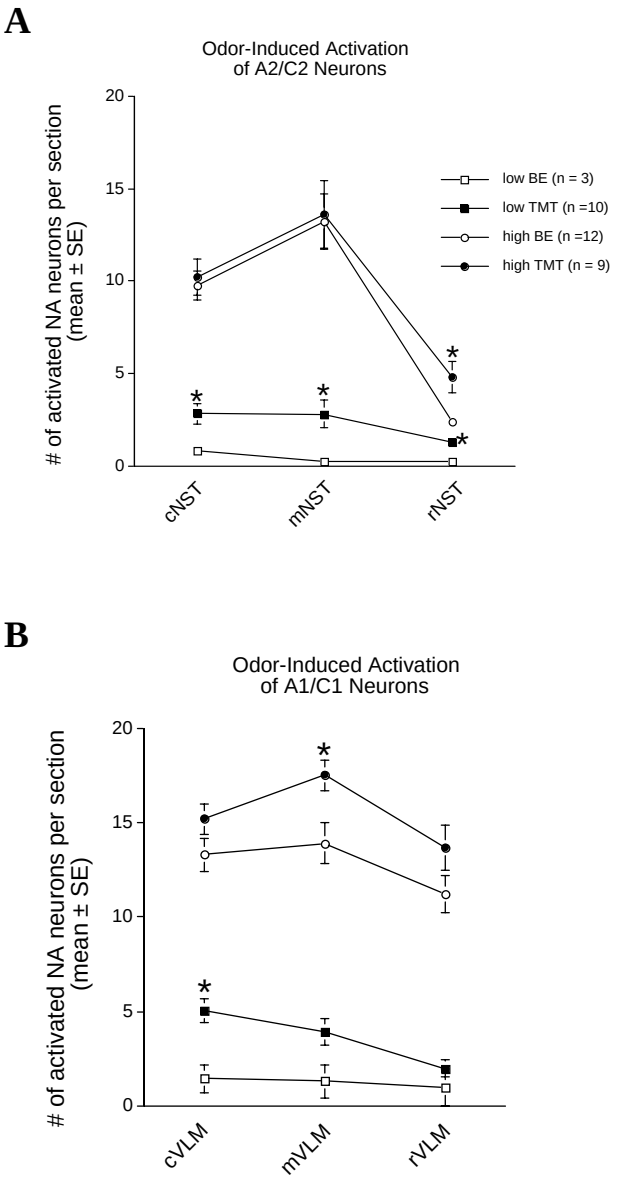

Figure 5. Odor-induced activation of NA neurons within the NST (A2/C2 cell groups; panel A) and VLM (A1/C1 cell groups; panel B) at three rostrocaudal levels: caudal to the area postrema (AP) (cNST, cVLM), through the level of the AP, i.e., middle levels (mNST, mVLM), and rostral to the AP (rNST, rVLM). Group sizes are indicated in the graph legend. * $P < 0.05$ compared to BE at same odor intensity level.

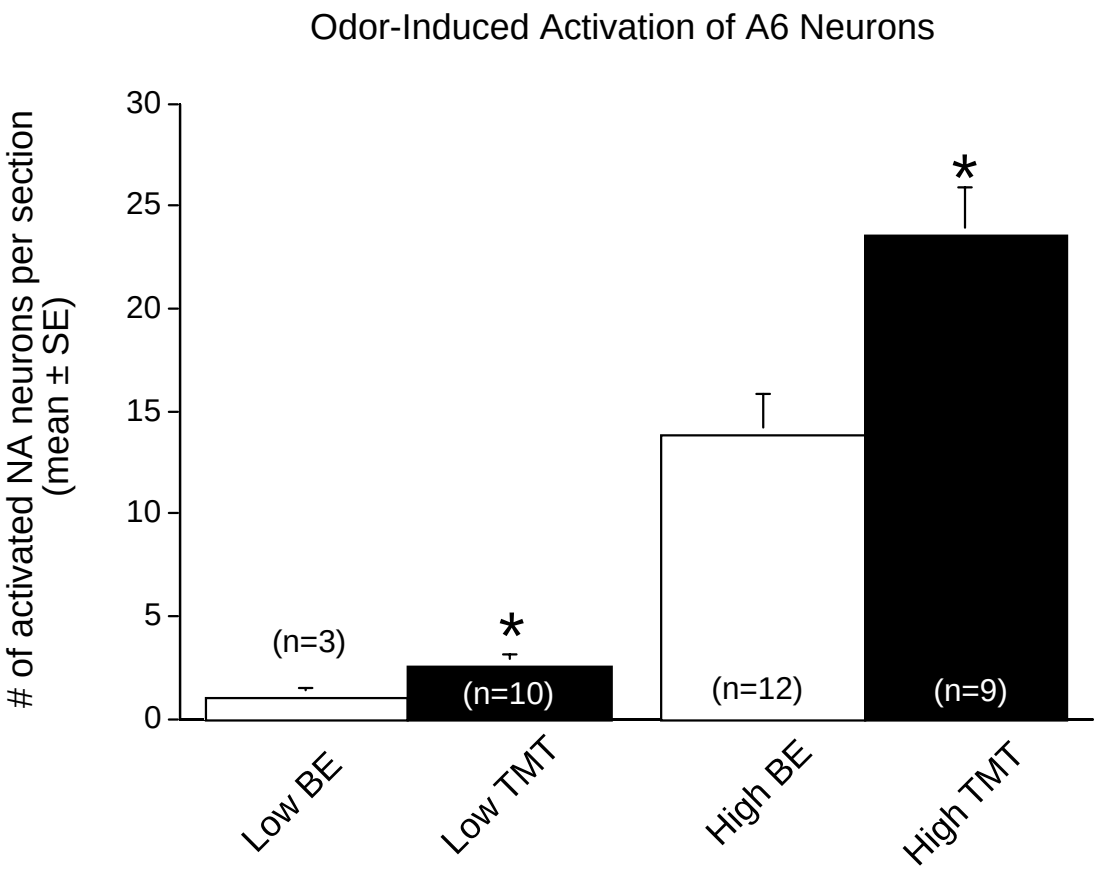

Figure 6. Odor-induced activation of NA neurons in the LC (A6 cell group). * $P < 0.05$ compared to BE at same odor intensity level. Group sizes are indicated above or within each bar.

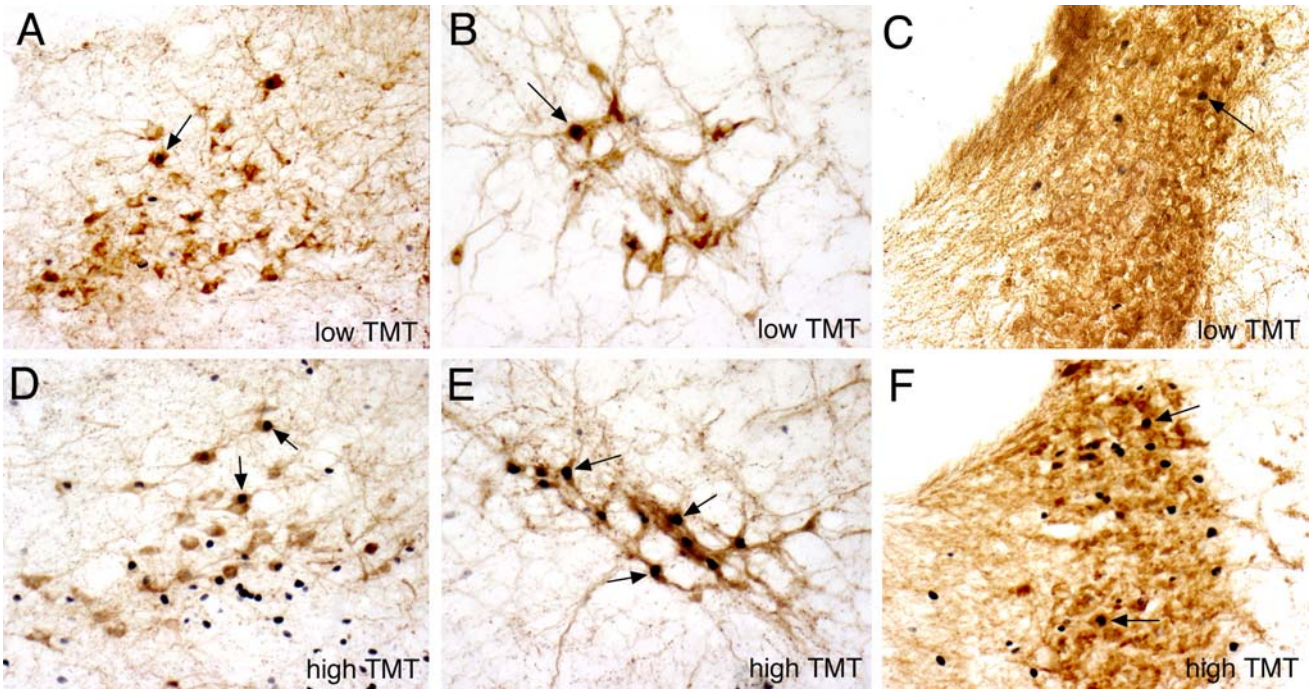

Figure 7. Photomicrographs depicting representative dual immunoperoxidase labeling for cFos (black nuclear label) and DβH (brown cytoplasmic label) within the mNST (A,D), mVLM (B,E) and LC (C,F) in rats after exposure to TMT at low intensity levels (A-C) or at high intensity levels (D-F). Arrows point out some of the activated (i.e., cFos-positive) NA neurons visible in each photomicrograph. Activation in each brainstem region is greater after exposure to high TMT levels compared to low TMT levels (see Figures 2 and 3 for quantitative data).

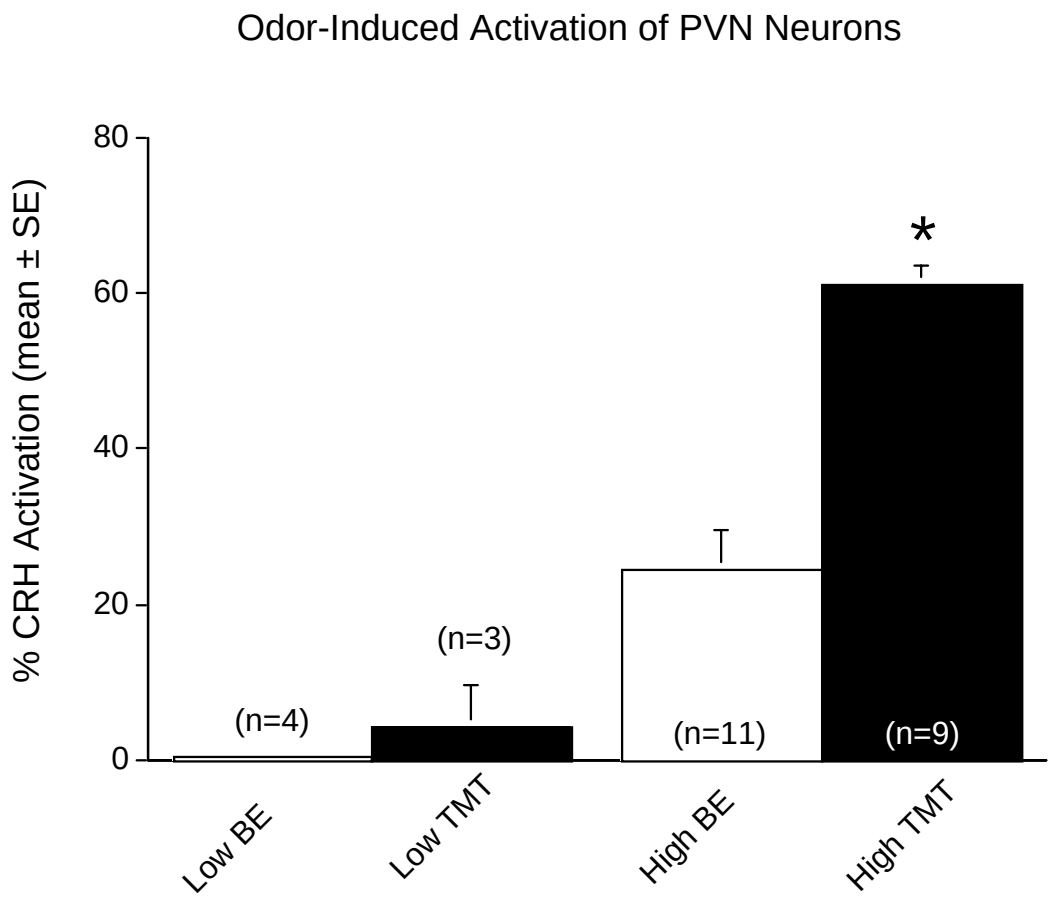

Figure 8. Odor-induced activation of CRH-immunopositive neurons within the medial parvocellular PVN. Bars represent group averages of the percentage of CRH-positive neurons that were double-labeled for cFos. * $P < 0.05$ compared to BE at same intensity level. Group sizes are indicated above or within each bar.

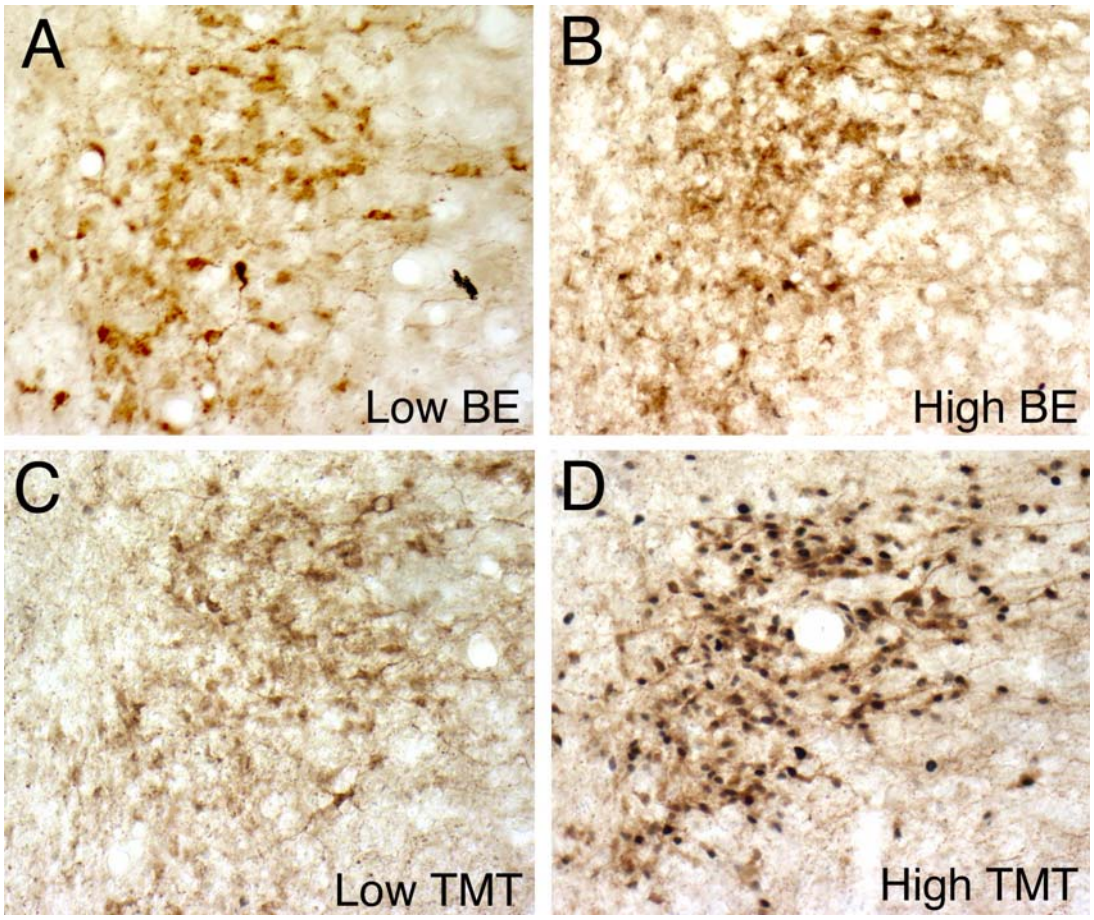

Figure 9. Photomicrographs depicting dual immunolabeling for cFos (black nuclear label) and CRH (brown cytoplasmic label) within the medial parvocellular subdivision of the PVN in rats after exposure to BE at low or high levels (A, B) or TMT at low or high levels (C, D). Activation of CRH-positive neurons is greatest after exposure to high TMT levels compared to all other conditions (see Figure 5 for quantitative data).

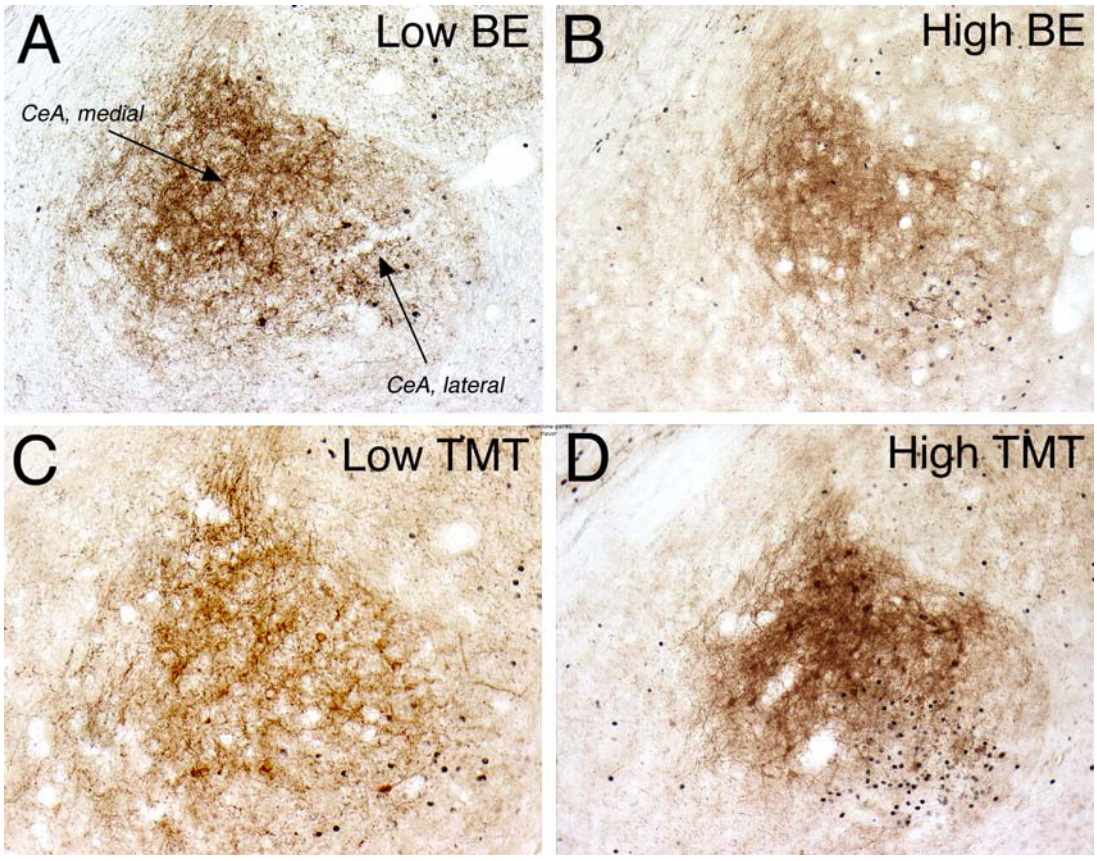

Figure 10. Photomicrographs depicting dual immunoperoxidase labeling for cFos (black nuclear label) and CRH (brown cytoplasmic label) within medial and lateral subregions of the central nucleus of the amygdala (CeA) in rats after exposure to BE at low or high levels (A, B) or TMT at low or high levels (C, D). cFos activation appears greatest within the lateral CeA after exposure to high levels of TMT compared to other treatment conditions.

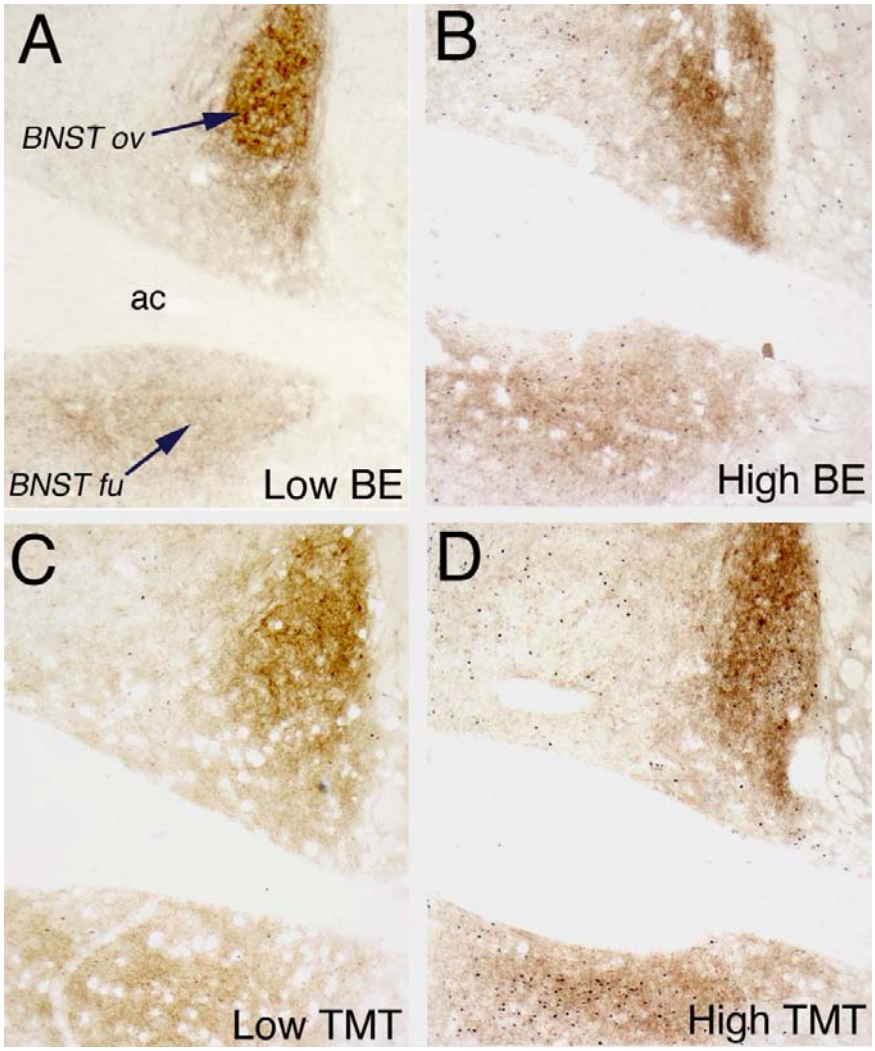

Figure 11. Photomicrographs depicting dual immunoperoxidase labeling for cFos (black nuclear label) and CRH (brown cytoplasmic label) within the oval (ov) and fusiform (fu) nuclei of the bed nucleus of the stria terminalis (BNST) in rats after exposure to BE at low or high levels (A, B) or TMT at low or high levels (C, D). anterior commissure (ac).

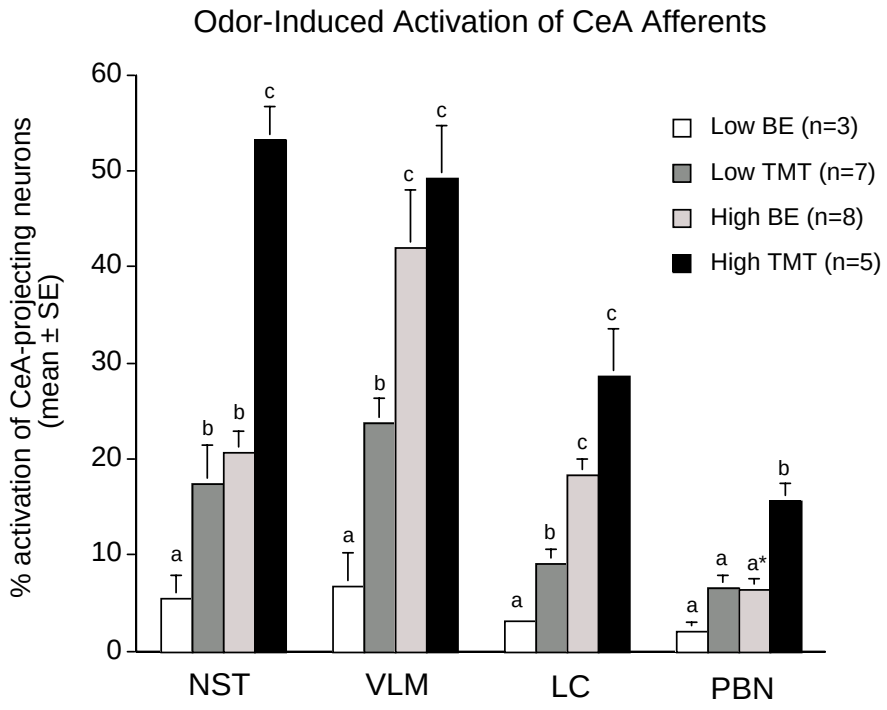

Figure 12. Odor-induced activation of retrogradely labeled brainstem neurons projecting to the CeA. Bars represent the percentage of retrogradely labeled neurons in each region (i.e., NST, VLM, LC, PBN) activated to express cFos in each treatment group. Within each region, bars with different letters (a, b, c) are significantly different ($P < 0.05$). For PBN values, a* over the high BE bar indicates $P < 0.05$ compared to low BE, but $P > 0.05$ compared to low TMT. Group sizes are indicated in graph legend. *Note, group numbers for PBN differ from graph legend: low BE (n=3), low TMT (n=5), high BE (n=4), and high TMT (n=3).

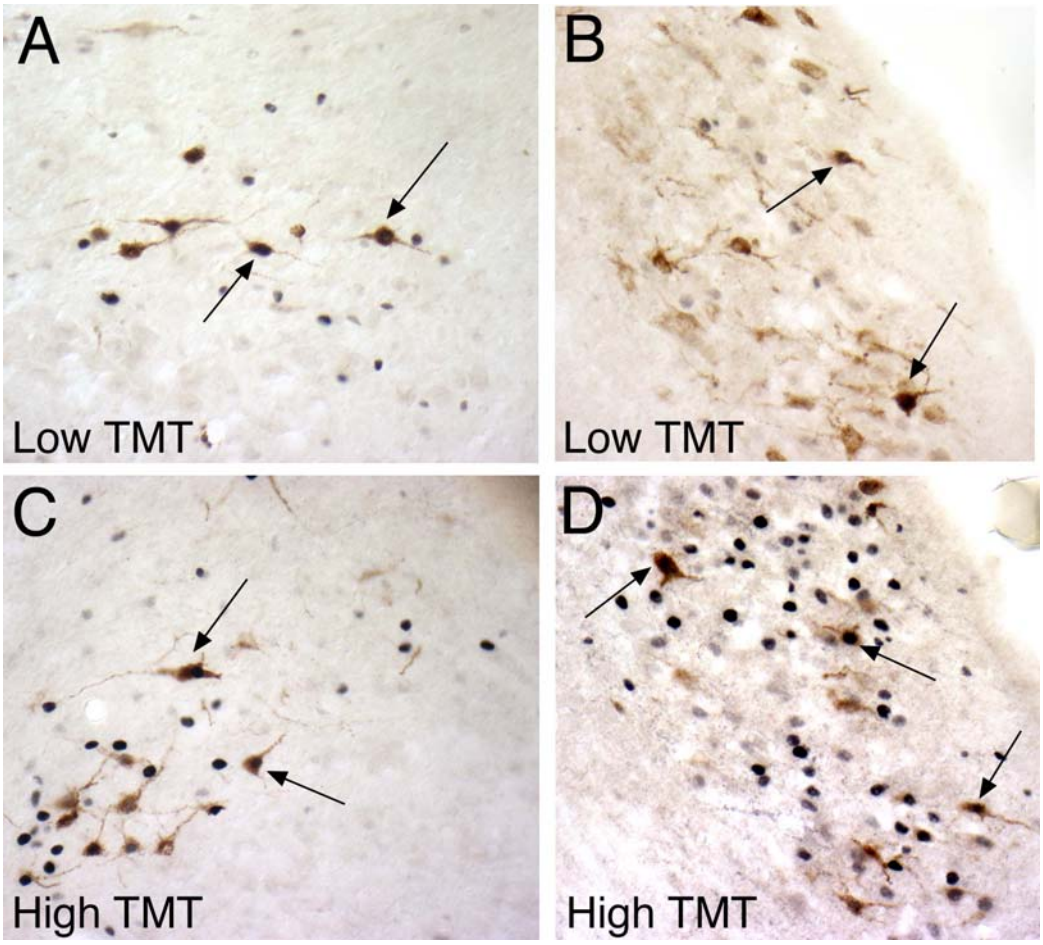

Figure 13. Photomicrographs depicting dual immunoperoxidase labeling for cFos (black nuclear label) and FG retrograde tracer (brown cytoplasmic label) within the mNST (A, C) and the LC (B, D) in rats after exposure to low or high levels of TMT. Arrows point out some of the activated (i.e., cFos-positive) retrogradely-labeled (i.e., CeA-projecting) neurons visible in each photomicrograph. See Figure 8 for quantitative data.

4. Chapter 4: Central neural activation and behavioral responses to systemic yohimbine in rats

Noradrenergic (NA) signaling in the central nucleus of the amygdala (CeA) and paraventricular nucleus of the hypothalamus (PVN) facilitates stress and anxiety responses to interoceptive and exteroceptive stimuli. The indole alkaloid yohimbine (YO) is a potent □2-adrenergic receptor antagonist that promotes excessive neurotransmitter release from central and peripheral NA terminals. Systemic YO activates the HPA stress axis and has anxiogenic effects. The present study further explored behavioral responses and central neural activation patterns in rats after acute YO treatment. YO (0 or 5 mg/kg, i.p.) significantly inhibited food intake and also supported the formation of a conditioned flavor avoidance response. Analysis of treatment-induced cFos expression confirmed previous reports that YO activates NA neurons in the pontine locus coeruleus (A6 cell group). YO also activated ~ 18-24% of NA neurons in the caudal dorsomedial medulla (A2/C2 cell groups) and ~ 50-65% of NA neurons in the caudal ventrolateral medulla (A1/C1 cell groups). YO activated ~ 75% of CRH-positive neurons in the PVN. Retrograde neural tracing demonstrated that YO activated ~ 40% of CeA-projecting neurons in medullary and pontine NA cell group regions, and ~15% of CeA-projecting neurons in the lateral parabrachial nucleus. In general, these data lend further support to the hypothesis that ascending NA inputs to the CeA play a key modulatory role in emotional learning, and that these inputs originate from both pontine and medullary NA cell groups.

4.1. Introduction

Brain noradrenergic systems play an important role in stress responses and emotional learning, and excessive central NA signaling has been implicated in anxiety-related disorders in humans. Several key symptoms commonly associated with anxiety (i.e., hyperarousal, tachycardia, autonomic dysfunction) are effectively mimicked by pharmacological agents that increase NA signaling, such as yohimbine (YO) (Charney et al., 1983; Southwick et al., 1993). Systemic YO is subjectively reported to induce nausea (Mattila et al., 1988; Linden et al., 1985), promotes subjective feelings of anxiety, and can induce panic attack (Charney et al., 1983; Uhde et al., 1984) in humans. YO also increases plasma ACTH (Kiem et al., 1995) and promotes behavioral signs of anxiety (Pellow et al., 1985; Schroeder et al., 2003) in rats, and reduces food intake in mice (Callahan et al., 1984).

YO is a selective antagonist of α2-adrenergic receptors located on both presynaptic and postsynaptic sites. The antagonistic effect of YO at presynaptic autoreceptors potentiates the release of endogenous transmitter from NA nerve terminals in both the central and peripheral nervous system. Consistent with this notion, experimental administration of YO produces a significant increase in plasma norepinephrine (NE) (Goldberg et al., 1983), a finding that is consistent with increased NE turnover in the CNS and with actions of α2 receptor antagonists. Systemically administered YO increases blood pressure, heart rate, and sympathetic outflow, all of which alter viscerosensory feedback to the CNS (Gurguis et al., 1997). YO elicits specific patterns of neuronal activation in limbic forebrain areas implicated in fear and anxiety, including the central nucleus of the amygdala (CeA) and hypothalamus (Singewald et al., 2003). Furthermore, systemic YO promotes activation of neurons in brainstem regions that contain NA neurons (Singewald and Sharp 2000) and are known to provide direct neural input to the

hypothalamic and limbic forebrain regions that shape emotional learning and modulate stress and anxiety.

The present study investigated whether YO treatment produces other behavioral effects relevant to stress and anxiety [(i.e., inhibition of food intake and formation of conditioned flavor avoidance (CFA)], and whether YO differentially activates anatomically specific NA cell groups within the brainstem. We further investigated whether YO activates central neural inputs to the central nucleus of the amygdala (CeA), because we hypothesize that the behaviorally aversive nature of YO treatment involves this limbic forebrain region.

4.2. Materials and Methods

Animals

Forty male Sprague-Dawley rats (Harlan Laboratories; 250-350 g body weight) were used in this investigation. Rats were housed singly in stainless steel cages in a controlled environment (20-22 °C, 12:12 h light/dark cycle, lights on at 7 am) with ad libitum access to water and pelleted chow (Purina 5001), except as noted. Rats were acclimated to this environment and to daily handling for at least one week before initiation of experiments.

Food Intake Experiment

Rats (n=8) were food deprived for 24 hrs, and then were injected i.p. with YO (Sigma-Aldrich; 5 mg/kg in 2.0 ml 0.15M NaCl vehicle; n = 4) or vehicle alone (n = 4). A pre-weighed measure of food was provided 30 min after injection, with paper towels placed beneath each cage to collect spillage. Cumulative food intake was recorded 30 min, 60 min and 14 hr later. After a subsequent 48 hr period of *ad libitum* chow access, the 24 hr deprivation and refeeding test was

repeated in a crossover design in which each rat received the treatment opposite to that received in the first test.

Conditioned Flavor Avoidance (CFA)

A sensitive two-bottle choice procedure (Deutsch and Hardy 1977) was used to determine whether systemic YO supports CFA. CFA training and testing were conducted during the light cycle of the photoperiod, between 1500 and 1700 hr. Prior to the start of the CFA experiment, rats were acclimated for 2 days to i.p. injections of 0.15M NaCl (2 ml, room temp).

Adult male rats (300 g BW; n=10) naïve to YO treatment underwent 22 hr water deprivation, then half of the rats were presented with almond flavored tap water to drink from a graduated tube, and the others with banana flavored water (both 0.5% McCormick flavor extract). The left-right position of the bottle on each testing cage was switched after 15 min, with fluid intake recorded at 15 and 30 min time points. Thirty min after the end of the flavor exposure session, each rat was injected with 0.15M NaCl (2.0 ml, i.p.). Water was returned 30 min later with *ad libitum* access for the next 24 h. Rats were then water deprived again for 22 hr and allowed to drink the alternate flavor for 30 min, with bottle positions switched after 15 min. Thirty min after the end of fluid access, each rat was injected with YO (5 mg/kg in 2.0 ml 0.15M NaCl, i.p.). Water was returned 30 min later with *ad libitum* access for the next 24 h. Rats were then again water deprived for 22 hr, then given 30 min simultaneous access to two bottles containing almond or banana-flavored water. The volume of each flavor consumed was recorded at 15 min, bottle positions were switched, and cumulative intake recorded at 30 min. Rats then were returned to *ad libitum* water access.

CFA data analysis: Within each CFA experiment, flavor preference ratios displayed by each rat were determined by dividing the volume consumed from each bottle during the 30-min choice test by the total volume consumed from both bottles. Outcomes indicating flavor preference ratios that do not differ significantly (i.e., 50%:50%) are interpreted as an absence of CFA, whereas an outcome indicating a preference ratio of 0%:100% would be interpreted as a complete avoidance of the flavor represented by the first value in the ratio. Individual rat preference ratio data were averaged to obtain group preference ratios (mean ± SE) for saline-paired flavors relative to YO-paired flavors within each experiment. Student's t-test was used to determine whether group preference ratios for saline-paired and YO-paired flavors were statistically different, with significance set at $P < 0.05$.

Yohimbine-induced neural activation

In a terminal cFos study, rats received an i.p. injection of either 0.15M NaCl (2.0 ml; n=7) or YO (5 mg/kg in 0.15M NaCl; n=16). Rats were then left undisturbed in their home cages for 90-120 min, then were anesthetized with sodium pentobarbital (Nembutal, 100 mg/kg i.p). Rats were transcardially perfused with a brief saline rinse followed by 500 ml of fixative (4% paraformaldehyde in 0.1 M phosphate buffer with lysine and sodium metaperiodate; McLean and Nakane 1974). Brains were post-fixed overnight at 4˚ C, then blocked and cryoprotected in 20% sucrose.

Neural tracer injections

A subset of rats in the terminal cFos study described above received CeA microinjections of retrograde neural tracer one week before experimental treatment and perfusion. Rats were

anesthetized with halothane (Halocarbon Laboratories; 1-3% in oxygen) and mounted into a stereotaxic frame. Two retrograde tracers were used: FluoroGold (FG, Fluorochrome, 2% in 150 mM NaCl) and cholera toxin (CTb, List Biological Laboratories; 0.25% in 150 mM NaCl). Rats received FG injections targeted to the left CeA and CTb injections targeted to the right CeA. CeA injection coordinates (2.20 mm posterior, 4.0 mm lateral, and 8.2 mm ventral relative to bregma) were based on a standard rat brain atlas (Paxinos and Watson 1997). FG (50 nl) or CTb (100-150 nl) was delivered by pressure injection over a 1-2 minute period through a 1.0 μl Hamilton syringe. The syringe was left in place for an additional 7 min after each injection to reduce tracer diffusion up the needle tract. A different syringe was used for each tracer. The skin was closed with stainless steel clips, 2.0% lidocaine was applied to the incision site, and rats were returned to their home cages after recovery from anesthesia. Rats were given one week to recover from surgery and permit retrograde tracer transport before YO or saline treatment and perfusion, as described above.

Histology and immunocytochemistry

Fixed brains were frozen and cut into serial coronal 35 μm sections from the caudal extent of the nucleus of the solitary tract (NST) through the rostral extent of the corpus callosum using a sliding microtome. Six adjacent sets of sections were collected into buffer for immediate use, or were stored at –20^{o}C in cryopreservant solution (Watson et al., 1986). Sections were rinsed for 1 h in buffer (0.1 M sodium phosphate, pH 7.4) prior to immunocytochemical procedures. Antisera were diluted in buffer containing 0.3% Triton-X and 1% normal donkey serum. Biotinylated secondary antisera (Jackson Immuochemicals) were used at a dilution of 1:500.

Tissue sections were processed for localization of cFos protein using a rabbit polyclonal antiserum (1:50,000; provided by Dr. Philip Larsen, Denmark) and Vectastain Elite ABC immunoperoxidase reagents (Vector Laboratories). The specificity of this antibody for cFos protein has previously been reported (Rinaman et al., 1997). Sections were processed using a nickel sulfate-intensified DAB reaction to generate a blue-black cFos nuclear reaction product of activated neurons. In tracer-injected rats, two sets of cFos-labeled tissue sections were subsequently processed for immunoperoxidase localization of either FG (rabbit anti-FG: Chemicon; 1:30,000) or CTb (goat anti-CTb; List Biological Laboratories; 1:50,000). Plain DAB was used to generate a brown reaction product at the amygdalar FG and CTb injection sites, and in the cytoplasm of retrogradely labeled brainstem neurons. Additional sets of cFos-labeled tissue sections from each rat were processed for immunoperoxidase localization of cytoplasmic corticotropin-releasing hormone (rabbit anti-CRH, 1:15,000; Penninsula) in forebrain sections and for the NA synthetic enzyme, dopamine beta hydroxylase, (mouse anti-DβH, 1:30,000; Chemicon) in hindbrain sections.

After immunocytochemical labeling, tissue sections were mounted onto Superfrost Plus glass microscope slides (Fisher Scientific), dehydrated and defatted in graded alcohols, cleared in xylene, and coverslipped using Cytoseal 60 (VWR).

Quantitative analysis

Dual immunoperoxidase-labeled sections were analyzed using a light microscope to determine the number and proportions of phenotypically identified neurons activated to express cFos. Criteria for counting a neuron as retrogradely labeled (i.e., CTb- or FG-positive), DβH-positive, or CRH-positive included the presence of brown cytoplasmic immunoreactivity and a

visible nucleus. Neurons were considered cFos-positive if their nucleus contained visible blue-black immunoreactivity, regardless of intensity, and cFos-negative if their nucleus was unlabeled. Cell counts thus obtained were used to determine the percentage of phenotypically identified neurons that were activated in each experimental case.

The distribution of CRH-positive PVN neurons and the proportion activated to express cFos in each rat was documented at 100x magnification using oil immersion with the assistance of Stereo Investigator X-Y plotting software (MicroBrightField, Inc). CRH-positive neurons in the PVN were summed bilaterally and averaged in each rat across two sections spaced by 210 μm that contained the highest density of CRH neural labeling. Activated CRH neurons (i.e., those with nuclear cFos labeling) were expressed as a percentage of the total number of CRH-positive neurons counted within the PVN bilaterally.

Quantitative analysis of cFos expression by retrogradely labeled neurons and DβH-positive NA neurons was conducted in brainstem regions that provide direct input to the CeA, including the pontine lateral parabrachial nucleus (PBN) and LC (location of the A6 NA cell group), the nucleus of the solitary tract (location of the A2/C2 cell groups), and the caudal ventrolateral medulla (location of the A1/C1 cell groups). Retrogradely labeled or DβH-positive neurons were counted bilaterally in each region at 40x magnification. Counts of activated DβH-positive LC neurons were summed bilaterally across 6-11 tissue sections spaced by 210 μm. Retrogradely labeled neurons within the lateral PBN ipsilateral to the tracer injection site were summed and averaged over two sections spaced by 210 μm that contained the highest density of retrograde labeling in each rat. Counts of retrogradely labeled and DβH-positive NST and VLM neurons were grouped according to 3 rostrocaudal levels of the visceral NST defined with respect to the area postrema (AP): (1) sections caudal to the AP (cNST and cVLM); (2) sections

at the level of the AP (mNST and mVLM); and (3) sections rostral to the AP (rNST and rVLM). Statistical comparisons were made using one- or two-way ANOVA. When F ratios indicated significant overall main effects of treatment and/or brain region, ANOVA was followed up with selected comparisons using planned t-tests. Differences were considered statistically significant when $P < 0.05$.

4.3. Results

YO-Induced Anorexia

Deprivation-induced food intake in rats (n=8) after YO treatment was significantly inhibited at the 30 and 60 min timepoints compared to food intake by the same rats after vehicle treatment ($P < 0.05$ for each comparison; Fig. 14). The anorexigenic effect of YO treatment was no longer evident at the 14 hr timepoint (Fig. 14).

YO-Induced Conditioned Flavor Avoidance

Results from the two-bottle choice test revealed a significant preference of rats (n=10) for saline-paired flavors compared to YO-paired flavors (Fig. 15). Group mean fluid intake in the 30 min choice test consisted of 9.6 ± 1.4 ml of saline-paired flavors and 4.8 ± 1.1 ml of YO-paired flavors ($P < 0.05$), evidence for a relatively strong CFA response to flavors previously paired with YO treatment.

YO-induced activation of brainstem noradrenergic neurons

Medulla

NST (A2/C2 cell groups): Two-way repeated measures ANOVA revealed a significant main effect (between subjects) of treatment group (saline vs. YO) [$F(1,28) = 26.78$, $P < 0.05$],

with YO activating significantly more NA neurons per tissue section than saline treatment (Fig. 16). Within subjects, there was a significant effect of rostrocaudal level (cNST, mNST, rNST) [$F(2,24) = 9.15$, $P < 0.05$] and a significant interaction between treatment group and NST rostrocaudal level [$F(2,24) = 7.11$, $P < 0.05$] in the average number of activated NA neurons per tissue section. Post hoc t comparisons revealed that YO activated significantly more NA neurons at all rostrocaudal levels of the NST compared to saline controls (Fig. 16). Figure 17 shows representative photomicrographs of cFos activation within the mNST in rats after YO (Fig. 17D) or saline treatment (Fig. 17A).

VLM (A1/C1 cell groups): Two-way repeated measures ANOVA revealed a significant main effect (between subjects) of treatment group (saline vs. YO) [$F(1,28) = 51.2$, $P < 0.05$], with YO activating significantly more NA neurons per tissue section compared to saline at all rostrocaudal levels of the VLM (Fig. 16). Within subjects, there was no significant effect of rostrocaudal level (cVLM, mVLM, rVLM) and no significant interaction between treatment group and rostrocaudal level in the average number of activated VLM NA neurons per tissue section. Figure 17 shows representative photomicrographs of cFos activation within the mVLM in rats after YO (Fig. 17E) or saline treatment (Fig. 17B).

The approximate proportions of NST and VLM NA neurons activated by YO treatment were determined by dividing the group mean number of activated NA neurons present within each tissue section by the total number of NA neurons at each rostrocaudal level of the NST and VLM (Fig. 16). YO treatment activated approximately 28% of NA neurons in the NST and approximately 68% of NA neurons in the VLM, with minimal differences in activation observed at different rostrocaudal levels of each region (Fig. 16).

Pons

LC (A6 cell group): Relatively few cFos-positive neurons were observed in the LC of vehicle-treated rats. Conversely, YO treatment produced a marked increase in the number of cells expressing cFos (Fig. 17). One-way ANOVA revealed a significant main effect of treatment on the number of activated NA neurons [$F(1,12) = 23.9$, $P < 0.05$], with YO activating significantly more NA neurons per tissue section compared to saline (Fig. 16). Figure 17 shows representative photomicrographs of cFos activation within the LC in rats after YO (Fig. 17F) or saline treatment (Fig. 17C). The proportion of NA neurons in the LC that were activated to express cFos could not be determined due to the high density of DβH immunolabeling and the resulting difficulty in visualizing unlabeled (i.e., cFos-negative) cell nuclei; however, it appeared that fewer than half of the DBH-positive neurons in the LC were activated to express cFos in rats after YO treatment (Fig. 17F).

YO-induced activation of hypothalamic CRH neurons

One-way ANOVA revealed a significant main effect of treatment (saline vs. YO) in the proportion of activated CRH neurons in the mpPVN [$F(1,7) = 78.7$, $P < 0.05$], with YO activating a significantly larger proportion of CRH neurons compared to saline (Fig. 18). Figure 19 shows representative photomicrographs of cFos expression by CRH-positive PVN neurons in rats after YO or saline treatment.

YO-induced activation of the lateral CeA

A robust increase in cFos expression was observed in the lateral subdivison of the CeA in rats after YO treatment, whereas very little cFos was observed in the same area in rats after saline treatment (Fig. 20).

CeA tracer injection sites

Twelve rats that received CeA tracer injections prior to the terminal cFos study had at least one tracer injection accurately targeted to the center of the CeA (n = 8 YO-treated, n=4 vehicle controls). FG produced the most accurate and effective tracer injection site in the majority of rats. Amygdalar regions adjacent to the CeA (i.e., basolateral and medical nuclei) were included within the outer boundaries of CeA-centered injection sites to varying degrees. Although these extra-CeA regions do not receive direct neural input from the NST or VLM (Myers and Rinaman 2002), neural tracer diffusing to these sites could contribute to some degree of retrograde labeling observed within the LC, as this region has projections to several subnuclei of the amygdala (Nitecka et al., 1980). A representative CeA neural tracer injection site is shown in Chapter 2 (see Fig. 1).

Distribution of activated brainstem inputs to the CeA

Retrogradely labeled neurons were observed in the NST, VLM, LC, and PBN in all experimental cases, although the absolute number of labeled neurons present in each region varied among experimental cases. Cell counts of retrogradely labeled neurons in the NST and VLM were discontinued at the level rostral to AP in which the NST moves laterally away from the floor of the fourth ventricle, because labeled NST and VLM neurons were rarely observed at

more rostral levels. The largest number of retrogradely labeled NST and VLM neurons was found at rostrocaudal levels through the AP, consistent with previous reports. Labeled neurons were present bilaterally in each brain region examined, but there was an ipsilateral predominance with respect to the injection site.

Two-way repeated measures ANOVA revealed a significant main effect (between subjects) of treatment group (saline vs. YO) in the proportion of activated retrogradely labeled neurons [$F(1,36) = 53.44$, $P < 0.05$], with YO activating significantly larger proportions of retrogradely labeled neurons in the NST, VLM, LC, and PBN in rats after YO treatment compared to saline treatment (Fig. 21). Within subjects, there was a significant effect of brainstem region (NST, VLM, LC, or PBN) [$F(3,30) = 5.89$, $P < 0.05$] on YO-induced activation of retrogradely labeled neurons, but no significant interaction between treatment group and brainstem region. Figure 22 shows representative photomicrographs of cFos expression by FG-labeled neurons in the NST, LC, and PBN in rats after YO or saline treatment.

4.4. Discussion

In several animal studies, yohimbine has been shown to be anxiogenic, causing decreased social interaction, decreased exploration, conditioned place aversion, and potentiated startle (Bhattacharya et al., 1997; Chopin et al., 1986; Davis et al., 1979; File 1986; Pellow et al., 1985). In the present study, we investigated possible neural correlates of additional behavioral responses associated with administration of the anxiogenic agent, yohimbine (YO). To our knowledge, the present report is the first to demonstrate a clear conditioned flavor avoidance response to YO, and to provide a detailed analysis of yohimbine-induced activation of phenotypically identified neuronal populations. We also report that YO decreases food intake, a finding that has

previously been reported in experiments using mice (Callahan et al., 1984). The results of the present experiment demonstrate that YO activates CRH neurons within the PVN and elicits a unique activation profile of brainstem NA cell populations, including those that provide direct afferent input to the CeA. Accordingly, previous studies report that YO increases NA release in several key anxiety-response brain regions that include the hypothalamus, amygdala, and LC (Ishii 1994; Oguchi 1988).

The fact that YO decreases food intake and supports the formation of CFA learning suggests that it functions as a behaviorally aversive unconditioned stimulus. It is clear that the inhibition of food intake is not likely attributable to satiating properties of YO given that it supports CFA learning as well. It is also questionable as to whether YO produces conditioned nausea that results in the avoidance of a particular flavor because nausea does not appear to be a necessary condition for the establishment of conditioned flavor avoidance (Parker 2003). However, YO has been subjectively reported to induce nausea in humans (Mattila et al., 1988; Linden et al., 1985. Our findings do not allow us to identify what specific property of YO is aversive to rats. Because YO crosses the blood brain barrier, it is conceivable that systemic administration of YO may have a direct effect on the neuronal populations of interest in the present study. Alternatively, YO may influence cFos expression in anxiety-related brain regions via transmitted actions subsequent to YO-induced peripheral alterations. Moreover, it is difficult to assess whether YO-induced increases in cFos expression in selective brain regions reflect neural pathways inducing anxiety or associated pathways adapting to this state.

Consistent with previous reports that YO increases plasma hormone levels (Kiem et al., 1995), our findings show that YO administration produced a statistically significant increase in the proportion of activated CRH neurons compared to saline controls. A seminal study reported

that systemic YO elicits activation of neurons in brainstem regions that contain key NA cell populations known to provide direct neural input to hypothalamic and limbic forebrain regions implicated in stress and anxiety (Singewald and Sharp 2000). Our findings confirm previous reports that YO activates NA neurons within the LC, which is generally thought to provide the source of relevant norepinephrine to anxiety-responsive forebrain regions. Additionally, our data reveal that NA cell populations in the caudal medulla provide important contributions to NA signaling during anxiety as YO was shown to activate ~23% and ~58% of NA neurons in the NST (A2 cell group) and VLM (A1 cell group), respectively.

It has been well documented that NST and VLM CeA-projection neurons are primarily catecholaminergic (Zardetto-Smith and Gray 1990, 1995) and that stimulation of NST neurons is reported to increase extracellular NE levels in the amygdala (Clayton and Williams 2000). However, it is currently unclear whether amygdalar-projecting NA projections are activated by YO. While YO produced a selective activation profile of NA neurons, it recruited a similar proportion of afferent inputs to the CeA arising in the NST, VLM, and LC compared to saline controls. Presumably, a large majority of these projections to the CeA are phenotypically NA given the known projection distributions. This suggests that the larger recruitment of NA in the VLM includes projections to both the CeA and additional brain regions, such as the PVN, which is known to also receive direct input from this cell population. Additionally, a moderate proportion of afferent inputs to the CeA arising in the lateral PBN were activated after systemic YO. Activation of the lateral PBN is consistent with the observed CFA learning in the present study, as this conditioned learning response is dependent on involvement of both the PBN and amygdala.

In conclusion, we report that YO is a behaviorally aversive stimulus in rats, as it supports conditioned flavor avoidance learning and reduces food intake. YO results in robust activation of hypothalamic neurons and recruits hindbrain NA neurons that provide afferent input to the amygdala. These results suggest that YO may potentially influence emotional learning via ascending NA projection pathways to the CeA, of which originate from both pontine and medullary NA cell groups. The behavioral responses and corresponding patterns of YO-induced neural activity reported here establishes the general groundwork for future experiments, which will probe the specific neural substrates necessary for the observed neural and behavioral responses to YO.

APPENDIX C: Chapter 4 Figures

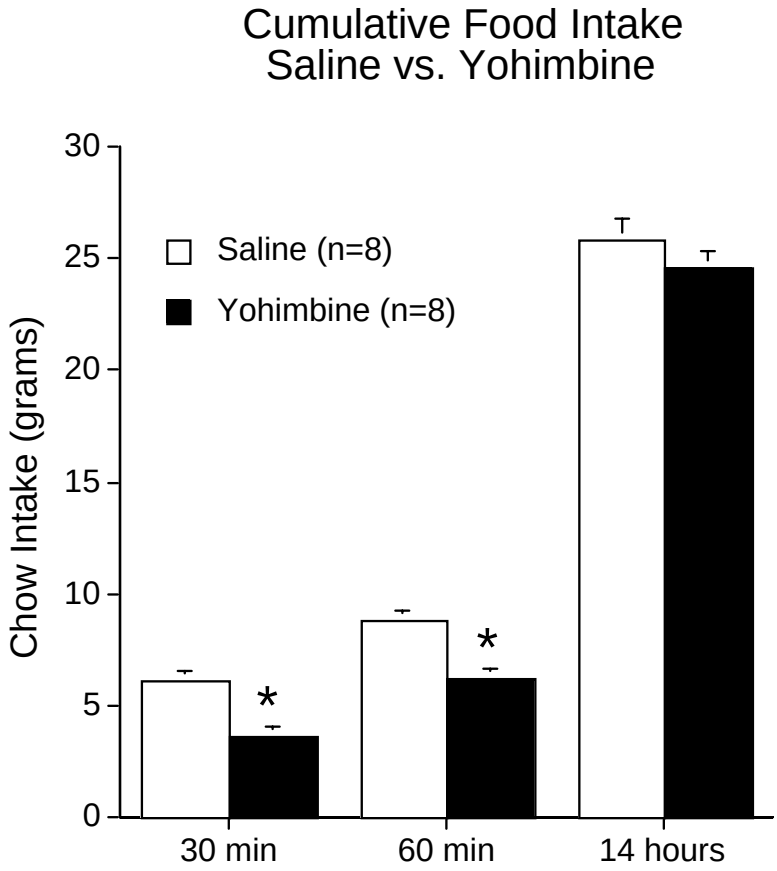

Figure 14. Deprivation-induced food intake in rats after YO treatment. YO significantly inhibited food intake at the 30 and 60 min compared to food intake by the same rats after vehicle treatment * $P < 0.05$ vs. saline.

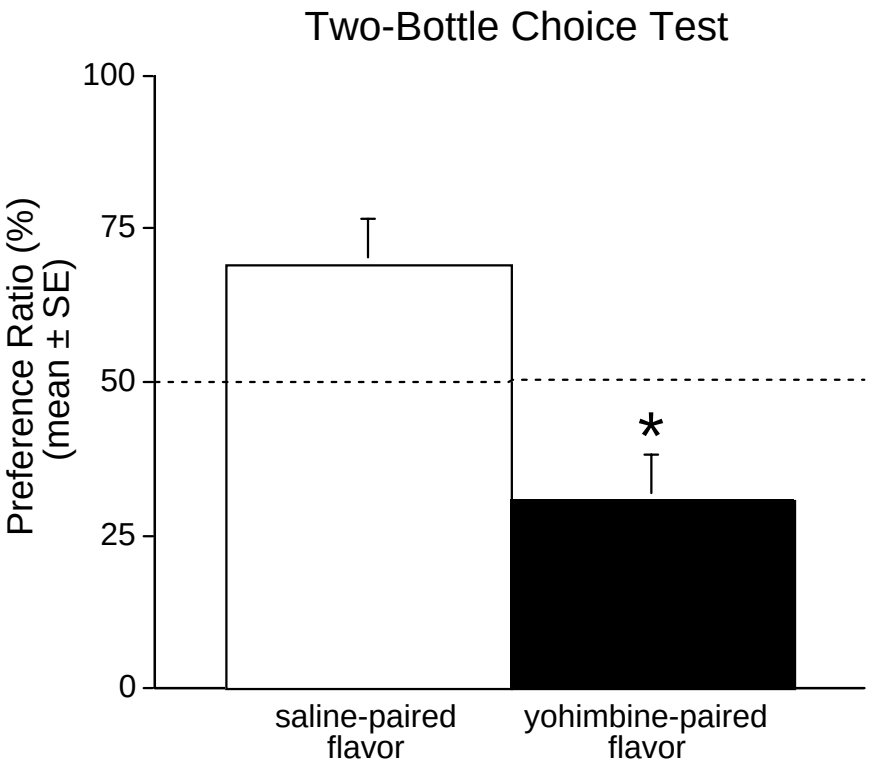

Figure 15. Average group preference ratios (n = 10) for novel flavors after pairing with saline or yohimbine. Dashed lines indicate expected ratio with no effect of treatment (50%). Yohimbine produces a clear CFA, * P = 0.0028 saline- vs. yohimbine-paired flavor.

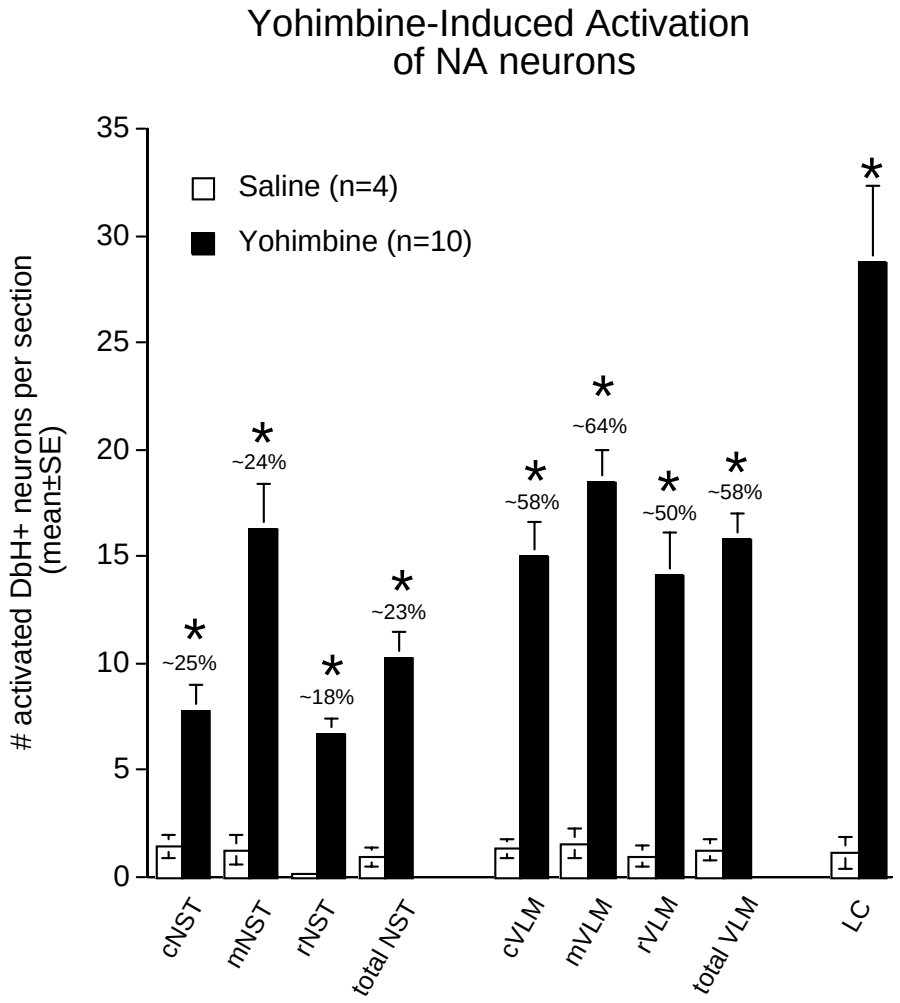

Figure 16. Yohimbine-induced activation of NA neurons in the LC, NST, and VLM across three rostrocaudal levels: caudal to the area postrema (AP) (cNST, cVLM), through the level of the AP, i.e., middle levels (mNST, mVLM), and rostral to the AP (rNST, rVLM). Group sizes are indicated in the graph legend. * P<.001 relative to saline.

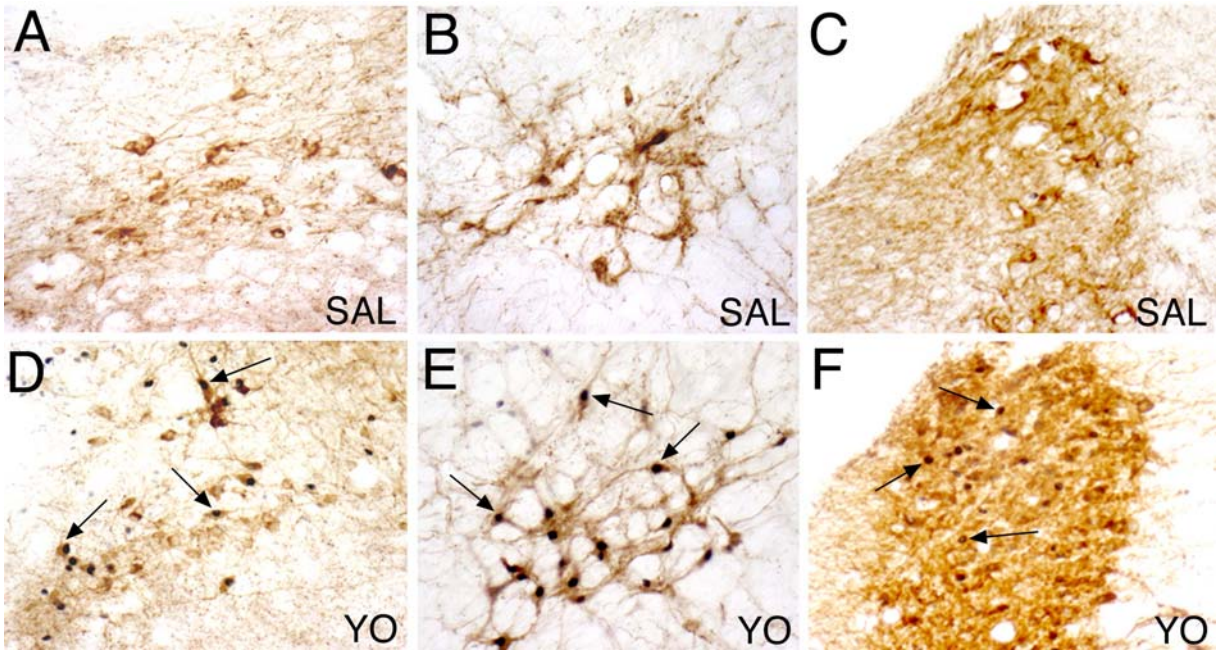

Figure 17. Photomicrographs depicting representative dual immunoperoxidase labeling for cFos (black nuclear label) and DβH (brown cytoplasmic label) within the mNST (A,D), mVLM (B,E) and LC (C,F) in rats after exposure to saline (A-C) or yohimbine (D-F). Arrows point out some of the activated (i.e., cFos-positive) NA neurons visible in each photomicrograph. Activation in each brainstem region is greater after yohimbine compared to saline (see Figure 3 for quantitative data).

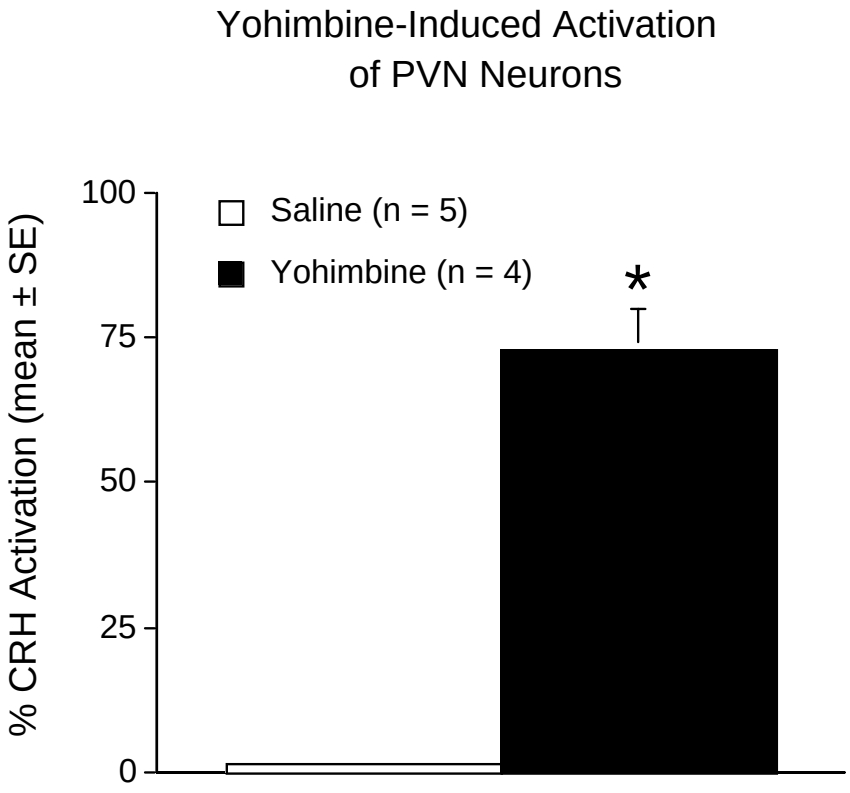

Figure 18. Yohimbine-induced activation of CRH-immunopositive neurons within the medial parvocellular PVN. Bars represent group averages of the percentage of CRH-positive neurons that were double-labeled for cFos. Group sizes are indicated in graph legend. * P=0.0006 relative to saline.

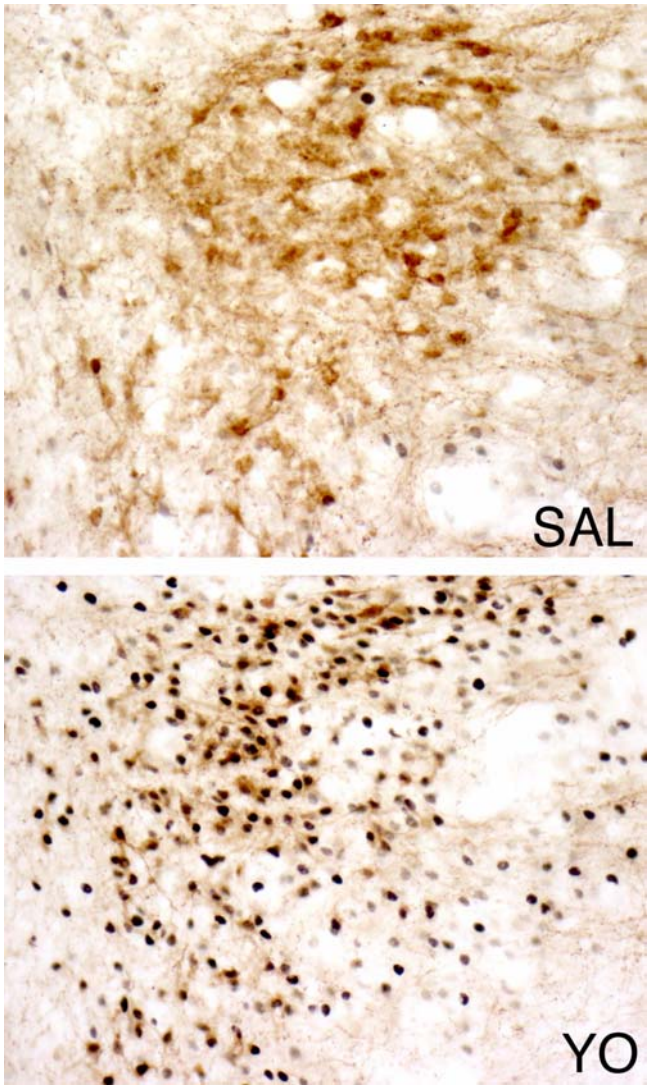

Figure 19. Photomicrographs depicting dual immunolabeling for cFos (black nuclear label) and CRH (brown cytoplasmic label) within the medial parvocellular subdivision of the PVN in rats after saline or yohimbine treatment. Activation of CRH-positive neurons is significantly greater after yohimbine treatment (see Figure 5 for quantitative data).

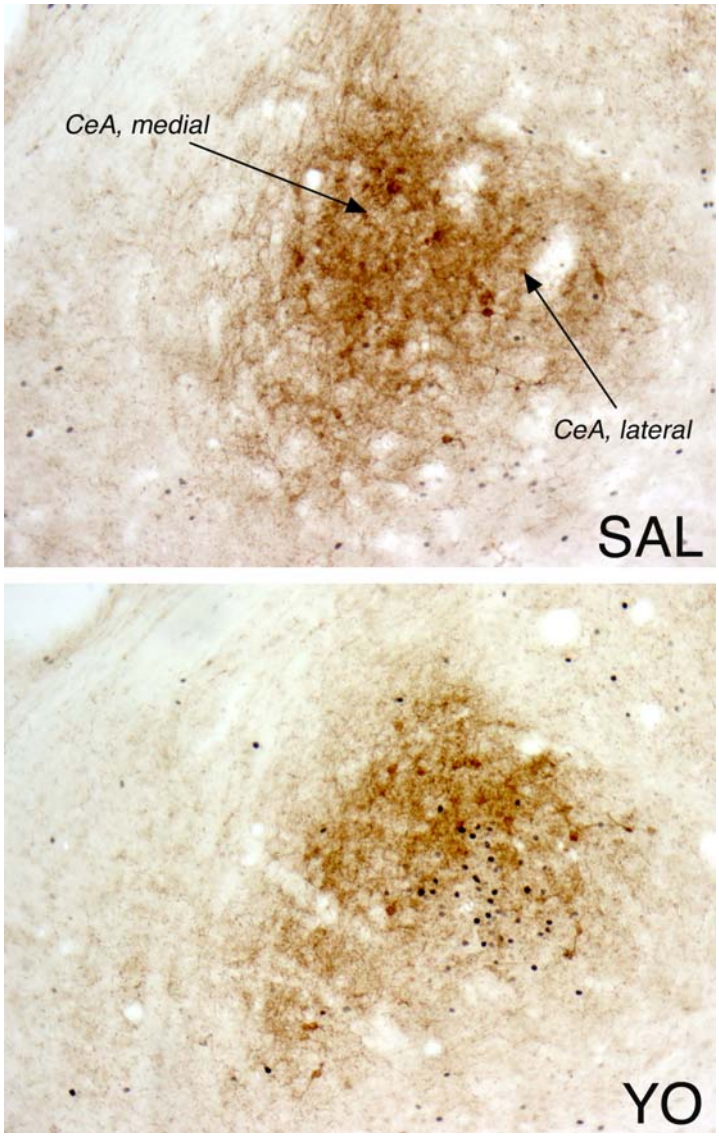

Figure 20. Photomicrographs depicting dual immunoperoxidase labeling for cFos (black nuclear label) and CRH (brown cytoplasmic label) within medial and lateral subregions of the central nucleus of the amygdala (CeA) in rats after saline or yohimbine treatment. cFos activation appears greatest within the lateral CeA after yohimbine treatment.

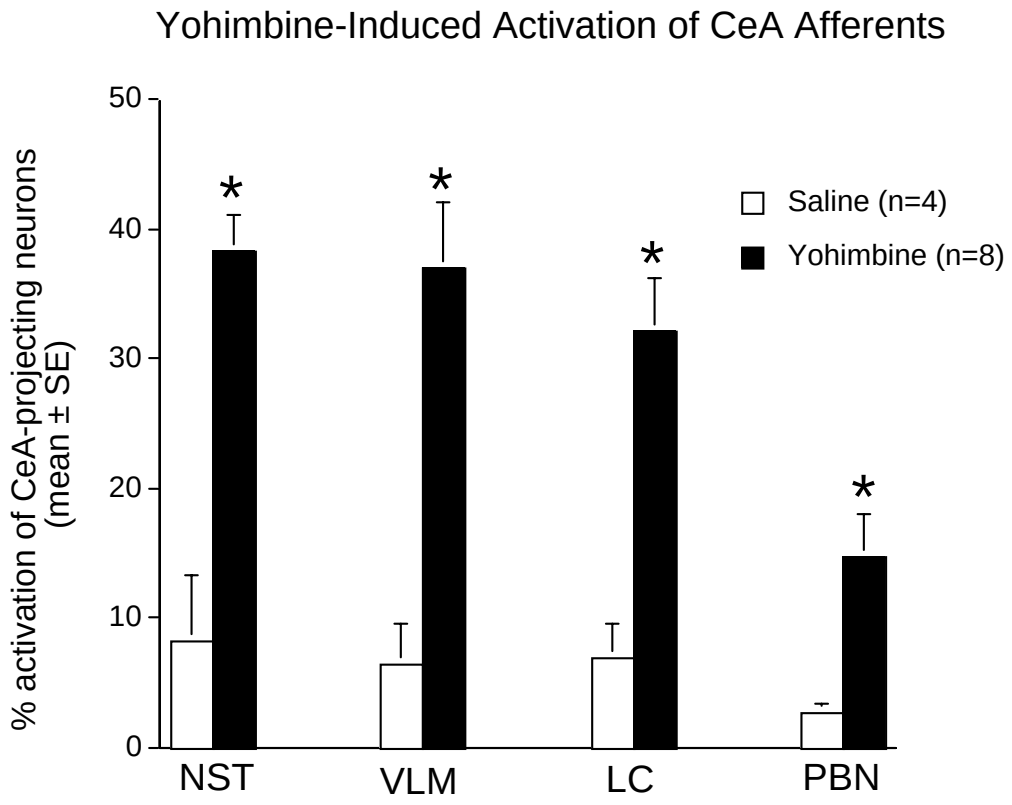

Figure 21. Yohimbine-induced activation of retrogradely labeled brainstem neurons projecting to the CeA. Bars represent the percentage of retrogradely labeled neurons in each region (i.e., NST, VLM, LC, PBN) activated to express cFos in each treatment group. Group sizes are indicted in graph legend. *Note, group numbers for PBN differ from graph legend: saline (n=3) and yohimbine (n=5). * P<.05 relative to saline within each brain region.

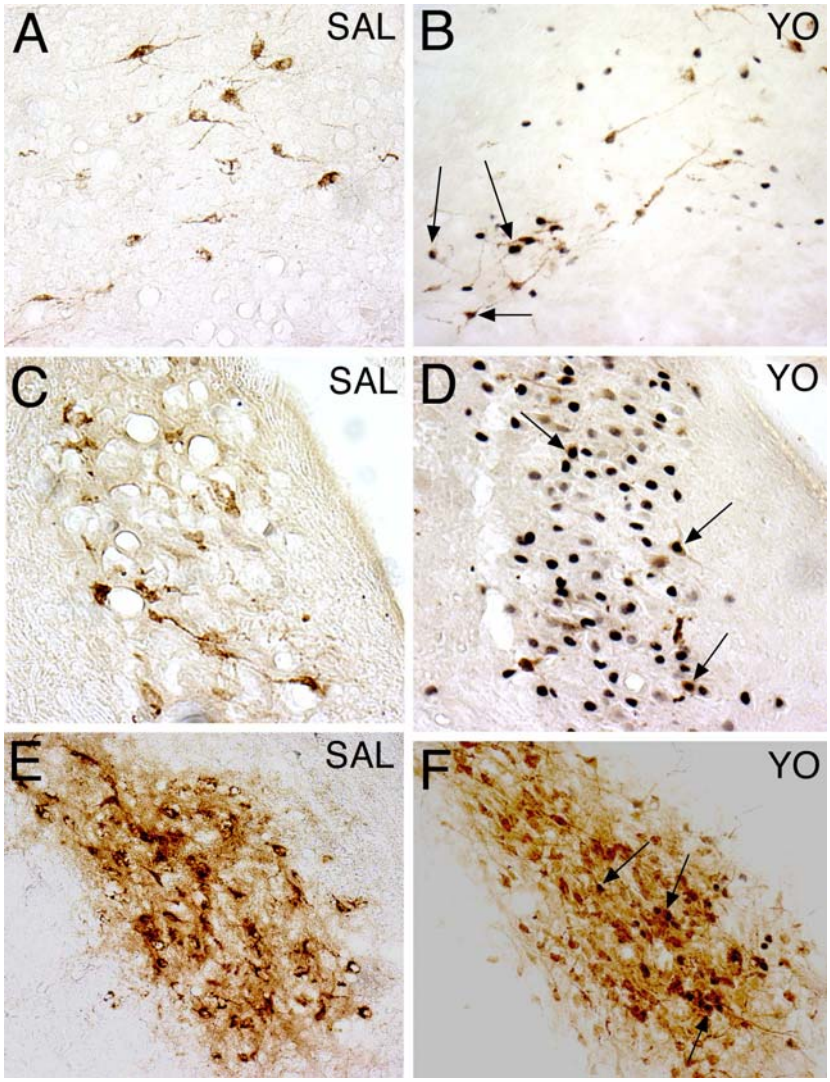

Figure 22. Photomicrographs depicting dual immunoperoxidase labeling for cFos (black nuclear label) and FG retrograde tracer (brown cytoplasmic label) within the mNST (A, B) LC (C, D), and PBN (E, F) in rats after exposure saline (A, C, E) or yohimbine (B, D, F) treatment. Arrows point out some of the activated (i.e., cFos-positive) retrogradely-labeled (i.e., CeA-projecting) neurons visible in each photomicrograph. See Figure 8 for quantitative data.

5. Chapter 5: Additional CCK Studies

Further analysis was performed on select CCK-treated cases from the previous study (see Chapter 2). These findings are presented as a separate chapter as they were completed following publication of the CCK study discussed in Chapter 2. Experimental findings are reported in this section and will subsequently be discussed in the Chapter 6 General Discussion section in relation to the other stressor paradigms. All experimental procedures are identical to the previous CCK study (Chapter 2) except those described below.

Experiment 1: Conditioned Flavor Avoidance (CFA)

Cholecystokinin-8 (CCK) stimulates gastric vagal afferents that carry viscerosensory signals to the brain. We recently demonstrated that CCK activates cFos in hindbrain noradrenergic (NA) neurons that project to the amygdala (Myers and Rinaman 2002), where NA signaling mechanisms are known to influence emotional learning (Chapter 2). CCK also activates peptidergic neurons in the lateral PBN that project directly to the CeA. Importantly, this direct PBN-to-CeA pathway is implicated in CFA learning (Lasiter and Glanzman 1985; Lamprecht and Dudai 1996; Yamamoto et al., 1997).

While endogenous levels of CCK play an important role in satiety, larger pharmacological doses are thought to inhibit feeding by inducing stereotypical sickness behavior indicative of nausea. Pharmacological doses of CCK (i.e., 10-100 μg/kg) are anorexigenic and stressful, producing plasma hormone and central neural response profiles that are largely indistinguishable from those produced by LiCl (McCann et al., 1989; Flanagan et al., 1992), a classic model of visceral illness that supports robust CFA learning. Results from previous studies are equivocal as to whether CCK treatment supports CFA learning. The behavioral

effects of CCK may be short-lived due to endogenous peptidases that shorten its half-life following acute systemic administration (i.e., ~10 min). The goal of the present study was to determine whether prolonging the effects of systemic CCK would promote CFA learning.

CFA Procedure: A sensitive two-bottle choice procedure (Deutsch and Hardy 1977) was used to determine whether systemic administration of CCK supports CFA learning. CFA training and testing were conducted during the light cycle of the photoperiod, between 1500 and 1700 h. Prior to the start of the CFA experiment, rats were acclimated for 2 days to i.p. injections of 0.15M NaCl (2 ml, room temp).

Adult male rats (300 g BW; n=33) naïve to CCK treatment underwent 22 h water deprivation, then half of the rats were presented with almond flavored tap water to drink from a graduated tube, and the others with banana flavored water (both 0.5% McCormick flavor extract). The left-right position of the bottle on each testing cage was switched after 15 min, with fluid intake recorded at 15 and 30 min time points. Thirty min after the end of the flavor exposure session, each rat received either a single or double injection(s) of 0.15M NaCl (2.0 ml, i.p.) in three separate experiments. Water was returned 30 min later with *ad libitum* access for the next 24 h. Rats were then water deprived again for 22 h and allowed to drink the alternate flavor for 30 min, with bottle positions switched after 15 min. Thirty min after the end of fluid access, each rat received either single or double injection(s) of CCK (3 or 10 μg/kg in 2.0 ml 0.15M NaCl, i.p.) in three separate experiments. Water was returned 30 min later with *ad libitum* access for the next 24 h. Rats were then again water deprived for 22 hr, then were given 30 min simultaneous access to two bottles containing almond or banana-flavored water. The

volume of each flavor consumed was recorded at 15 min, bottle positions were switched, and cumulative intake recorded at 30 min. Rats then were returned to *ad libitum* water access.

CFA data analysis: Within each CFA experiment, flavor preference ratios displayed by each rat were determined by dividing the volume consumed from each bottle during the 30-min choice test by the total volume consumed from both bottles. Outcomes indicating flavor preference ratios that do not differ significantly (i.e., 50%:50%) are interpreted as an absence of CFA, whereas an outcome indicating a preference ratio of 0%:100% would be interpreted as a complete avoidance of the flavor represented by the first value in the ratio. Individual rat preference ratio data were averaged to obtain group preference ratios (mean ± SE) for saline-paired flavors relative to CCK-paired flavors within each experiment. Student's t-test was used to determine whether group preference ratios for saline-paired and CCK-paired flavors were statistically different, with significance set at $P < 0.05$.

CFA Results: A single injection of CCK (10 μg/kg) did not produce a CFA (Fig. 23A). Conversely, double CCK injections (10 μg/kg) spaced 15 min apart produced a clear CFA response ($P < 0.001$; Fig. 23B). Double injections of a lower dose of CCK (3 μg/kg) did not produce a statistically significant CFA (Fig. 23C). However, results in individual rats were quite variable, as shown in Table 2. Half of the rats showed a strong CFA response to the CCK-paired flavor (bold), but half of the animals did not. An unusual response in one rat (the last one in the table) clearly skewed the group results. Qualitative observations suggest that double-dose CCK activates more cFos expression in the NST and lateral PBN compared to single-dose CCK (Fig. 24, 25).

Experiment 2: Phenotypic characterization of activated neurons after CCK treatment

Our previous study (Myers and Rinaman 2002) examined CCK-induced activation of hindbrain afferent inputs to the CeA. As reported in previous studies, we noted that a large majority of these neuronal inputs to the CeA were phenotypically noradrenergic, though we did not perform a quantitative analysis on this. We subsequently carried out an in depth phenotypic analysis of CCK-induced (10 μg/kg, single i.p. injection) activation of both hypothalamic CRH neurons and hindbrain NA cell groups implicated to play a role in stress and anxiety.

Distribution of activated noradrenergic neurons

Medulla

NST (A2 cell group): Two-way repeated measures ANOVA revealed a main effect (between subjects) of treatment group (saline vs. CCK) [$F(1,18) = 24.7$, $P = 0.0016$], a main within subjects effect of brain region (cNST, mNST, rNST) [$F(2,14) = 18.3$, $P = 0.0001$], and a significant interaction between treatment group and brain region [$F(2,14) = 12.2$, $P = 0.0009$] in the number of activated NA neurons per tissue section in the NST. Post hoc *t* comparisons revealed that CCK produced a significant increase in the number of activated NA neurons at all rostrocaudal levels of the NST compared to vehicle treatment (Fig. 26).

VLM (A1 cell group): Two-way repeated measures ANOVA revealed a main effect (between subjects) of treatment group (saline vs. CCK) [$F(1,18) = 40.6$, $P = 0.0004$], a main within subjects effect of brain region (cVLM, mVLM, rVLM) [$F(2,14) = 9.03$, $P = 0.003$], and a significant interaction between treatment group and brain region [$F(2,14) = 6.92$, $P = 0.008$] in the number of activated NA neurons per tissue section in the VLM. Post hoc *t* comparisons

indicated that CCK treatment significantly increased the number of activated NA neurons at all rostrocaudal levels of the VLM in comparison to vehicle treatment (Fig. 26).

Pons

LC (A6 cell group): One-way ANOVA revealed no significant effect of treatment group (saline vs. CCK) in the number of activated NA neurons per tissue section in the LC. Quantitative analysis revealed that CCK administration did not produce a significant increase in the number of activated LC NA neurons in comparison to saline ($P = 0.115$; Fig. 26).

Activation of hypothalamic CRH neurons

Relatively few cFos-positive neurons were observed in the PVN of saline-treated animals in comparison to CCK-treated cases. One-way ANOVA revealed a significant effect of treatment (saline vs. CCK) in the proportion of activated CRH neurons in the mpPVN [$F(1,6) = 93.2$, $P < 0.0001$). A post hoc *t* comparison revealed that significantly larger proportions of CRH neurons were activated after CCK compared to saline (Fig. 27).

APPENDIX D: Chapter 5 Figures

A

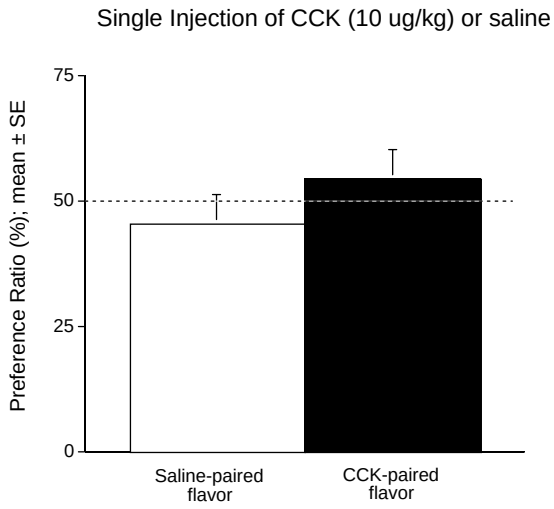

B

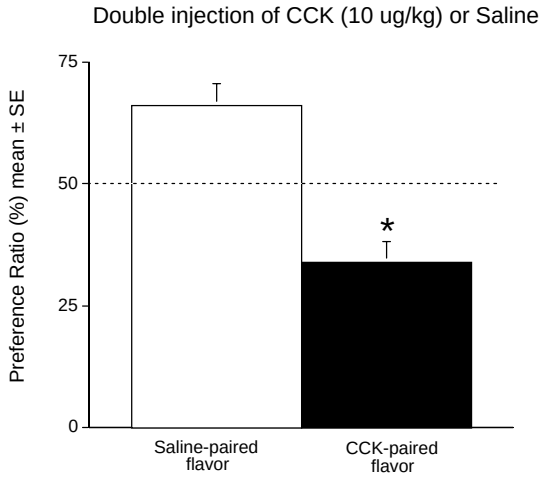

C

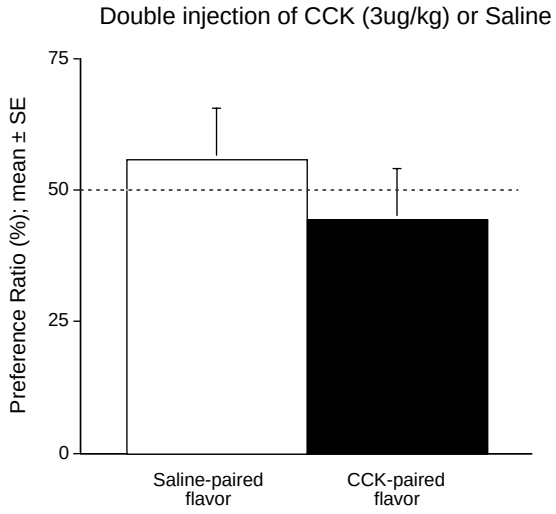

Figure 23. Preference ratios for a novel flavor after pairing with saline vs. CCK. (A) Single CCK injection (10 µg/kg; n=12), (B) Double CCK injections (10 µg/kg; n=11), (C) Double CCK injections (3µg/kg; n=10). Dashed lines indicate expected ratio with no effect of treatment (50%). Double injections of CCK (10 µg/kg) produce a clear CFA, *P < 0.001 saline- vs. CCK-paired flavor.

Table 2. Preference Ratios in 2-Bottle Choice Test (3 μg/kg CCK, dual injections spaced by 15 min)

Rat	saline-paired flavor	CCK-paired flavor
#03-25	**93.80%**	**6.25%**
#03-26	43.80%	56.30%
#03-27	16.70%	83.30%
#03-28	42.10%	57.90%
#03-29	**83.30%**	**16.70%**
#03-30	**73.30%**	**26.70%**
#03-53	**76.50%**	**23.50%**
#03-54	**77.80%**	**22.20%**
#03-55	50%	50%
#03-56	0%	100%

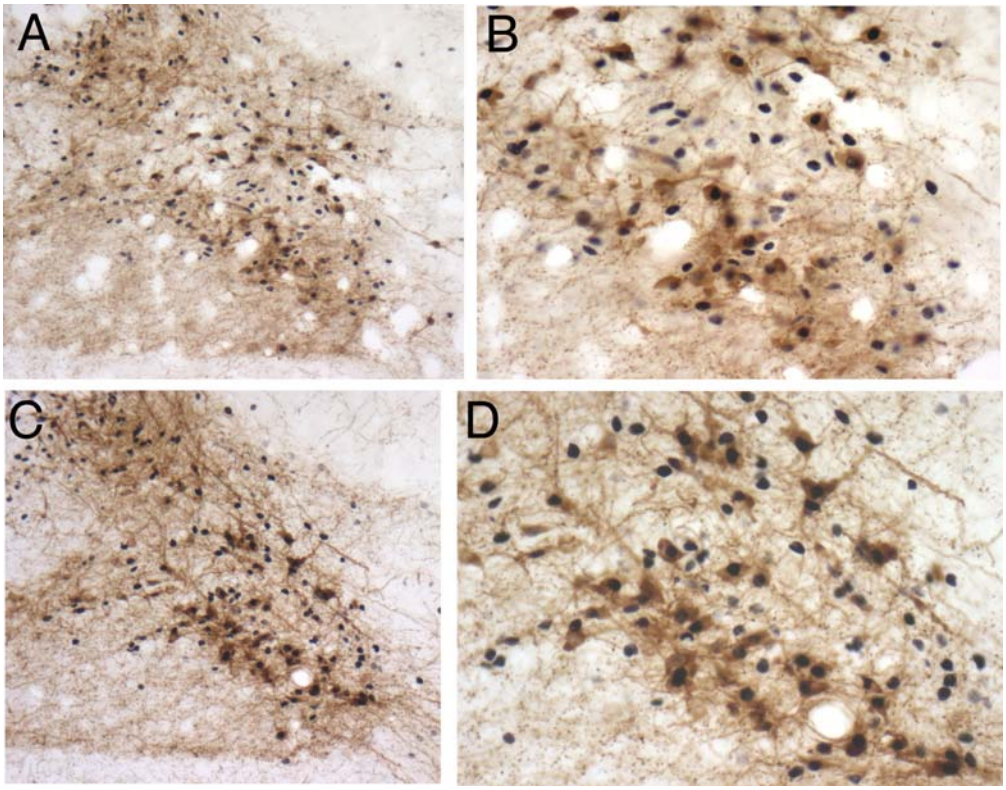

Figure 24. DβH immunolabeling (brown) and cFos expression in the NTS after: (A, B) a single CCK (10 µg/kg) injection i.p. or (C, D) a double CCK (10 µg/kg) injection i.p. (A,C) 10x and (B, D) 20x magnification.

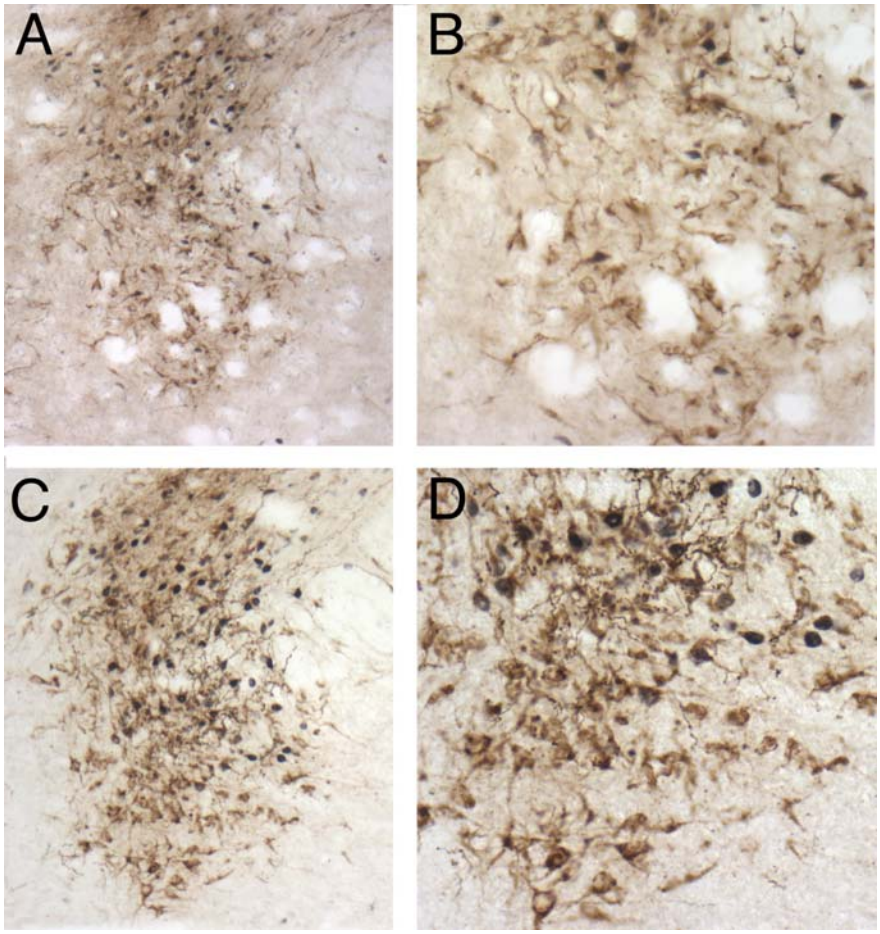

Figure 25. CGRP immunolabeling (brown) and cFos expression (black) in the PBN after: (A, B) a single CCK (10 µg/kg) injection i.p or (C, D) a double CCK (10 µg/kg) injection i.p. (A, C) 10x and (B,D) 20x magnification.

A

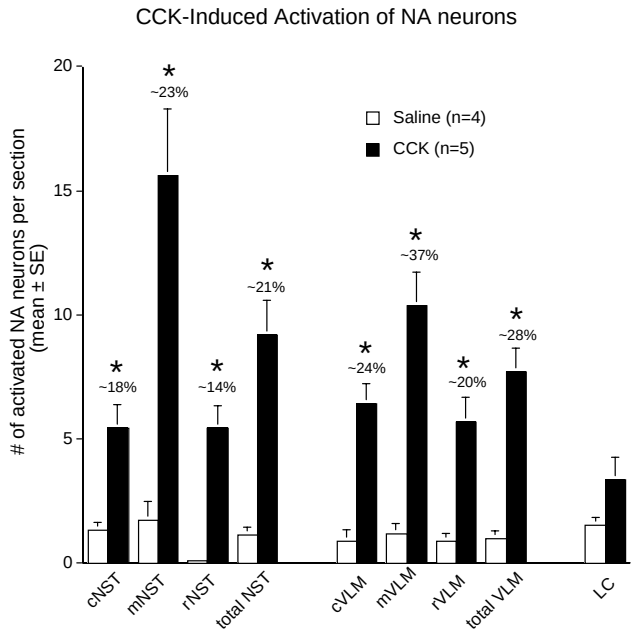

B

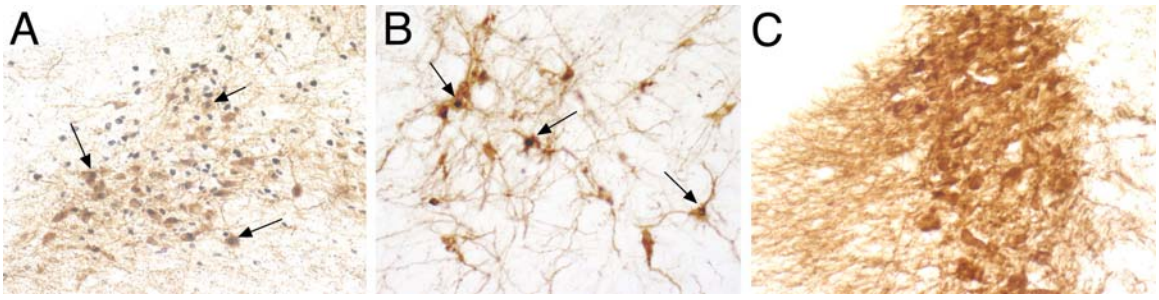

Figure 26. CCK treatment recruits NA neurons in the NST and VLM, but not the LC. (A) CCK-induced activation of NA neurons across the rostrocaudal axis of the NST and VLM, and in the LC. Bars represent the average number of activated NA neurons per tissue section. Group sizes are indicated in graph legend. * $P < 0.05$ relative to saline. (B) Photomicrographs showing dual immunolabeling for cFos (blue-black nuclear label) and DβH-positive NA neurons (brown cytoplasmic label) in a single tissue section through the: NTS (A), VLM (*B)*, and LC *(C)*. Arrows indicate activated (i.e., cFos-positive) NA neurons.

A **B**

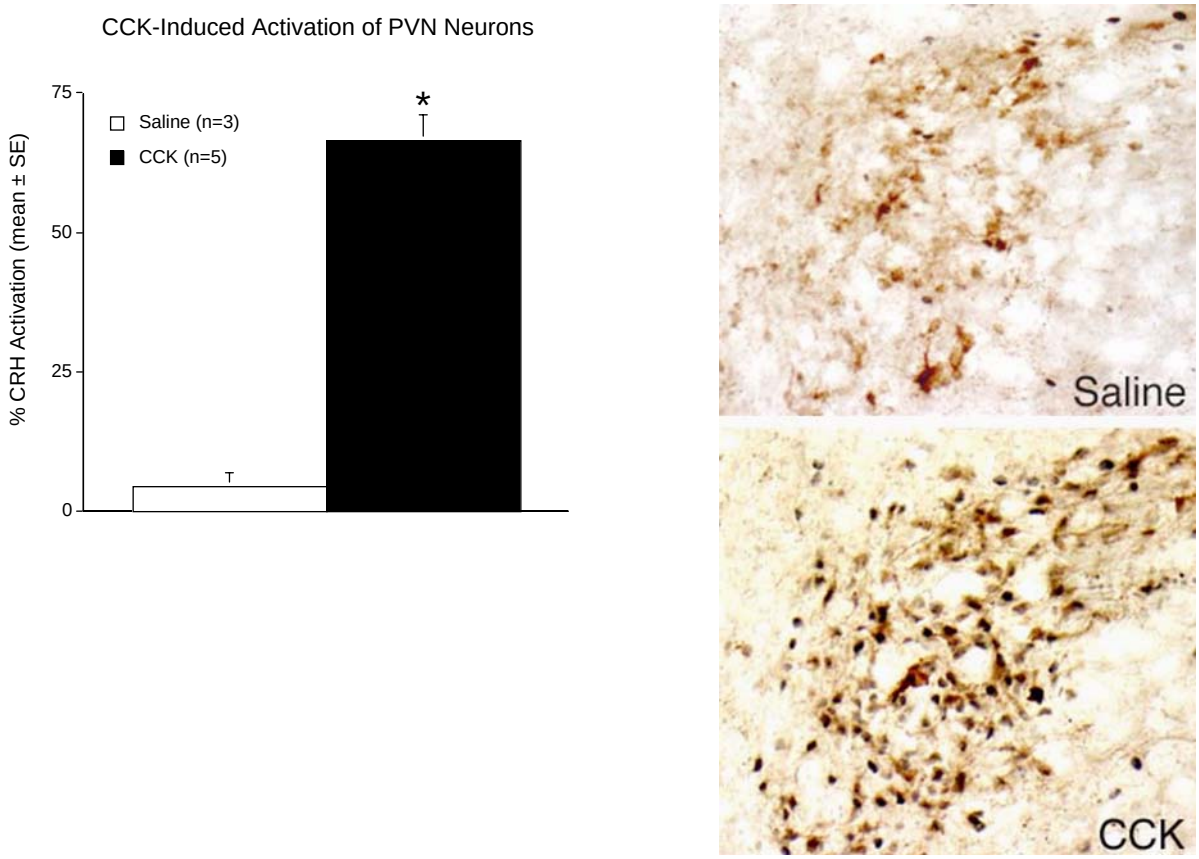

Figure 27. CCK treatment activated CRH neurons in the PVN. (A) Each set of bars represents the percent activation of CRH neurons averaged across cases in each experimental group. Group sizes are indicated in graph legend. * P = 0.0002 relative to saline. (B) Photomicrographs showing dual immunolabeling for cFos (black label) and CRH (brown cytoplasmic label) within the medial parvocellular subdivision of\ the PVN.

6. Chapter 6: General Discussion

*Note: see APPENDIX E for discussed comparisons.

The amygdala is thought to be an essential brain region for detecting emotional events and generating appropriate behavioral and physiological responses (i.e., autonomic and neuroendocrine) to these stimuli. Specifically, the central nucleus of the amygdala (CeA) appears necessary for a large array of conditioned learning paradigms and is implicated as a key limbic structure in the neural circuits that mediate fear, stress, and anxiety. The CeA, the major output nucleus of amygdala, receives input from both cortical areas and other amygdaloid nuclei, integrates this information, and subsequently influences behavioral, autonomic, and endocrine responses to stress through output projections to the brainstem, hypothalamus, and other limbic forebrain regions.

Importantly, brainstem catecholamine systems are thought to provide essential noradrenergic (NA) drive to forebrain regions that mediate endocrine, autonomic, and behavioral responses to stress and anxiety. Specifically, NA cell populations of the caudal medulla (NST and VLM) and pons (LC) provide a dense innervation of the CeA, BNST, and PVN, where they exert influence on HPA function (Sawchenko and Swanson 1982) and influence emotional processing. A wide range of interoceptive and exteroceptive stimuli produce an increase in cFos expression by these NA brainstem cell populations that is paralleled by an observed increase in NA activity within the amydala**.**

While a diverse range of stimuli are known to activate these medullary and pontine NA cell groups, it is currently unclear if stressor-specific patterns of cell activation are elicited in these regions. However, a growing number of studies are providing convincing evidence that there in fact is stressor-specific recruitment of these hindbrain NA cell populations (Dayas et al.,

2001; Li et al., 1996). Whereas few studies to date have directly compared multiple stressors simultaneously, an advantage of the present investigation is that it provides a within-study comparison of neuronal recruitment patterns elicited by categorically different stressors.

The results of the present study are consistent with previously reported findings in that the different stressors (i.e., CCK, TMT, and YO) implemented in our study elicit unique activation profiles of brainstem NA cell populations, including those that provide direct input to the CeA. We further demonstrate that these stressors support aversive conditioned learning and induce a similar robust activation of CRH neurons at the apex of the HPA axis (Fig. 28), suggesting that these stimuli are comparable in their ability to recruit the neuroendocrine stress axis. We recognize that examining stressor-induced plasma hormone levels would likely provide a better indicator of stressor intensity/magnitude; however, our findings are consistent with previous reports that CCK and TMT treatment increase plasma CORT levels to a similar degree in rats (Miaskiewicz et al., 1989; Morrow et al., 2000; Vernet-Maury et al., 1999, 1984). Though evidence for YO-induced increases in plasma CORT is lacking, one study reports YO-induced increases in plasma ACTH in rats (Kiem et al., 1995), which predict a likely increase in CORT. Interestingly, each stressor recruited a significant and similar number of NA neurons within the NST (~21-23%; Fig. 29A). In contrast, a more selective activation profile of VLM and LC NA neurons was observed, with TMT and YO recruiting similar numbers of cells and significantly more neurons compared to CCK (Fig. 29B, 30). In general, TMT and YO appeared to recruit a larger proportion of NA neurons in the VLM (~58%) compared to those in the NST, and the degree of activation did not seem to differ across rostrocaudal level of the VLM. The apparently selective response of the VLM and LC to TMT and YO may reflect heightened arousal associated with these particular stimuli, whereas other similarities in NA cell activation observed

in the NST may reflect novelty and/or the effects of nonspecific peripheral feedback unrelated to the potential behavioral significance of these stimuli. Alternatively, the selective TMT- and YO-induced recruitment of the VLM and LC may reflect a maximal NA activation level reached in these brain regions.

Similar to the apparently selective NA activation profiles observed in this study, differential recruitment profiles of afferent inputs to the CeA arising from the hindbrain were observed among stressors. Presumably, a large majority of these projections to the CeA are phenotypically NA given the known projection distributions (see Introduction). Significantly greater proportions of CeA-projecting neurons in the VLM and LC were recruited by TMT and YO compared to CCK (Fig. 31). Afferent inputs to the CeA arising in the NST were similarly recruited by CCK and YO, whereas TMT exposure recruited a significantly greater proportion of these neurons in comparison, although it is questionable as to how biologically significant this finding is (Fig. 31). Overall, these activation patterns of CeA-projection neurons seem to parallel the NA neuronal activation profiles observed across these brain regions in this study. In view of this, it is possible that afferent NA drive arising from the NST may stimulate the increase in CRH activity observed across all stressors in this study. This is fitting with the observation that the greatest number of activated NA neurons were at the mid-NST level (i.e., at the level of the area postrema), which is the rostrocaudal level of the NST known to provide the densest input to the PVN (Rinaman et al., 1995).

An additional finding of the present study was that a moderate and similar proportion of afferent inputs to the CeA arising in the external portion of the lateral PBN (elPBN) were activated with each stressor (Fig. 31, 32). The observed cFos expression in the elPBN and the activation of CeA inputs arising from this region parallels the observed conditioned flavor

avoidance (CFA) learning with each stressor, as conditioned aversion/avoidance responses are dependent on involvement of both the PBN and amygdala (Lasiter and Glanzman 1985; Lamprecht and Dudai 1996; Yamamoto et al., 1997; Sakai and Yamamoto 1998; Grigson et al., 1998; Reilly 1999; Wang and Chambers 2002). Furthermore, robust stressor-induced increases in cFos expression were observed in both the amygdala and PBN in the present study (Fig. 32, 33). On the whole, these findings lend additional support to the view that dissimilar stressors generate interoceptive feedback, as CCK, TMT, and YO all recruited the well-defined classical viscerosensory circuit between the PBN and CeA (see Introduction).

The fact that each stressor supported CFA learning suggests that these stimuli are highly aversive to rats, although the specific properties which make them aversive cannot be identified based on our experimental findings. It is possible that these stressors are nauseogenic as CCK and YO have been subjectively reported to cause nausea in humans (Miaskiewicz et al., 1989; Mattila et al., 1988; Linden et al., 1985); however, support for this is lacking with TMT. Presumably, these stressors may also elicit autonomic feedback that the brain may interpret as malaise.

While our findings clearly demonstrate that there are specific neural correlates associated with select stressors of this study, it is remarkable that there is a large degree of overlap in the recruitment patterns of a number of neuronal populations by these stressors despite the clear differences in the both the general characteristics and relevant sensory modalities associated with these stimuli. The findings of our study indicate that the activation of hindbrain NA systems is a common thread among the stimuli examined, though the mechanisms by which these neuronal populations are recruited likely differ markedly depending on the stimulus.

Systemic CCK administration operates as a model of interoceptive stress in the present study. Accordingly, the actions of systemic CCK are initiated by activation of CCK_A receptors located on gastric vagal afferents which terminate in the NST near or on local catecholaminergic (i.e., noradrenergic and adrenergic) cell populations. It is assumed that subsequent neurotransmission from the NST to limbic forebrain regions carries viscerosensory information that strongly influences emotional processing.

TMT, on the other hand, operates as a model of exteroceptive stress and is routed through the olfactory system. Olfactory information is sent directly to the anterior amygdala as this limbic region is continuous with the primary olfactory cortex (Price 1991; Switzer et al., 1985). These anatomical relationships suggest a high level of functional connectivity between the olfactory and limbic systems. Moreover, approximately 40% of the neurons in the rodent amygdala are reported to respond to olfactory stimulation (Cain and Bindra 1972), and evidence suggests that the human amygdala participates in hedonic or emotional processing of olfactory stimuli (Zald and Pardo 1997). Subsequent descending projections from the amygdala likely recruit these very same hindbrain NA cell populations. It is generally assumed that exteroceptive stressors recruit medullary NA neurons via descending inputs from the forebrain, particularly through direct projections from the amygdala (Li et al., 1996). Consistent with this view is experimental evidence demonstrating that electrical stimulation of the amygdala elicits cFos expression in medullary NA cells, and that destruction of the amygdala alters medullary NA cell responses to restraint stress (Petrov et al., 1995; Dayas and Day 2001).

Administration of systemic yohimbine (YO), a sympathomimetic agent, influences both the peripheral and central nervous system due to its ability to cross the blood brain barrier. Therefore, YO may activate the sympathetic nervous system via the stimulation of central NA

pathways involved in mediating anxiety, by activating central autonomic nuclei which regulate sympathetic responses, or through the blockade of presynaptic peripheral sympathetic nerves. It is currently unclear whether the central effects of YO occur subsequent to peripheral feedback or vice versa. In view of this, YO cannot be easily assigned to either interoceptive or exteroceptive stressor classes; instead this stimulus likely sits along a spectrum between these two general categories. Consequently, YO likely recruits global ascending and descending circuitry alike that influences hindbrain NA cell populations.

TMT and YO produced similar NA and CeA-projection activation profiles that differed significantly from CCK treatment. Parallel similarities were observed between TMT and YO upon examining cFos responses in several brain structures implicated as key areas of the defense circuit. Both stressors produced marked increases in cFos expression within the piriform and endopiriform cortices, periaqueductal gray (PAG), and lateral septum, although these responses appeared to be more robust with TMT exposure (data not shown). Additionally, TMT exposure produced a robust increase in cFos expression within the ventromedial hypothalamus, interpeduncular nucleus, and the dorsal and ventral premammillary nuclei of the hypothalamus (data not shown). Notably, the ventromedial and premammillary nuclei of the hypothalamus provide moderate input to the medial amygdala (MeA) that contributes to a brain defense circuit. In contrast, CCK treatment did not induce remarkable increases in cFos expression within these brain regions.

Accordingly, TMT and YO produced apparent activation of the MeA whereas CCK elicited a robust response in the CeA only (data not shown). This finding is not surprising given the observed TMT- and YO-induced increase in cFos activity within the endopiriform cortex, a region known to provide direct input to the MeA (Behan and Haberly 1999). Furthermore,

chemosensory signals, such as TMT, can reach the MeA directly via projections from the accessory olfactory bulb and main olfactory bulbs (Scalia and Winans 1975; McDonald 1998). TMT and YO, but not CCK, recruited NA neurons within the LC and VLM as well. Although the source of the noradrenergic input to the MeA is sparse compared to the other nuclei, observations made in the course of mapping studies focused on other amygdalar nuclei suggest that noradrenergic input to the dorsal component of the MeA may originate from the VLM A1 cell group (Zardetto-Smith and Gray, 1990; Roder and Ciriello, 1993) or the LC, which provides diffuse innervation of the entire amygdaloid complex, including sparse inputs to the MeA (Jones and Moore 1977; Fallon et al., 1978). Accordingly, "missed" injection sites that targeted the MeA instead of the CeA in the present study, produced a small amount of retrograde labeling in the medullary and pontine regions analyzed. Diffuse NA terminals were also observed in the MeA upon histological examination in the present study (observational results). Moreover, the LC provides diffuse NA drive to the entire cortex, which presumably includes olfactory regions that communicate directly with the MeA. Therefore, NA inputs from these brainstem regions might contribute to the increased activity observed within the MeA with these selective stressors via either direct or indirect routes through the cortex.

Previous studies report that "emotional stressors" (i.e., exteroceptive) elicit cFos more consistently in the MeA than the CeA (Arnold et al., 1992; Pezzone et al., 1992; Bhatnager and Dallman 1998; Li and Sawchenko 1998; Dayas et al., 2001) whereas several physical stressors (i.e., interoceptive) evoke cFos more strongly in CeA than MeA (Ericsson et al 1994; Li et al., 1996; Thrivikraman et al., 1997; Yamamoto et al., 1997; Buller et al., 1998). Moreover, it is generally assumed that the MeA is critical for unconditioned emotional stressors to influence HPA axis, while CeA is for conditioned emotional stressors (Van der Kar et al., 1991;

Roozendaal et al., 1992). A recent study demonstrated that CeA lesions suppress PVN CRH cell responses to physical stressors (Xu et al., 1998). Interestingly, TMT appeared to produce a selective and robust activation of the lateral subdivision of the CeA (Fig. 33) in addition to the MeA. The fact that TMT, an exteroceptive stressor, robustly activates both the MeA and CeA abates the notion that distinct components of amygdala may mediate the neuroendocrine responses to categorically different types of stressors. However, in view of the fact that the olfactory system provides direct input to the MeA, which in turn provides a substantial input to the CeA (Canteras et al., 1995), it is possible that observed increase in cFos expression within the CeA is generated via this route.

Nonetheless, specific stressor-induced activation of the lateral subdivision of the CeA (CeAL) is functionally meaningful given its selective projection district to brain regions implicated in stress and anxiety and given the observed increase in cFos expression within these brain regions in the present investigation. The CeAL receives a wide array of input from cortical areas and exhibits a relatively simple bidirectional projection pattern with three major brain regions: the medial subdivision of the CeA, the lateral BNST, and the elPBN (Petrovich and Swanson 1997).

The caudal aspect of the CeAL has projections that terminate heavily and selectively in both the oval and fusiform nuclei of the lateral division of the BNST, which together are collectively termed the lateral extended amygdala (Sun et al., 1991; Alheid et al., 1995; Petrovich and Swanson 1997). Therefore, stimulation or manipulations of the CeA are presumably going to have profound influences on the BNST. Furthermore, the CeA and BNST share strong reciprocal projections between each other and with the PBN and dorsal vagal complex (Moga et al., 1990; Veening et al., 1984; Higgins and Schwaber 1983), and both have

high γ-aminobutyric acid (GABA) content (Sun and Cassell 1993). Likewise, the MeA contains GABAergic neurons and is known to provide heavy inputs to the BNST (Canteras et al., 1995); therefore, manipulations of this nucleus may also influence activity of the BNST. Of further interest is the observation that the MeA projects to caudal regions of the anterolateral region of the BNST, which also receive dense input from the CeA (Sun et al., 1991). Given the intricate neurochemical and anatomical relationships between the BNST, CeA, and MeA, coupled with a large body of literature implicating both structures in emotional processing, it is imperative that further studies be carried out to elucidate whether, and how, these similar brain structures operate in a concerted or differential manner to mediate responses to stress and anxiety.

In the present study, robust stressor-induced increases in cFos expression were observed in the lateral BNST (both oval and fusiform nuclei), similar to the CeA and MeA (Fig. 34). Accordingly, previous studies report that the BNST receives NA inputs from the pontine and medullary cell groups, (Pickel et al., 1974; Sawchenko and Swanson 1982; Riche et al., 1990; Roder and Ciriello 1994) which are much denser than those going to the CeA. One preliminary study demonstrates that YO activates neural inputs to the BNST, in addition to the CeA, that arise in the NST, VLM, and lateral PBN (Myers et al., 2004 Exp Bio Abstract). Therefore, it is plausible that NA drive, originating from these hindbrain cell populations, to the BNST may serve as an additional neural correlate of the behavioral effects associated with the stressor paradigms implemented in the present study. However, it is currently unclear if different subsets of hindbrain NA cell groups project to the CeA and BNST, or if the same NA neurons provide input to both structures via collateral projections. Moreover, future studies are necessary to determine if the CeA or BNST, or both, are critical to the behavioral and neural responses observed with the each of the stressors used in the current study.

In summary, the present findings demonstrate that CCK, TMT, and YO are behaviorally aversive stimuli in rats, as they support conditioned flavor avoidance learning and have been shown or are known to reduce food intake. These emotional stimuli also result in robust activation of hypothalamic neurons and recruit hindbrain NA neurons that provide afferent input to the amygdala. These results suggest that these differential emotional learning paradigms may potentially influence emotional learning via stressor-specific ascending NA projection pathways to the CeA (and likely via the BNST), of which originate from both pontine and medullary NA cell groups. The behavioral responses and corresponding patterns of stressor-induced neural activity reported here establishes the general groundwork for future experiments to probe the specific neural substrates necessary for the observed responses to the emotionally provoking stimuli of the present study.

Specifically, selective NA cell groups, and their selective projection districts to the CeA, BNST, and PVN, could be lesioned to determine which hindbrain populations drive the associated behavioral responses to a given stressor, and whether projections to the CeA or BNST are more crucial for mediating these effects. Furthermore, removing NA afferent drive to the forebrain from brainstem viscerosensory nuclei, or disrupting autonomic feedback by using an autonomic ganglion blocker, may elucidate a more defined role for interoceptive feedback in emotional processing. Inquiries such as these remain to be answered and demand further experimental consideration. Investigations that focus on identifying stressor-specific neuronal phenotypes and associated behavioral and neural correlates, such as the present study, offer the benefit of new insight into our understanding of stress-related pathogeneses and provide information relevant to current clinical practice.

APPENDIX E: Chapter 6 Statistical Analysis & Figures

Stressor-Induced activation of CRH-positive hypothalamic neurons

One-way ANOVA revealed no significant effect of treatment group (CCK, high TMT, or YO) in the proportion of activated CRH neurons in the mpPVN [$F(2,16) = 1.92$, $P = 0.18$]. CCK, high TMT exposure, and YO activated CRH neurons in the PVN to a similar extent (~61-73%; Fig. 28).

Stressor-Induced activation of DβH-positive NA neurons

NST (A2 cell group): Two-way repeated measures ANOVA revealed no significant main effect (between subjects) of treatment group (CCK, high TMT, YO) in the number of activated NA neurons per tissue section in the NST. Within subjects, there was a significant main effect of rostrocaudal level (cNST, mNST, rNST) [$F(2,42) = 46.1$, $P < 0.0001$], but no significant interaction between treatment group and rostrocaudal level in the number of activated NA neurons per tissue section in the NST. CCK, high TMT exposure, and YO activated similar numbers of NA neurons at all rostrocaudal levels of the NST, except the cNST where high TMT activated significantly more NA neurons compared to CCK ($P = 0.005$; Fig. 29A).

VLM (A1 cell group): Two-way repeated measures ANOVA revealed a significant main effect (between subjects) of treatment group (CCK, high TMT, YO) [$F(2,48) = 18.7$, $P < 0.0001$] and a significant within subjects effect of rostrocaudal level (cVLM, mVLM, rVLM) [$F(2,42) = 8.86$, $P = 0.0006$], but no significant interaction between treatment group and rostrocaudal level in the number of activated NA neurons per tissue section in the VLM. Post hoc *t* comparisons revealed that high TMT exposure and YO activated similar numbers of NA neurons at each

rostrocaudal level of the VLM that were significantly greater then the number of NA neurons activated by CCK in this region ($P < 0.05$ for each comparison; Fig. 29B).

LC (A6 cell group): One-way ANOVA revealed a significant main effect of treatment group (CCK, high TMT, YO) in the number of activated NA neurons per tissue section in the LC [$F(2,21) = 15.4$, $P < 0.0001$]. Post hoc *t* comparisons indicated that high TMT exposure and YO activated similar numbers of NA neurons in the LC that were significantly greater then the number of NA neurons activated by CCK in this region ($P < 0.0001$ for each comparison; Fig. 30).

Quantitative analysis of stressor-induced activation of brainstem inputs to the CeA

Two-way repeated measures ANOVA revealed a significant main effect (between subjects) of treatment group (CCK, high TMT, YO) [$F(2,54) = 20.1$, $P < 0.0001$], a significant within subjects effect of brainstem region (NST, VLM, LC, PBN) [$F(3,45) = 27.5$, $P < 0.0001$], and a significant interaction between treatment group and brainstem region on the proportion of treatment-induced activation of retrogradely labeled brainstem neurons [$F(6,45) = 6.93$, $P < 0.0001$].

Post hoc *t* comparisons revealed that high TMT exposure activated a greater proportion of retrogradely labeled CeA inputs in the NST (~52%) compared to both CCK (~30%) and YO (~38%) ($P < 0.05$ for each comparison; Fig. 31). In the VLM, high TMT exposure and YO recruited similar proportions of retrogradely labeled CeA inputs (~37-49%), both of which differed significantly from CCK (~19%) ($P < 0.05$ for each comparison; Fig. 31). Similarly, high TMT exposure and YO recruited similar proportions of retrogradely labeled CeA afferents in the LC (~29-32%), which differed significantly from CCK (~4%) ($P < 0.05$ for each

comparison; Fig. 31). CCK, high TMT exposure, and YO activated retrogradely labeled CeA inputs in the PBN to a similar extent (~15-21%; $P < 0.05$ for each comparison; Fig. 31, 32).

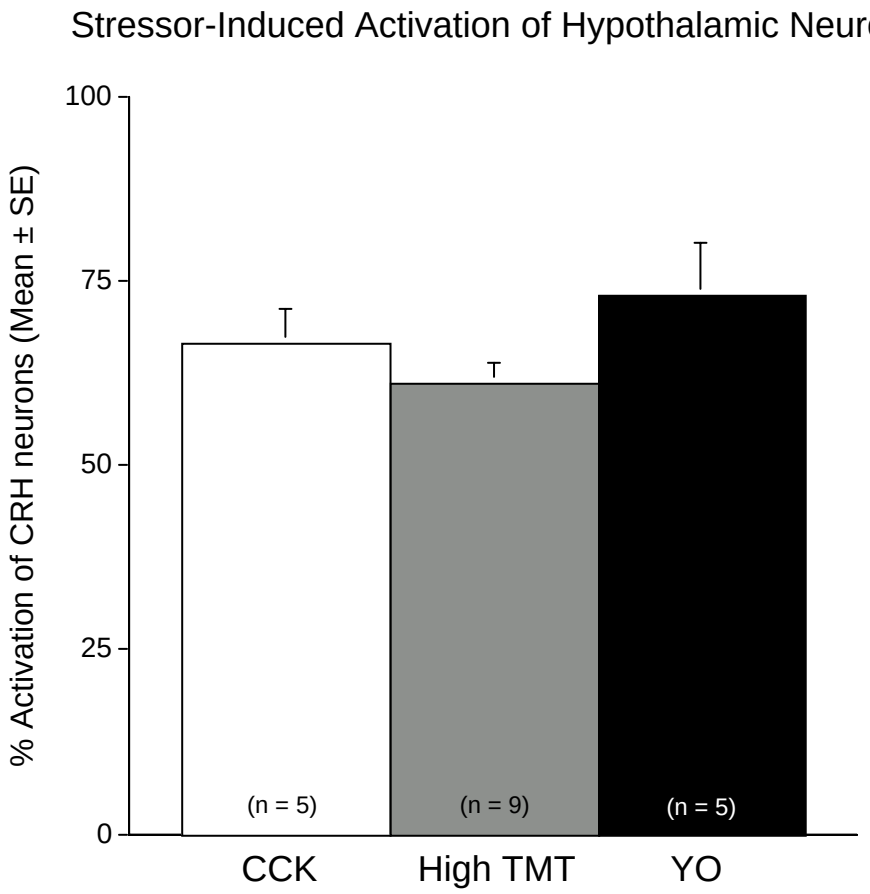

Figure 28. Stressor--induced activation of CRH-immunopositive neurons within the medial parvocellular PVN. Bars represent group averages of the percentage of CRH-positive neurons that were double-labeled for cFos. Group sizes are indicated in within bars of graph (n). CCK, high TMT exposure, and YO activated similar proportions of CRH neurons.

A

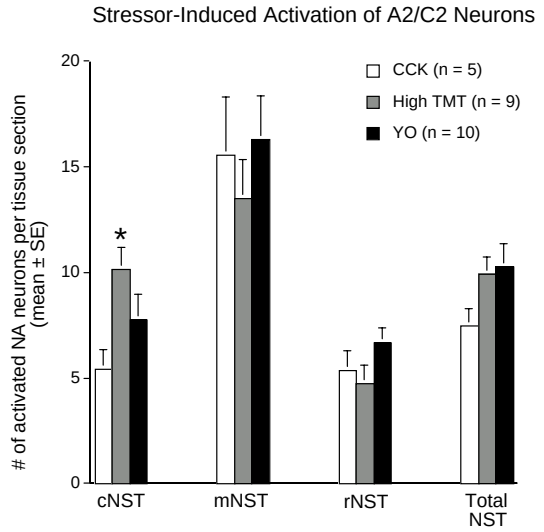

B

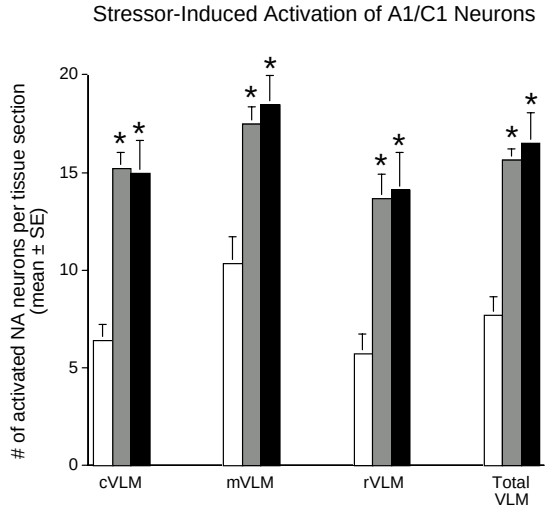

Figure 29. Stressor-induced activation of NA neurons in the NST and VLM across three rostrocaudal levels: caudal to the area postrema (AP) (cNST, cVLM), through the level of the AP, i.e., middle levels (mNST, mVLM), and rostral to the AP (rNST, rVLM). (A) Activation of NA neurons in the NST, * $P < 0.05$ relative to CCK in cNST and (B) Activation of NA neurons in theVLM, * $P < 0.05$ relative to CCK. Group sizes are indicated in the graph legend.

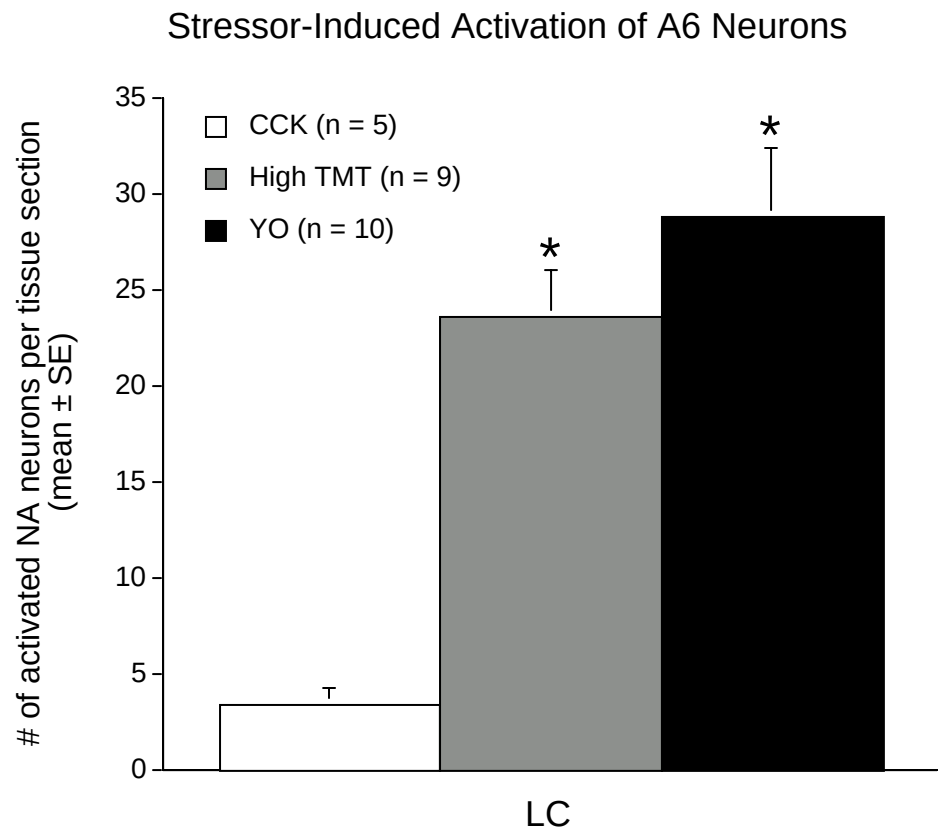

Figure 30. Stressor-induced activation of NA neurons in the LC. * $P < 0.0001$ compared to CCK. Group sizes are indicated in graph legend. High TMT and YO activated significantly greater numbers of NA neurons compared to CCK.

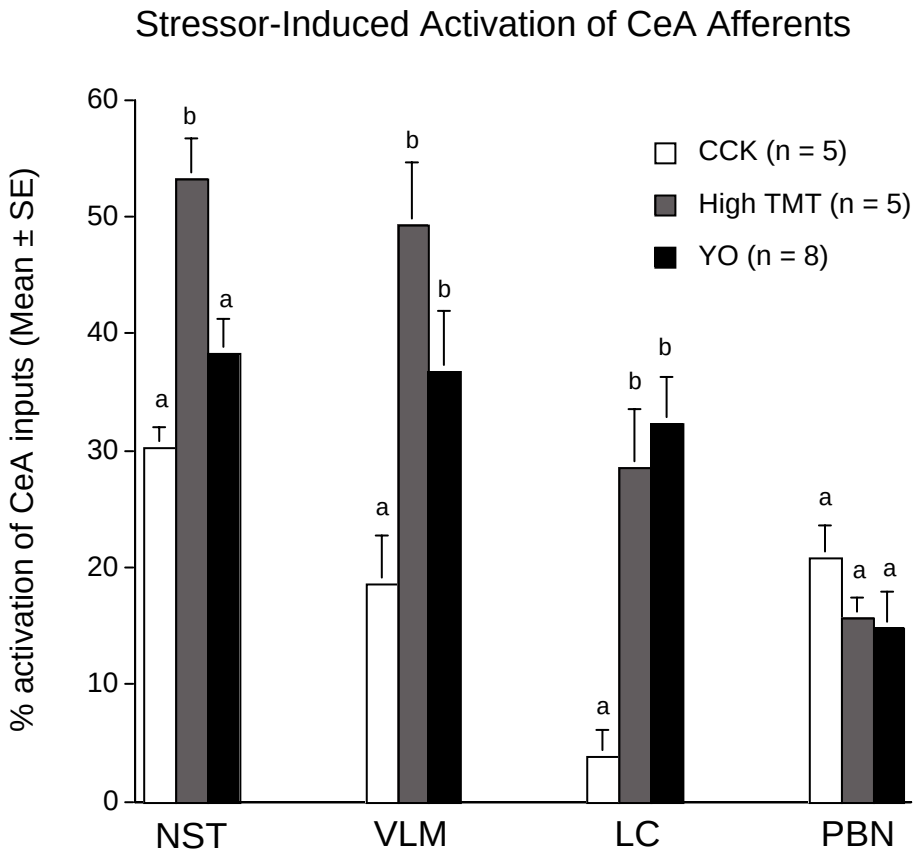

Figure 31. Stressor-induced activation of retrogradely labeled brainstem neurons projecting to the CeA. Bars represent the percentage of retrogradely labeled neurons in each region (i.e., NST, VLM, LC, PBN) activated to express cFos in each treatment group. Within each region, bars with different letters (a, b) are significantly different ($P < 0.05$). For PBN values, a* over the high BE bar indicates $P < 0.05$ compared to low BE, but $P > 0.05$ compared to low TMT. Group sizes are indicated in graph legend. *Note, group numbers for PBN differ from graph legend: CCK (n = 4), high TMT (n = 3), and YO (n = 5).

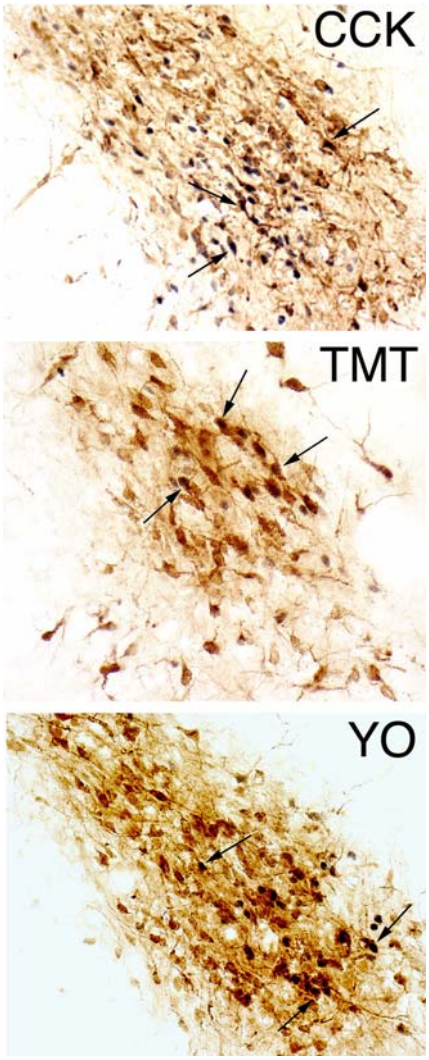

Figure 32. Photomicrographs depicting dual immunoperoxidase labeling for cFos (black nuclear label) and FG retrograde tracer (brown cytoplasmic label) within the PBN after CCK, TMT, or YO treatment. Arrows point out some of the activated (i.e., cFos-positive) retrogradely-labeled (i.e., CeA-projecting) neurons visible in each photomicrograph. See Figure 31 for quantitative data.

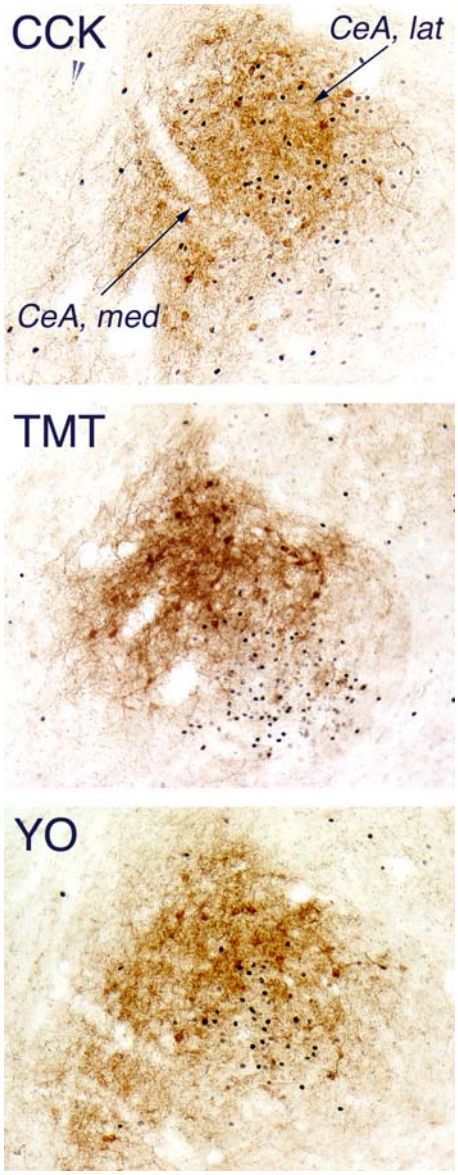

Figure 33. Photomicrographs depicting dual immunoperoxidase labeling for cFos (black nuclear label) and CRH (brown cytoplasmic label) within medial and lateral subregions of the central nucleus of the amygdala (CeA) in rats after CCK, high TMT, or YO treatment. cFos activation appears greatest within the lateral CeA after each stressor treatment.

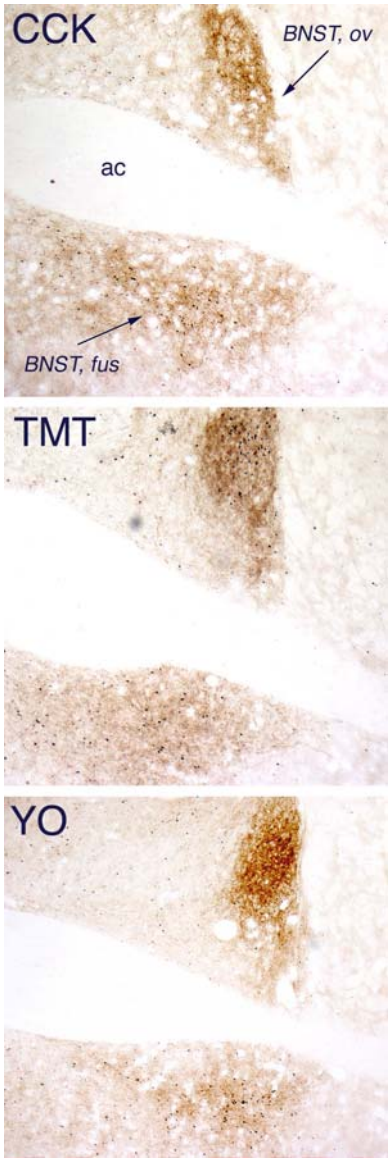

Figure 34. Photomicrographs depicting dual immunoperoxidase labeling for cFos (black nuclear label) and CRH (brown cytoplasmic label) within the oval (ov) and fusiform (fus) nuclei of the bed nucleus of the stria terminalis (BNST) in rats after exposure to CCK, TMT, or YO. anterior commissure (ac).

Bibliography

Alheid G, de Olmos JS, Beltramino CA (1995). Amygdala and extended amygdala. In: Paxinos, G. (Ed.), The Rat Nervous System. Academic Press, New York, pp. 495-578.

Arnold FJ, De Lucas Bueno M, Shiers H, Hancock DC, Evan GI, Herbert J (1992). Expression of c-fos in regions of the basal limbic forebrain following intracerebroventricular corticotrophin-releasing factor in unstressed and stressed male rats. Neuroscience 51:377-390.

Beaulieu S, DiPaolo T, Cote J, Barden N (1987). Participation of the central amygdaloid nucleus in the response of adrenocorticotropin secretion to immobilization stress: Opposing roles of the noradrenergic and dopaminergic systems. Neuroendocrinology 45:37-46.

Behan M, Haberly LC (1999). Intrinsic and efferent connections of the endopiriform nucleus in the rat. J Comp Neurol 408:532-548.

Benarroch EE (1993). The central autonomic network: Functional organization, dysfunction, and perspective. Mayo Clin Proceedings 68:988-1001.

Bhatnager S, Dallman M (1998). Neuroanatomical basis for facilitation of hypothalamic-pituitary-adrenal responses to a novel stressor after chronic stress. Neuroscience 84:1025-1039.

Bhattacharya SK, Satyan KS, Chakrabarti A (1997). Anxiogenic action of caffeine: an experimental study in rats. J Psychopharmacol 11:219-224.

Blanchard DC, Blanchard RJ (1973). Innate and conditioned reactions to threat in rats with amygdaloid lesions. J Comp Physiol Psychol 81:281-290.

Blanchard DC, Griebel G, Blanchard RJ (2003). Conditioning and residual emotionality effects of predator stimuli: some reflections on stress and emotion. Prog Neuro-Psychopharmacol Biolog Psych 27:1177-1185.

Buller KM, Xu Y, Day TA (1998). Indomethacin attenuates oxytocin and hypothalamic-pituitary-adrenal axis responses to systemic interleukin-1β. J Neuroendocrinol 10:519-528.

Burwash MD, Tobin ME, Woolhouse AD, Sullivan TP (1998). Laboratory evaluation of predator odors for eliciting an avoidance response in roof rats (Rattus rattus). J Chem Ecology 24:49-66.

Cain DP, Bindra D (1972). Responses of amygdala single units to odors in the rat. Exp Neurol 35: 98-110.

Callahan MF, Beales M, Oltmans GA (1984). Yohimbine and Rauwolscine Reduce Food Intake of Genetically Obses *(obob)* and Lean Mice. Pharmacol Biochem Behav 20:591-99.

Cannon WB (1929). Organization for physiological homeostasis. Physiol Rev 9:399-431.

Canteras NS, Simerly RB, Swanson LW (1995). Organization of projections from the medial nucleus of the amygdala: a PHAL study in the rat. J Comp Neurol 360:213-245.

Canteras NS, Goto M. Fos-like immunoreactivity in the periaqueductal gray of rats exposed to a natural predator (1999). *NeuroReport* 10:413-8.

Casada JH, Dafny N (1991). Restraint and stimulation of bed nucleus of the stria terminalis produce similar stress-like behaviors. Brain Res Bull 27:207-212.

Ceccatelli S, Villar MJ, Goldstein M, Hokfelt T (1989). Expression of c-Fos immunoreactivity in transmitter-characterized neurons after stress. Proc Natl Acad Sci USA 86:9569-9573.

Charney DS, Heninger GR, Redmond DE (1983). Yohimbine induced anxiety and increased noradrenergic function in humans: Effects of diazepam and clonidine. Life Science 33:19-29.

Chopin P, Pellow S, File SE (1986). The effects of yohimbine on exploratory and locomotor behaviour are attributable to its effects at noradrenaline and not at benzodiazepine receptors. Neuropharmacology 25:53-57.

Chun-I Li, Maglinao TL, Takahashi LK (2004). Medial amygdala modulation of predator odor-induced unconditioned fear in the rat. Behav Neurosci 118:324-332.

Ciriello J, Calaresu FR (1980). Monosynaptic pathway from cardiovascular neurons in the nucleus tractus solitarii to the paraventricular nucleus in the cat. Brain Res 193:529-533.

Clark KB, Smith DC, Hassert DL, Browning RA, Naritoku DK, Jensen RA (1998). Posttraining electrical stimulation of vagal afferents with concomitant vagal efferent inactivation enhances memory storage processes in the rat. Neurobio Learning and Memory 70:364-373.

Clark KB, Naritoku DK, Smith DC, Browning RA, Jensen RA (1999). Enhanced recognition memory following vagus nerve stimulation in human subjects. Nature Neurosci 2:94-98.

Clayton EC, Williams CL (2000). Adrenergic activation of the nucleus tractus solitarius potentiates amygdala norepinephrine release and enhances retention performance in emotionally arousing and spatial memory tasks. Behav Brain Research 112:151-158.

Crane JW, Buller KM, Day TA (2003). Evidence that the bed nucleus of the stria terminalis contributes to the modulation of hypophysiotropic corticotrophin-releasing factor cell responses to systemic interleukin-1β. J Comp Neurol 467:232-242.

Critchley HD, Corfield DR, Chandler M, Mathias, CJ, Dolan RJ (2000). Cerebral correlates of peripheral cardiovascular arousal: a functional neuroimaging study. J Physiol 523:259-270.

Critchley HD, Mathias CJ, Dolan RJ (2001). Neural correlates of first and second-order representation of bodily states. Nat Neurosci 4:207-212.

Cullinan WE, Herman JP, Battaglia DF, Akil H, Watson SJ (1995). Pattern and time course of immediate early gene expression in rat brain following acute stress. Neuroscience 64:477-505.

Cunningham Jr. ET, Sawchenko PE (1988). Anatomical specificity of noradrenergic inputs to the paraventricular and supraoptic nuclei of the rat hypothalamus. J Comp Neurol 274:60-76.

Davis M, Redmond Jr DE, Baraban JM (1979). Noradrenergic agonists and antagonists: effects on conditioned fear as measured by potentiated startle paradigm. Psychopharmacology (Berl) 65:111-118.

Davis M (1992a). The role of the amygdala in conditioned fear, in The Amygdala: Neurobiological Aspects of Emotion, Memory, and Mental Dysfunction, Aggleton, J.P., Ed., Wiley Liss, New York, p 255.

Davis M (1992b). The role of the amygdala in fear and anxiety. Annu Rev Neurosci 15:353-375.

Davis M (2001). The role of the amygdala in conditioned and unconditioned fear and anxiety. In: Aggleton, JP (Ed.), The Amygdala: A Functional Analysis. Oxford University Press, New York, pp. 232-234.

Day HEW, McKnight AT, Poat JA, Hughes J (1994). Evidence that cholecystokinin induces immediate early gene expression in the brainstem, hypothalamus and amygdala of the rat by a CCK_A receptor mechanism. Neuropharmacol. 33:719-727.

Dayas CV, Buller KM, Day TA (1999). Neuroendocrine responses to an emotional stressor: evidence for involvement of the medial but not the central amygdala. Eur J Neurosci 11:2312-2322.

Dayas CV, Day TA (2001). Opposing roles for medial and central amygdala in the initiation of noradrenergic cell responses to a psychological stressor. Eur J Neurosci 15:1712-1718.

Dayas CV, Buller KM, Crane JW, Xu Y, Day TA (2001). Stressor categorization: acute physical and psychological stressors elicit distinctive recruitment patterns in the amygdala and in medullary noradrenergic cell groups. Eur J Neurosci 14:1143-1152.

Deutsch JA, Hardy WT (1977). Cholecystokinin produces bait shyness in rats. Nature 266:196.

Dielenberg R A, Hunt GE, McGregor IS (2001). When a Rat Smells a Cat: The Distribution of Fos immunoreactivity in rat brain following exposure to a predatory odor. Neuroscience 104:1085-1097.

Dielenberg RA, McGregor IS (2001). Defensive behavior in rats towards predatory odors: a review. *Neuroscience and Biobehavioral Reviews* 25:597-609.

Dong Hong-Wei, Petrovich GD, Watts AG, Swanson LW (2001). Basic Organization of Projections From the Oval and Fusiform Nuclei of the Bed Nuclei of the Stria Terminalis in Adult Rat Brain. J Comp Neurol 436:430-455.

Dunn JD (1987). Plasma corticosterone responses to electrical stimulation of the bed nucleus of the stria terminalis. Brain Res 407:327–331.

Ericcson A, Kovacs KJ, Sawchenko PE (1994). A functional anatomical analysis of central pathways subserving the effects of interleukin-1 on stress-related neuroendocrine neurons. J Neurosci 14:897-913.

ETC Jr., Bohn MC, Sawchenko PE (1990). Organization of adrenergic inputs to the paraventricular and supraoptic nuclei of the hypothalamus in that rat. Journal of Comparative Neurology 292:651-667.

Fallon JH, Koziell DA, Moore RY (1978). Catecholamine innervation of the basal forebrain. II. Amygdala, suprahinal cortex and entorhinal cortex. J Comp Neurol 180:509-32.

Fendt M, Endres T, Apfelbach R (2003). Temporary Inactivation of the Bed Nucleus of the Stria Terminalis But Not of the Amygdala Blocks Freezing Induced by Trimethylthiazoline, a Component of Fox Feces. J Neurosci 23:23-8.

Ferry B, Roozendaal B, McGaugh JL (1999). Role of norepinephrine in mediating stress hormone regulation of long-term memory storage: a critical involvement of the amygdala. Biol. Psychiat. 46:1140-1152.

File SE (1986). Aversive and appetitive properties of anxiogenic and anxiolytic agents. Behav Brain Res 21:189-194.

Flanagan LM, Dohanics J, Verbalis JG, Stricker EM (1992). Gastric motility and food intake in rats after lesions of hypothalamic paraventricular nucleus. Am J Physiol 263:R39-44.

Flood JF, Smith GE, Morley JE (1987). Modulation of memory processing by cholecystokinin: dependence on the vagus nerve. Science 236:832-834.

Flood JF, Merbaum MO, Morley JE (1995). The memory enhancing effects of cholecystokinin octapeptide are dependent on an intact stria terminalis. Neurobiol. of Learning and Memory 64:139-145.

Fortier C (1951). Dual control of adrenocorticotropin release. Endocrinology 49:782-788.

Fox RJ, Sorenson CA (1994). Bilateral lesions of the amygdala attenuate analgesia induced y diverse environmental challenges. Brain Res 648:215-221.

Fulwiler CE, Saper CB (1984). Subnuclear organization of the efferent connections to the parabrachial nucleus in rats. Brain Res 7:229-259.

Funk D, Amir S (2000). Circadian modulation of Fos responses to odor of the red fox, a rodent predator, in the rat olfactory system. *Brain Res* 866:262-7.

Gallagher M, Chiba AA (1996). The amygdala and emotion. Curr Opin Neurobiol 6:221-227.

Gerhardt P, Voits M, Fink H, Huston JP (1994). Evidence for mnemotropic action of cholecystokinin fragments Boc-CCK-4 and CCK-8S. Peptides 15:689-697.

Goldberg MR, Hollister AS, Robertson D (1983). Influence of yohimbine ob blood pressure, autonomic reflexes, and plasma catecholamines in humans. Hypertension 5:772-778.

Gray TS, Carney ME, Magnuson D J (1989). Direct projections from the central amygdaloid nucleus to the hypothalamic paraventricular nucleus: possible role in stress-induced adrenocorticotropin release. Neuroendocrinology 50:433–446.

Grigson PS, Reilly S, Scalera G, Norgren R (1998). The parabrachial nucleus is essential for acquisition of a conditioned odor aversion in rats. Behav Neurosci 112:1104-13.

Gurguis G, Vitton BJ, Uhde TW (1997). Behavioral, sympathetic and adrenocortical responses to yohimbine in panic disorder patients and normal controls. Psychiatry Res 71:27-39.

Herbert H, Saper CB (1990). Cholecystokinin-, galanin-, and corticotropin releasing factor-like immunoreactive projections from the nucleus of the solitary tract to the parabrachial nucleus in the rat. J Comp Neurol 293:581–598.

Herman JP and Cullinan WE (1997). Neurocircuitry of stress: central control of the hypothalamo-pituitary-adrenocortical axis. TINS 20:78-84.

Herman JP, Figueiredo H, Mueller NK, Ulrich-Lai Yvonne, Ostrander MM, Choi DC, Cullinan WE (2003). Central Mechanisms of stress integration: hierarchical circuitry controlling hypothalamo-pituitary-adrenocortical responsiveness. Frontiers in Neuroendocrinology 24:151-180.

Higgins GA, Schwaber JS (1983). Somatostatinergic projections from the central nucleus of the amygdala to vagal nuclei. Peptides 4:657-662.

Hotsenpillar G, Williams JL (1997). A synthetic predator odor (TMT) enhances conditioned analgesia and fear when paired with a benzodiazepine receptor inverse agonist (FG-7142). Psychobiology 25:83-88.

Ishii H (1994). The activation of noradrenergic neurons in the rat locus coeruleus and stress responses. J Kurume Med Assoc 57:1-13.

Jhamandas JH, Petrov T, Harris KH, Vu T, Krukoff TL (1996). Parabrachial nucleus projection to the amygdala in the rat: electrophysiological and anatomical observations. Brain Res Bull 39:115-126.

Jia HG, Rao ZR, Shi JW (1994). An indirect projection from the nucleus of the solitary tract to the central nucleus of the amygdala via the parabrachial nucleus in the rat: a light and electron microscopic study. Brain Res 663:181–190.

Jones BJ, Moore RY (1977). Ascending projections of the locus ceruleus in the rat. II. Autoradiographic study. Brain Res 127:23-53.

Kaneyuki T, Morimasa T, Shohmori (1989). T. Action of peripherally administered cholecystokinin on monoaminergic and GABAergic neurons in the rat brain. Acta Med Okayama 43:153-159.

Kannan H, Yamashita H (1985). Connections of neurons in the region of the nucleus tractus solitarius with hypothalamic paraventricular nucleus: their possible involvement in neural control of the cardiovascular system in rats. Brain Res 329:205-212.

Kiem DT, Barna I, Koenig JI, Makara GB (1995). Adrenocorticotropin, Prolactin and Beta-Endorphin Stimulatory Actions of Alpha-2-Adrenoceptor Antagonists. Neuroendocrinology 61:152-58.

Kovacs KJ (1998). c-Fos as a transcription factor: a stressful (re)view from a functional map. Neurochem Int 33:297-297.

Lamprecht R, Dudai Y (1996). Transient expression of c-Fos in rat amygdala during training is required for encoding conditioned taste aversion memory. Learn Mem 31:31-41.

Lasiter PS, Glanzman DL (1985). Cortical substrates of taste aversion learning: involvement of dorsolateral amygdaloid nuclei and temporal neocortex in taste aversion learning. Behav Neurosci 99:257-276.

LeDoux JE, Sakaguchi A, Reis DJ (1984). Subcortical efferent projections of the medial geniculate nucleus mediate emotional responses conditioned to acoustic stimuli. J Neurosci 4:683-698.

LeDoux JE, Iwata J, Pearl D, Reis DJ (1986). Disruption of auditory but not visual learning by destruction of intrinsic neurons in the rat medial geniculate body. Brain Res 371:395-399.

LeDoux JE (1992). In search of an emotional system in the brain: leaping from fear to emotion and consciousness. In The Cognitive Neurosciences, M.S. Gazzaniga, ed. (Cambridge, MA: MIT press), pp, 1049-1061.

LeDoux JE (1995). Emotion: Clues from the brain. Ann Rev Psychol 46:209-235.

LeDoux J (1996). The Emotional Brain. Simon and Schuster (Ed.), New York.

LeDoux JE, Iwata J, Cicchetti P, Reis DJ (1988). Different projections of the central amygdaloid nucleus mediate autonomic and behavioral correlates of conditioned fear. J. Neurosci. 8:2517-2529.

LeDoux JE (2003). The Emotional Brain, Fear, and the Amygdala. Cellular and Molecular Neurobiology 23:727-737.

Lemaire M, Bohme GA, Piot O, Roques BP, Blanchard JC (1994). CCK-A and CCK-B selective receptor agonists and antagonists modulate olfactory recognition in male rats. Psychopharmacol. 115:435-440.

Li HY, Ericsson A, Sawchenko PE (1996). Distinct mechanisms underlie activation of hypothalamic neurosecretory neurons and their medullary catecholaminergic afferents in categorically different stress paradigms. Proc. Natl Acad Sci USA 93:2359-2364.

Li HY, Sawchenko PE (1998). Hypothalamic effector neurons and extended circuitries activated in 'neurogenic' stress: a comparison of footshock effects exerted acutely, chronically, and in animals with controlled glucocorticoid levels, J Comp Neurol 393:244-266.

Linden CH, Vellman WP, Rumack B (1985). Yohimbine: a new street drug. Ann Emerg Med 14:1002-4.

Magnuson DJ, Gray TS (1989). Bed nucleus of the stria terminalis directly innervate parvocellular paraventricular hypothalamic CRF, vasopressin and oxytocin containing cells. Neurosci Abstr 15:135.

Marcilhac A, Siaud P (1996). Regulation of the adrenocorticotrophin response to stress by the central nucleus of the amygdala in rats depends upon the nature of the stressor. Exp Physiology 81:1035-1038.

Mattila M, Seppala T, Mattila MJ (1988). Anxiogenic effect of yohimbine in healthy subjects: comparison with caffeine and antagonism by clonidine and diazepam. Int Clin Psychopharmacol 3: 215-29.

Mayer EA, Naliboff B, Munakata J (2000). The evolving neurobiology of gut feelings. Progress in Brain Res 122:195-206.

McCann MJ, Verbalis JG, Stricker EM (1989). LiCl and CCK inhibit gastric emptying and feeding and stimulate OT secretion in rats. Am J Physiol 256:R463-8.

McDonald AJ (1998). Cortical pathways to the mammalian amygdala. Prog Neurbiol 55:257-332.

McLean IW, Nakane PK (1974). Periodate-lysine-paraformldehyde fixative. A new fixative for immunoelectron microscopy. J Histochem Cytochem 22:1077-1083.

Miaskiewicz SL, Stricker EM, Verbalis JG (1989). Neurohypophyseal secretion in response to cholecystokinin but not meal-induced gastric distention in humans. J Clin Endocrinol Metab 68:837-843.

Moga MM, Saper CB, Gray TS (1990). The bed nucleus of the stria terminalis: Cytoarchitecture, immunohistochemistry and projection to the parabrachial nucleus in the rat, J Comp Neurol 283:315-332.

Morrow BA, Redmond AJ, Roth RH, Elsworth JD (2000). The predator odor, TMT, displays a unique, stress-like pattern on dopaminergic and endocrinological activation in the rat. Brain Res 864:146-151.

Morrow BA, Elsworth JD, Roth RH (2002). Fear-Like Biochemical and Behavioral Responses in Rats to the Predator Odor, TMT, Are Dependent on the Exposure Environment. Synapse 46:11-18.

Myers, EA, Rinaman L (2002). Viscerosensory Activation of Noradrenergic Inputs to the Amygdala in Rats. Physio Behav 723:

Myers, EA, Banihashemi L, Sprute L, Rinaman L (2004). Central Neural Activation and Behavioral Responses to Systemic Yohimbine in Rats. Exp Bio Abstract.

Nitecka L, Amerski L, Panek-Mikula J, Narkiewicz O (1980). Tegmental afferents of the amygdaloid body in the rat. Acta Neurobio. Exp. 40:609-624.

Norgren R. (1995). Gustatory system. In: Paxinos G, editor. The rat nervous system. San Diego: Academic Press. p 751–771.

Oguchi M (1988). Effects of anxiogenic drugs on noradrenaline metabolism in rat brain regions, J Kurume Med Assoc 51:943-957.

Pacak K, McCarty R, Palkovits M, Kopin IJ, Goldstein DS (1995). Effects of immobilization on in vivo release of norepinephrine in the bed nucleus of the stria terminalis in conscious rats. Brain Res 688:242-246.

Parker Linda (2003). Taste avoidance and taste aversion: evidence for two different processes. Learn Behav 31:165-72.

Paxinos G, Watson C (1997). The Rat Brain in Stereotaxic Coordinates. San Diego: Academic Press.

Pellow S, Chopin P, File SE, Briley M (1985). Validation of open:closed arm entries in an elevated plus-maze as a measure of anxiety in the rat. Journal of Neuroscience Methods 14:149-67.

Perrot-Sinal TS, Ossenkopp KP, Kavaliers M (1999). Brief predator odour exposure activated the HPA axis independent of locomotor changes. Neuroreport 10:775-780.

Petrov T, Krukoff TL, Jhamandas JH (1995). Convergent influence of the central nucleus of the amygdala and the paraventricular hypothalamic nucleus upon brainstem autonomic neurons as revealed by c-fos expression and anatomical tracing. J Neurosci Res 42:835-845.

Petrovich GD, Swanson LW (1997). Projections from the lateral part of the central amygdalar nucleus to the postulated fear conditioning circuit. Brain Res 763:247-254.

Pezzone MA, Lee WS, Hoffman GE, Rabin BS (1992). Induction of c-Fos immunoreactivity in the rat forebrain by conditioned and unconditioned aversive stimuli. Brain Res 597:41-50.

Pickel VM, Segal M, Bloom FE (1974). A radioautographic study of the efferent pathways of the nucleus locus coeruleus. J Comp Neurol. 155:15-42.

Pitkanen A, Savander P, LeDoux JE (1997). Organization of intra-amygdaloid circuitries in the rat: an emerging framework for understanding functions of the amygdala. TINS 20:517-523.

Plotsky PM (1987). Facilitation of immunoreactive corticotrophin-releasing factor secretion into the hypophysial –portal circulation after activation of catecholaminergic pathways or central norepinephrine injection. Endocrinology 121:924-934.

Price JL (1991). The Human Nervous System, ed. Paxinos, G Academic, New York pp 979-998.

Reilly S (1999). The parabrachial nucleus and conditioned taste aversion. Brain Res Bull 48:239-54.

Ricardo JA, Koh ET (1978). Anatomical evidence of direct projections from the nucleus of the solitary tract to the hypothalamus, amygdala, and other forebrain structures in the rat. Brain Research 153:1-26.

Riche D, De Pommery J, Menetrey D (1990). Neuropeptides and catecholamines in efferent projections of the nuclei of the solitary tract in the rat. J Comp Neurol 293:399-424.

Rinaman L, Stricker EM, Hoffman GE, Verbalis JG (1997). Central c-fos expression in neonatal and adult rats after subcutaneous injection of hypertonic saline. Neuroscience 79:1165-1175.

Rinaman L, Verbalis JG, Stricker EM, Hoffman GE (1993). Distribution and neurochemical phenotypes of caudal medullary neurons activated to express cFos following peripheral administration of cholecystokinin. J. Comp. Neurol. 338:475-90.

Rinaman L, Hoffman GE, Dohanics J, Le WW, Stricker EM, Verbalis JG (1995). Cholecystokinin activates catecholaminergic neurons in the caudal medulla that innervate the paraventricular nucleus of the hypothalamus in rats. J. Comp. Neurol. 360:246-56.

Rinaman L, Baker EA, Hoffman GE, Stricker EM, Verbalis JG (1998). Medullary c-Fos activation in rats after ingestion of a satiating meal. Am. J. Physiol. Reg. Integrat. Comp. Physiol. 275:R262-R268.

Roder S, Ciriello J (1993). Innervation of the amygdaloid complex by catecholaminergic cell groups of the ventrolateral medulla. J. Comp. Neurol. 332:105-122.

Roder S, Ciriello J (1994). Collateral axonal projections to limbic structures from ventrolateral medullary A1 noradrenergic neurons. Brain Res 182-188.

Roozendaal B, Koolhaas JM, Bohus B (1992). Central amygdaloid involvement in neuroendocrine correlates of conditioned stress responses. J Neuroendocrinol 4:483-489.

Sagar SM, Sharp FR, Curran T (1988). Expression of c-Fos protein in brain: metabolic mapping at the cellular level. Science 240:1328-1331.

Sakai N, Yamamoto T (1998). Role of the medial and lateral parabrachial nucleus in acquisition and retention of conditioned taste aversion in rats. Behav Brain Res 93:63-70.

Saper CB, Loewy AD (1980). Efferent connections of the parabrachial nucleus in the rat. Brain Res 197:291–317.

Sawchenko PE, Swanson LW (1981). Central noradrenergic pathways for the integration of hypothalamic neuroendocrine and autonomic responses. Science 214:685-687.

Sawchenko PE, Swanson LW (1982). The organization of noradrenergic pathways from the brainstem to the paraventricular and supraoptic nuclei in the rat. Brain Research Reviews 4:275-325.

Sawchenko PE, Swanson LW (1983). The organization of forebrain afferents to the paraventricular and supraoptic nuclei of the rat. J Comp Neurol 218:121-144.

Sawchenko PE, Brown ER, Chan RK, Ericsson A, Li HY, Roland BL, Kovacs KJ (1996). The paraventricular nucleus of the hypothalamus and the functional neuroanatomy of visceromotor responses to stress. Prog Brain Res 107:201-225.

Sawchenko PE, Li H, Ericcson A (2000). Circuits and mechanisms governing hypothalamic responses to stress: a tale of two paradigms. Prog Brain Res 122:61-80.

Scalia F, Winans SS (1975). The differential projections of the olfactory bulb and accessory bulb in mammals. J Comp Neurol 161:31-55.

Schroeder BE, Schiltz CA, Kelley AE (2003). Neural activation profile elicited by cues associated with the anxiogenic drug yohimbine differs from that observed for reward-paired cues. Neuropsychopharmacology 28:14-21.

Schwaber JS, Sternini C, Brecha NC, Rogers WT, Card JP (1988). Neurons containing calcitonin gene-related peptide in the parabrachial nucleus project to the central nucleus of the amygdala. J Comp Neurol 270:416-26.

Selye H (1936). A syndrome produced by diverse noxious agents. Nature 138:32.

Selye H (1946). The general adaptation syndrome and the diseases of adaptation. J Clin Endocrinol Metab 6:117-230.

Schwaber JD, Kapp BS, Higgins GA, Rapp PR (1982). J Neurosci 2:1424-1438.

Schwartz GJ, Moran TH (1998). Integrative gastrointestinal actions of the brain-gut peptide cholecystokinin in satiety. Prog. Psychobiol. Physiol. Psych. 17:1-34.

Shapiro RE, Miselis RR. (1985). The central neural connections of the area postrema. J Comp Neurol 234:344–364.

Singewald N, Sharp T (2000). Neuroanatomical targets of anxiogenic drugs in the hindbrain as revealed by Fos immunocytochemistry. Neuroscience 98:759-770.

Singewald N, Salchner P, Sharp T (2003). Induction of c-Fos Expression in Specific Areas of the Fear Circuitry in Rat Forebrain by Anxiogenic Drugs. Biol Psychiatry 53:275-83.

Slaughter JS, Hahn WW (1974). Effects on avoidance performance of vagal stimulation during previous fear conditioning in rats. J. Comp. Physiol. Psych. 86:283-287.

Southwick SM, Krystal JH, Morgan CA, Johnson D, Nagy LM, Nicolaou A, Heninger GR, Charney DS (1993). Abnormal noradrenergic function in post-traumatic stress disorder. Arch Gen Psychiatry 50:266-74.

Spyer KM (1982). Central nervous integration of cardiovascular control. J Exp Bio 100:109-128.

Sun N, Roberts L, Cassell M.D (1991). Rat central amygdaloid nucleus projections to the bed nucleus of the stria terminalis. Brain Res. Bull 27:651–662.

Sun N, Cassell MD (1993). Intrinsic GABAergic neurons in the rat central extended amygdala. J Comp Neurol 330:381-404.

Switzer RC, de Olmos J, Heimer L (1985). Olfactory system. In: The Rat Nervous System, pp 1-36 Ed. G. Paxinos. Academic Press: Sydney.

Thrivikraman KV, Su Y, Plotsky PM (1997). Patterns of Fos-immunoreactivity in the CNS induced by repeated hemorrhage in conscious rats: Correlations with pituitary-adrenal axis activity. Stress 2:145-158.

Uhde TW, Boulenger JP, Post RM, Siever LJ, Vittone BJ, Jimerson DC, Roy-Byrne PP (1984). Fear and anxiety: relationship to noradrenergic function. 17:8-23.

Van der Kar LD, Piechowski RA, Rittenhouse PA, Gray TS (1991). Amygdaloid lesions: differential effect on conditioned stress and immobilization-induced increases in corticosterone and rennin secretion. Neuroendocrinology 54:89-95.

Van Der Kooy D, Koda LY, McGinty JR, Gerfen CR, Bloom FE (1984). The organization of projections from the cortex, amygdala, and hypothalamus to the nucleus of the solitary tract in rat. J Comp Neurol 224:1-24.

Veening JG, Swanson LW, Sawchenko PE (1984). The organization of projections of the central nucleus of the amygdala to brainstem sites involved in central autonomic regulation: a combined retrograde transport-immunocytochemical study. Brain Res 303:337-357.

Vernet-Maury E, Polak EH, Demael A (1984). Structure–activity relationship of stress-inducing odorants in the rat. J Chem Ecology 10:1007-1018.

Vernet-Maury E, Alaoui-Ismaili O, Dittmar A, Delhomme G, Chanel J (1999). Basic emotions induced by odorants: a new approach based on autonomic pattern results. J Auton Nerv Syst. 75:176-83.

Voits M, Hasenohrl RU, Huston JP, Fink H (2001). Repeated treatment with cholecystokinin octapeptide improves maze performance in aged Fischer 344 rats. Peptides 22:1325-1330.

Walker DL, Toufexis DJ, Davis M (2003). Role of the bed nucleus of the stria terminalis versus the amygdala in fear, stress, and anxiety. European Journal of Pharmacology 463:199-216.

Wallace KJ, Rosen JB (2000). Predator odor as an unconditioned fear stimulus in rats: elicitation of freezing by trimethylthiazoline, a component of fox feces. Behav Neurosci 114:912-922.

Wallace KJ, Rosen JB (2001). Neurotoxic lesions of the lateral nucleus of the amygdala decrease conditioned fear but not unconditioned fear of a predator odor: comparison with electrolytic lesions. J Neurosci 21:3619-27.

Wang Y and Chambers KC (2002). Cooling lesions of the lateral parabrachial nucleus during LiCl activation block acquisition of conditioned taste avoidance in male rats. Brain Res 934:7-22.

Watson RE, Wiegand SJ, Clough RW, Hoffman GE (1986). Use of cryoprotectant to maintain long-term peptide immunoreactivity and tissue morphology. Peptides 7:155-159.

Weiskrantz L (1956). Behavioral changes associated with ablations of the amygdaloid complex in monkeys. J Comp Physiological Psychol 49:381-391.

Werka T (1997). The effects of the medial and cortical amygdala lesions on post-stress analgesia in rats. Behav Brain Res 86:59-65.

Williams CL, Men D, Clayton EC (2000). The effects of noradrenergic activation of the nucleus tractus solitarius on memory and potentiating norepinephrine release in the amygdala. Behav. Neurosci. 114:1131-1144.

Xu Y, Buller KM, Day TA (1998). Role of the central amygdala in HPA axis, oxytocin and central catecholamine responses to systemic IL-1β. Eur J Neurosci 10:295.

Xu Y, Day TA, Buller KM (1999). The central amygdala modulates hypothalamic-pituitary-adrenal axis responses to systemic immune challenge. Neuroscience 94:175-183.

Yamamoto T, Saki N, Sakai N, Iwafune A (1997). Gustatory and visceral inputs to the amygdala of the rat: conditioned taste aversion and induction of c-fos-like immunoreactivity. Neurosci Lett 226:127-130.

Zald DH, Pardo JV (1997). Emotion, olfaction, and the human amygdala: Amygdala activation during aversive olfactory stimulation. Proc Natl Acad Sci USA 94: 4119-4124.

Zardetto-Smith AM, Gray TS (1990). Organization of peptidergic and catecholaminergic efferents from the nucleus of the solitary tract to the rat amygdala. Brain Research Bull. 25:875-887.

Zardetto-Smith AM, Gray TS (1995). Catecholamine and NPY efferents from the ventrolateral medulla to the amygdala in the rat. Brain Research Bull. 38:253-260.